THE ROLE OF THE TRANSMEMBRANE DOMAIN OF SYNAPTOBREVIN IN EXOCYTOSIS

by Annita Nganso Ngatchou

THE ROLE OF THE TRANSMEMBRANE DOMAIN OF SYNAPTOBREVIN IN EXOCYTOSIS

A Dissertation

Presented to the Faculty of the Graduate School

of Cornell University

in Partial Fulfillment of the Requirements for the Degree of

Doctor of Philosophy

by

Annita Nganso Ngatchou

August 2010

THE ROLE OF THE TRANSMEMBRANE DOMAIN OF SYNAPTOBREVIN IN EXOCYTOSIS

Annita Nganso Ngatchou, Ph.D.

Cornell University 2010

Exocytosis is a process used by many cells to move material out of the cell. This process is used by nerve cells to communicate with one another at synapses. This communication is achieved in part by the release of neurotransmitters at the nerve terminal into the extracellular space. Neurotransmitters are contained in membrane bound organelles called vesicles. These vesicles dock and fuse with the plasma membrane of the cell, where a fusion pore is created to allow for the diffusion of neurotransmitters into the extracellular space. The study of exocytosis has led to the identification of the SNARE proteins, located on the vesicle (v-SNARE) and on the plasma membrane (t-SNARE). The v-SNARE and the t-SNARE form a tight complex that holds the vesicle close to the cell plasma membrane. However, it is unclear whether the SNARE proteins also participate in the creation the fusion pore. In this thesis, the role of the v-SNARE protein, synaptobrevin-2 is explored, in particular the role of its transmembrane domain which is embedded into the vesicle membrane. It turns out that the formation of the SNARE complex formed by the association of the v-SNARE and the t-SNARE pulls the C-terminus of synaptobrevin into the vesicle lipid membrane, and with this movement, it disrupts the membrane continuity leading the formation of the fusion pore. In addition, the transmembrane domain of synaptobrevin-2 is located at the vincinity of the fusion pore during the fusion pore expansion.

BIOGRAPHICAL SKETCH

Annita Nganso Ngatchou was born on June 24, 1980 in Yaounde, Cameroon. Growing up in a large family with many cousins and relatives she experienced an easygoing childhood. After finishing High school, she spent 3 years completing her undergraduate studies at Rutgers University in Camden, NJ. After graduating in 2003, and undecided about her future career, she spent a year in the post-baccalaureate program at Johns Hopkins University, where she worked in the laboratory of Prof. Rachel Green. However, it was clear that she wanted to pursue her education thus, after being accepted at Cornell University, she started her PhD study in the field of Biophysics and worked in the department of Applied Physics and Engineering under the supervision of Prof. Manfred Lindau. During her PhD time at Cornell, she spent all together 18 months in Germany where she enjoyed working at the Max Planck Institute for Biophysical Chemistry in Göttingen under the supervision of Prof. Jakob Sørensen.

In memory of my mother and grand-mother, Jeanne Yomba and Miyo

To my father, Jean-Claude Ngatchou
-with love always

Beung nsi nag youm ngam si shou dô
-Medumba (Bagangté)

ACKNOWLEDGEMENTS

I first would like to thank Prof. Manfred Lindau for the opportunity of working in his lab and for supervising this research.

I also would like to acknowledge Prof. Sørensen for the amazing learning experience during the time I spent in his group at the Max Planck Institute in Göttingen.

A big thanks goes out to the whole **The Lindau group and The Sørensen group!**

Thank you to Prof. Jerry Feigenson for all the advice.

I am acknowledging Stephan Weiss for cross-reading this thesis.

I shall not proceed without saying many thanks to Tchefor Ndukum who was my unofficial physics tutor.

To Patricia Kegne, Clarice Njike and Michael Grabchak, and to my siblings N-Neka, Zanne, Zania, Tchoufa and Celia thank you for the fun years.

A special thank to my parents Jean-Claude and Catherine who, not only provided the logistics but also the moral support, without which I could not have finished graduate school.

TABLE OF CONTENTS

LIST OF TABLES

LIST OF FIGURES

ABBREVIATIONS

C – terminal	Carboxyl- terminal
ceb	cellubrevin
GFP	Green Fluorescent Protein
GFP – SybII	GFP-synaptobrevin-2
N – terminal	Animo-terminal
NP – EGTA	NP-EGTA/o-nitrophenyl EGTA tetrapotassium salt
pHlourin	pH-sensitive green fluorescent protein-based sensor
RRP	Readily Releasable Pool
SNAP – 25	Synaptosomal-associated protein of 25 KD
SNARE	Soluble N-ethylmaleimide-sensitive-factor Attachement protein REceptor
SRP	Slowly Releasable Pool
SybII	Synaptobrevin-2

TMD	Transmembrane Domain
VAMP	Vesicle-Associated Membrane Protein

CHAPTER 1

INTRODUCTION

Neuron to neuron communication is one of the most important activities occurring in living animals. The main task of neurons is to transmit information throughout our body. In order to achieve this task, the information needs to travel within neurons and, from one neuron to the next. While the information travels along a neuron in the form of electrical pulses called action potential, it is sent to the neighboring neuron by neurotransmitter molecules that are released in one cell, diffuse through the extracellular space and stimulate the next neuron. Before their release, neurotransmitters are generally encapsulated inside small membrane bound packets, called vesicles. At the arrival of a stimulus, these vesicles fuse with the nerve terminal's plasma membrane and thereby release their content into the extracellular space. This process is called *exocytosis*.

Neurotransmitters are therefore essential for all kinds of brain activities such as memory, attention, mood and the coordination of voluntary movement, hence it is important for our body to sustain its functionality. One example for the consequence of a neurotransmitter deficiency is Parkison's disease, a chronic movement disorder, where the release of the neurotransmitter dopamine is profoundly impaired.

The study of the exocytotic process has advanced the understanding of the mechanism of neurosecretion. For example, it was found that a high concentration of calcium stimulates the fusion of vesicles in neurons. Furthermore the proteins that mediate the fusion could be identified as members of the so-called SNARE (Soluble N-ethylmaleimide-sensitive-factor Attachement protein REceptor) family [31, 34].

A system widely used to study neuronal exocytosis is the chromaffin cell from the adrenal gland [Fig 1.1]. Similar to neurons, this cell type also encom-

passes vesicles that undergo calcium dependent exocytosis and the fusion of their vesicles is also mediated by the neuronal SNAREs.

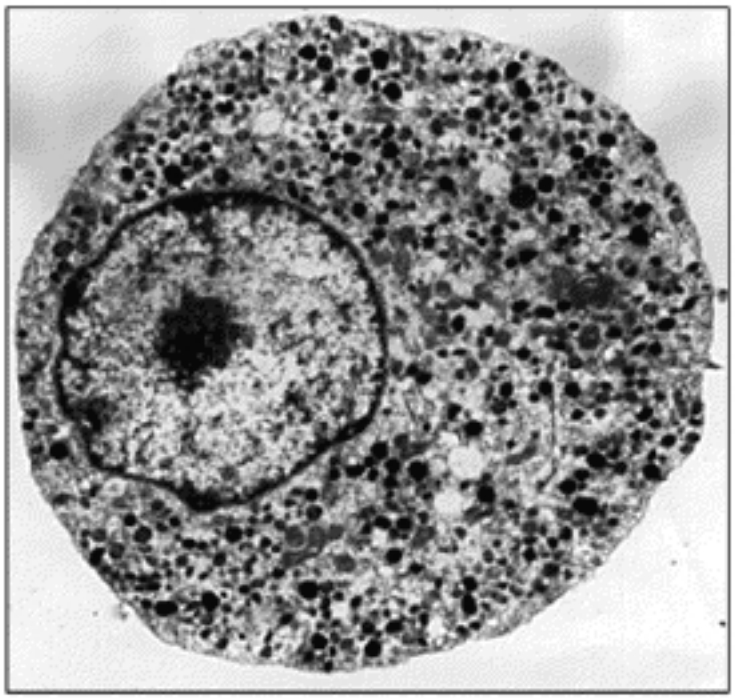

Figure 1.1: Electron Micrograph of a bovine chromaffin cell. The small dark dots are the dense core vesicles, located in the cytoplasm (Horstmann and Lindau, unpublished).

The SNARE proteins can be divided into two subgroups, the vesicle SNARE (v-SNARE) found on the vesicle membrane and the target SNARE (t-SNARE) located on the plasma membrane of the cell . The original SNARE hypothesis stipulated that when a vesicle is near the cell membrane, the t-SNARE and the v-SNARE paired up side by side in opposite directions to form a SNARE complex that leads to the fusion of the vesicle [31]. However, when the crystal structure of the complex was solved, it was observed that although the t-SNARE and the v-SNARE fold into an helical bundle [Fig.1.2 A], they adopt a parallel orientation with respect to each other [38, 36, 20]. Nevertheless, numerous experiments

have confirmed that the formation of the SNARE complex leads to exocytosis as initially postulated. For example, when toxins are used that specifically cleave the SNARE proteins, neuronal exocytosis is abolished [28, 23, 27, 17]. Additional evidence supporting the essential role of SNAREs in vesicle fusion also comes from experiments showing that mice that are genetically deprived of one of the SNARE proteins are deficient in exocytosis [7, 3, 32, 29, 42]. Based on these observations, it was proposed that the SNAREs constitute the scaffold of the fusion machinery. However the specifics of the mechanisms by which the SNARE proteins mediate the fusion of vesicles is still not fully understood.

1.1 SNARE complex formation

The neuronal v-SNARE also called synaptobrevin has a SNARE motif that is located in the cytosol and a transmembrane domain, which is anchored into the lipid membrane of the vesicle. The t-SNARE on the other hand, is comprised of syntaxin and SNAP-25. Syntaxin has a similar structure to that of synaptobrevin with the exception that it is anchored to the plasma membrane of the cell, whereas SNAP-25 is covalently attached to the lipid plasma membrane by means of cysteine residues.

The SNARE complex is formed by a 4-α-helical bundle [38], where synaptobrevin and syntaxin each provide one helix, and SNAP-25 provides the remaining two [Fig.1.2]. The helices are aligned in such a way that the interacting amino acids (between 60 to 70 amino acids) are grouped into layers [Fig.1.2 B] [9].

To understand the steps leading to the formation of the SNARE complex, Sørensen and coworkers investigated how the complex assembles by interfering with its stability [33]. By introducing point mutations in layer 5 or 8 of the

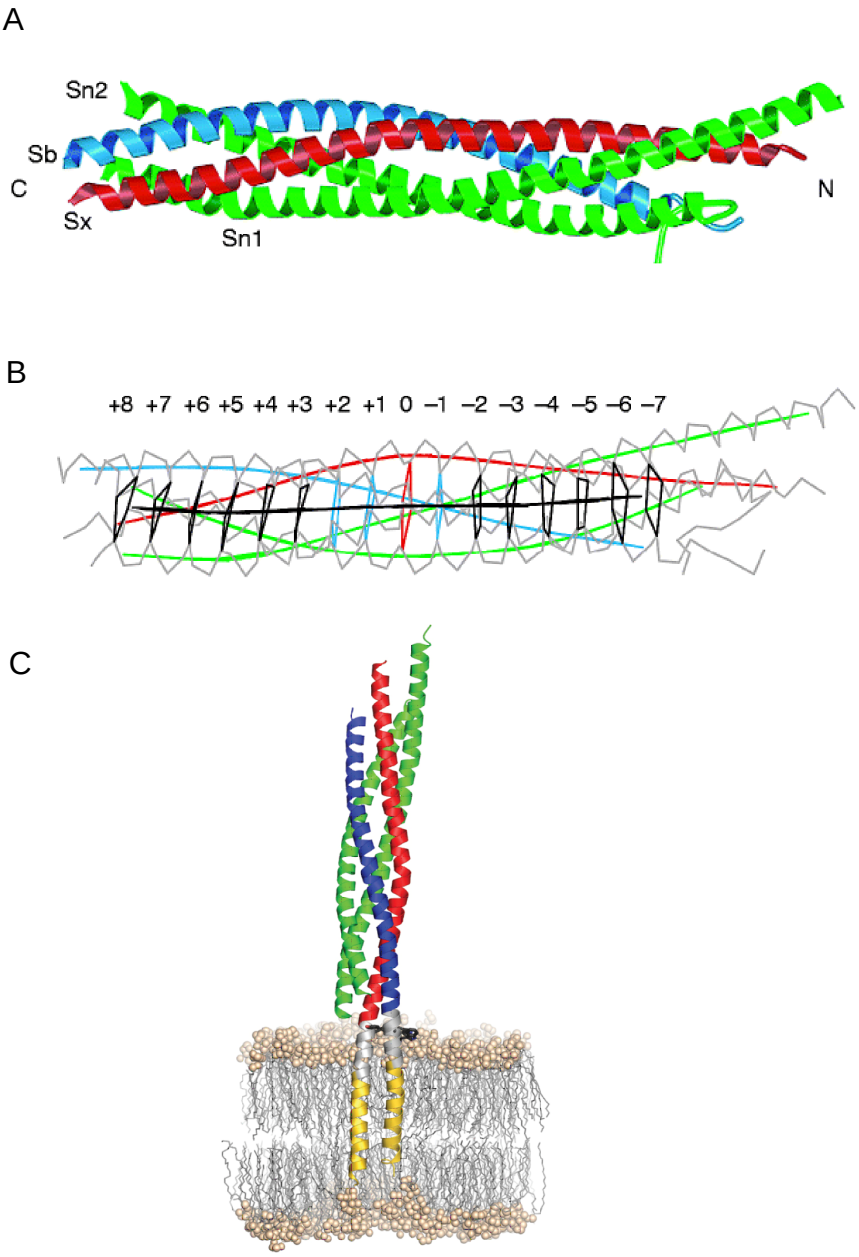

Figure 1.2: Crystal structure of the SNARE complex. (A,C) The complex is composed of 4 helices, synaptobrevin-2 (blue), syntaxin-1A (red), and SNAP-25 which provide an additional two strands (Sn1 and Sn2 in green) as seen in this backbone ribbons drawing of the SNARE complex structure. (B) Structural alignments of the SNARE proteins around the super helix axis (black). The layers (+8 to -7) was inferred based on the virtual bonds between the helices [38]. (C) The parallel arrangement of the SNARE proteins into the complex continues into the lipid membrane [36]. (Modified Figures from [36] and [38]).

carboxyl-terminal of SNAP-25 helices [Fig.1.2 B] , they destabilized the helical interaction within the complex and observed that these mutations slowed down the kinetics of rapid exocytosis. However, when the mutations were located at the amino terminal, the kinetics of rapid exocytosis was unchanged. This suggests that the SNARE complex folds in two steps from the amino-terminal to the carboxyl (C)- terminal .

The SNARE complex stability was also investigated by circular dichroism spectroscopy technique [10]. It was estimated that the N-terminal domain of the complex melts at ~66 °C, whereas the C-terminal domain melts at ~44 °C, indicating that the C-terminal region of the SNARE complex is less stable. From these experimental results, it was proposed that the SNARE complex formation proceeds in a zipper-like fashion from the N- to the C- terminus (although this model has been challenged [15]), thus pulling the vesicle and the membrane together to lead to vesicle-plasma membrane fusion and exocytosis [33, 25, 30].

1.2 The SNARE complex energy output and the fusion pore

During exocytosis, vesicles at the plasma membrane, dock, fuse and release neurotransmitters through a fusion pore. As we have previously discussed, 50 to 70 residues (SNARE motif) of SNAP-25, syntaxin and synaptobrevin assemble themselves into a complex [38] [Fig.1.2 A]. However, it was recently shown that this helical bundle continues into the membrane through the interaction of the synaptobrevin and syntaxin transmembrane domains [36] [Fig.1.2 C]. From this observation, it was proposed that the transition from unstructured single SNARE proteins to a zipped complex releases energy which is transferred to the lipid membranes via the transmembrane domains (TMD) of synaptobrevin and syntaxin [Fig.1.2 C, yellow]. But, is this energy sufficient to drive the fu-

sion of the vesicle with the plasma membrane or to create a pore through which molecules can be secreted?

1.2.1 The SNAREs: Minimum machinery for exocytosis?

Weber and colleagues initially reconstituted the basic fusion machinery in a liposome system [43], that is to say only the SNARE proteins and lipid membranes were used. They observed that the liposomes exchanged their contents, suggesting that the SNARE proteins were sufficient to induce liposome-liposome fusion. However the kinetics of this fusion was extremely slow, taking hours for completion, in comparison to millisecond kinetics of neurotransmitter secretion observed in cells [1]. This inconsistency in the time scale of the reactions between the liposomes and the cells data was attributed to the fact that in cells, the calcium sensor protein synaptotagmin also catalyzes the merger of the membranes [45, 11, 22]. Hence, when the liposome assay was reconstituted with the addition of the full length synaptotagmin protein or only its calcium sensing domain, C2AB, sped up the fusion reaction [35, 39, 22], thus leading to faster pore formation.

1.2.2 The SNARE complex energy

Inherent to exocytosis is the apposition of the vesicular and the plasma lipid bilayers. It was suggested that for the SNAREs to overcome the electrostatic repulsion induced by the apposition of the charged phospholipid head groups of the membranes, the SNAREs would need to provide a free energy of activation of about 40 KT [18]. However, it has not been possible to determine with accuracy the energy release by the SNARE complex formation *in vivo*, accordingly it has been a challenge figuring out whether the SNAREs alone can lower this

activation energy for fast vesicle fusion. Nevertheless, Li and colleagues [19] have rather elegantly attempted to provide an estimate of the energy stored by the complex. Using a surface forces apparatus, they estimated 35 KT for the stabilization energy of the complex. However in this study, 12 to 25 residues of the C-terminal regions were unstructured and the TMDs of synaptobrevin and syntaxin were deleted, suggesting that the 35 KT may represent the energy stored by 3/4 of the SNARE complex. Thus, this would suggest that the formation of one SNARE complex alone would already provide enough energy to deform the membranes for the creation of a pore [40]. However, these studies were performed *in vitro* where synaptotagmin was omitted. Synaptotagmin along with other accessory proteins bind the SNARE complex at various stages prior to vesicle fusion [4, 5, 37], thus the transition to generate the fusion of a vesicle is not simply the assembly of the individual SNARE complex components.

1.3 Genesis of the fusion pore

The creation of a fusion pore is a rate limiting step in exocytosis, and is therefore the process that determines the speed at which vesicles fuse with the plasma membrane [26]. Over the years, several experiments have been designed to assess whether the SNARE complex formation affect the fusion pore properties. The standard approach has been to mutate the SNARE proteins and to introduce them into cells, then the fusion pore conductance and the flux of neurotransmitters through the fusion pore is acquired from these cells and compared to cells having non mutated proteins. The flux of catecholamine neurotransmitter molecules through the fusion pore can be detected because they oxidize when they make contact with a carbon fiber electrode held at a positive potential (amperomtry) [44, 13, 24]. In the amperometry technique, the electrode is pressed

down onto the cell membrane. When a vesicle fuses with the plasma membrane and releases its contents, neurotransmitters oxidize at the surface of the carbon fiber where they give up two electrons per molecule [Fig.1.3 A]. This transfer of electrons can be observed as transient spikes on the amperometry trace [Fig.1.3 B]. From the analysis of the amperometry spikes properties [Fig.1.3 B], the fusion pore properties can be inferred. For example, the amperometry spikes are often preceded by a pre-spike or "foot" [6] which provides a read out of the initial neurotransmitter flux through the fusion pore [1].

To assess whether the SNARE complex conformational change is reflected in the fusion pore properties, the foot signal that precedes the spikes was analyzed. When the complex was destabilized by mutating synaptobrevin-2 SNARE motif in layer 8 of the C-terminal domain, the foot duration was reduced, indicating the shortening of the fusion pore lifetime [41]. However, when the last nine amino acids of the SNARE motif of SNAP-25 were deleted, the foot duration increased [8] reflecting the elongation of the pore lifetime. Hence it is evident that the stability of the SNARE complex is reflected in the properties of the fusion pore.

Although there is a clear link between the SNARE proteins and the fusion pore, it is not fully understood how the fusion pore is created, however several models have been proposed to explain the genesis of the fusion pore. The proteinaceous fusion pore model which postulates that the TMD of syntaxin and probably synaptobrevin-2 line the fusion pore channel in the first few milliseconds of its existence [14]. This model is drawn from neurotransmitter flux analysis done by Han et al. [14], which showed that when some residues of the TMD of syntaxin were replaced by a bulky tryptophan amino acid, the pre-spike amperometric amplitude during exocytosis was reduced. This model also postulates that, the pore expands because the TMDs dissociate during the fusion

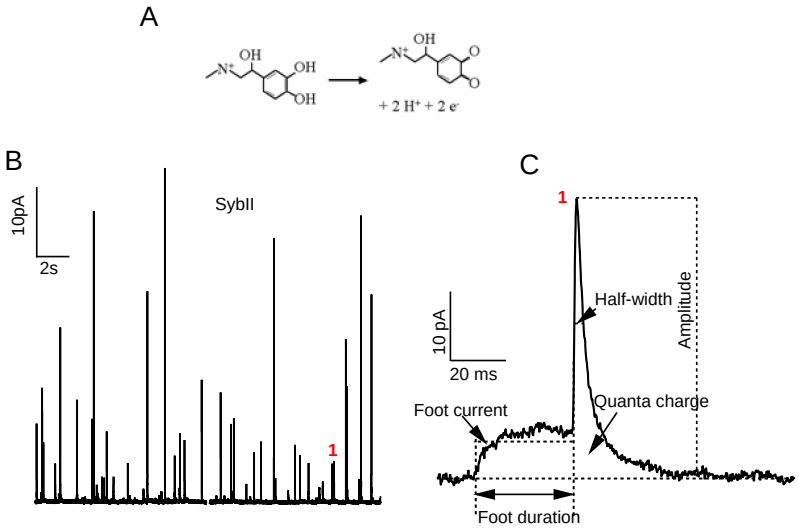

Figure 1.3: (A) The oxidation of catecholamine releases two electrons. (B) Amperometric current trace recorded from a chromaffin cell. (C) Representation of amperometry event parameters. (Modified figure from Chapter V).

pore expansion [Fig 1.4 A] [16]. The caveat with this view is that the TMD of synaptobrevin and syntaxin are composed of hydrophobic residues, hence it is difficult to picture a pore formation with hydrophobic residues that allows for the diffusion of hydrated cations [12].

To circumvent this problem, the proteolipidic fusion pore model was proposed [Fig 1.4 B] [46]. In this model, the fusion pore lines up with lipids and proteins, such that the hydrophilic lipid head groups would face the interior of the pore, thus providing a means for the cation molecules to diffuse. Although, the steps leading to such a fusion pore structure are unclear.

Unlike the previous models, a purely lipidic pore is an alternative model that excludes the participation of the SNARE proteins. In this model, the two membranes initially in apposition, create a stable link between the outer leaflets. As the lipid membranes expand, the structure transits to a hemifusion state, and

the formation of a fluidic connection between two membranes follows [Fig 1.4 C]. In SNAREs dependent exocytosis, this model has faced conceptual limitation as reviewed in [46, 21].

In conclusion, mutating the SNARE proteins and using the amperometry technique has offered an unprecedented means to link the SNARE complex and the fusion pore. However, there is still not enough consistent data to discriminate between the different fusion pore models.

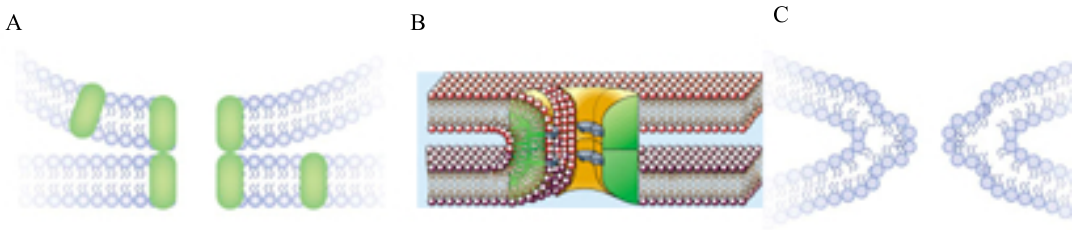

Figure 1.4: (A) The proteinous pore model proposes an initial pore composed solely of proteins. (B) The proteolipidic model suggests that both lipids and proteins constitute the fusion pore. (C) In the lipidic pore model, the lipids form the pore (Figures modified from [2, 16]).

1.4 Current contribution

In this thesis, the role of the transmembrane domain of synaptobrevin in exocytosis will be studied. This work was motivated by the fact that synaptobrevin is essential for SNARE dependent exocytosis, and it is the only protein of the SNARE complex which is linked to the vesicle. Although the function of its SNARE motif has been determined, the role of its transmembrane domain has only been speculative. It has been proposed for instance that the binding of the

C-terminal domain of the SNARE motifs releases energy which is transfered to the membranes by means of the transmembrane domains of synaptobrevin and syntaxin [36] and, it has also been suggested that the transmembrane domain of synaptobrevin lines the fusion pore [15]. However, there is no experimental evidence backing up these claims. Here, by mutating the transmembrane domain of synaptobrevin and by using caged-calcium flash photolysis, amperometry, TIRF microscopy, and fluorescence techniques, we attempt to elucidate the function of synaptobrevin transmembrane domain. This thesis is divided in chapters, where each chapter discuss different regions of the transmembrane domain and its potential role.

Chapter II will give a brief overview of the caged-calcium flash photolysis technique. Chapter III focuses on the C-terminal end of synaptobrevin-2 and its function for exocytosis. Chapter IV explores the effect of adding a GFP tag at the N- or C-terminal end synaptobrevin on exocytosis in chromaffin cells. Chapter V addresses the question as to whether the transmembrane domain of synaptobrevin line the fusion pore. Chapter VI explores the topic of the transmembrane dimerization and will discuss its potential function in exocytosis. Finally in the conclusion, all the results will be summarized and future work will be discussed.

BIBLIOGRAPHY

[1] A. Albillos, G. Dernick, H. Horstmann, W. Almers, G. Alvarez de Toledo, and M. Lindau. The exocytotic event in chromaffin cells revealed by patch amperometry. *Nature*, 389:509–512, 1997.

[2] W. Almers. Fusion needs more than SNAREs. *Nature*, 409(6820):567–8, 2001.

[3] M. Borisovska, Y. Zhao, Y. Tsytsyura, N. Glyvuk, S. Takamori, U. Matti, J. Rettig, T. Südhof, and D. Bruns. v-snares control exocytosis of vesicles from priming to fusion. *Embo. J.*, 24(12):2114–26, 2005.

[4] Nils Brose. For better or for worse: complexins regulate SNARE function and vesicle fusion. *Traffic*, 9(9):1403–13, 2008.

[5] Edwin R Chapman. How does synaptotagmin trigger neurotransmitter release? *Annu Rev Biochem*, 77(NIL):615–41, 2008.

[6] R H Chow, L von Ruden, and E Neher. Delay in vesicle fusion revealed by electrochemical monitoring of single secretory events in adrenal chromaffin cells. *Nature*, 356(6364):60–3, 1992.

[7] Ferenc Deak, Ok-Ho Shin, Ege T Kavalali, and Thomas C Südhof. Structural determinants of synaptobrevin 2 function in synaptic vesicle fusion. *J Neurosci*, 26(25):6668–76, 2006.

[8] Q. Fang, K. Berberian, L. W. Gong, I. Hafez, J. B. Sø rensen, and M. Lindau. The role of the c terminus of the snare protein snap-25 in fusion pore opening and a model for fusion pore mechanics. *Proc Natl Acad Sci U S A*, 105(40):15388–92, 2008.

[9] D Fasshauer, R B Sutton, A T Brunger, and R Jahn. Conserved structural features of the synaptic fusion complex: SNARE proteins reclassified as Q- and R-SNAREs. *Proc Natl Acad Sci U S A*, 95(26):15781–6, 1998.

[10] Dirk Fasshauer, Wolfram Antonin, Vinod Subramaniam, and Reinhard Jahn. SNARE assembly and disassembly exhibit a pronounced hysteresis. *Nat Struct Biol*, 9(2):144–51, 2002.

[11] Claudio G Giraudo, Alejandro Garcia-Diaz, William S Eng, Ai Yamamoto, Thomas J Melia, and James E Rothman. Distinct domains of complexins bind SNARE complexes and clamp fusion in vitro. *J Biol Chem*, 283(30):21211–9, 2008.

[12] Liang-Wei Gong, Guillermo Alvarez de Toledo, and Manfred Lindau. Exocytotic catecholamine release is not associated with cation flux through channels in the vesicle membrane but Na+ influx through the fusion pore. *Nat Cell Biol*, 9(8):915–22, 2007.

[13] Ismail Hafez, Kassandra Kisler, Khajak Berberian, Gregor Dernick, Vicente Valero, Ming G Yong, Harold G Craighead, and Manfred Lindau. Electrochemical imaging of fusion pore openings by electrochemical detector arrays. *Proc Natl Acad Sci U S A*, 102(39):13879–84, 2005.

[14] X. Han, C. T. Wang, J. Bai, E. R. Chapman, and M. B. Jackson. Transmembrane segments of syntaxin line the fusion pore of ca2+-triggered exocytosis. *Science*, 304(5668):289–92, 2004.

[15] Xue Han and Meyer B Jackson. Structural transitions in the synaptic SNARE complex during Ca2+-triggered exocytosis. *J Cell Biol*, 172(2):281–93, 2006.

[16] Meyer B Jackson and Edwin R Chapman. Fusion pores and fusion machines in Ca2+-triggered exocytosis. *Annu Rev Biophys Biomol Struct*, 35(NIL):135–60, 2006.

[17] R Jahn, P I Hanson, H Otto, and G Ahnert-Hilger. Botulinum and tetanus neurotoxins: emerging tools for the study of membrane fusion. *Cold Spring Harb Symp Quant Biol*, 60(NIL):329–35, 1995.

[18] Yonathan Kozlovsky and Michael M Kozlov. Stalk model of membrane fusion: solution of energy crisis. *Biophys J*, 82(2):882–95, 2002.

[19] Feng Li, Frederic Pincet, Eric Perez, William S Eng, Thomas J Melia, James E Rothman, and David Tareste. Energetics and dynamics of SNAREpin folding across lipid bilayers. *Nat Struct Mol Biol*, 14(10):890–6, 2007.

[20] R C Lin and R H Scheller. Structural organization of the synaptic exocytosis core complex. *Neuron*, 19(5):1087–94, 1997.

[21] M. Lindau and W. Almers. Structure and function of fusion pores in exocytosis and ectoplasmic membrane fusion. *Current Opinion in Cell Biology*, 7:509–517, 1995.

[22] Sascha Martens, Michael M Kozlov, and Harvey T McMahon. How synaptotagmin promotes membrane fusion. *Science*, 316(5828):1205–8, 2007.

[23] C. Montecucco and G. Schiavo. Mechanism of action of tetanus and botulinum neurotoxins. *Mol. Microbiol.*, 13:1–8, 1994.

[24] Eugene V Mosharov and David Sulzer. Analysis of exocytotic events recorded by amperometry. *Nat Methods*, 2(9):651–8, 2005.

[25] A. V. Pobbati, A. , and D. Fasshauer. N- to c-terminal snare complex assembly promotes rapid membrane fusion. *Science*, 313(5787):673–6, 2006.

[26] Christoph Reese and Andreas Mayer. Transition from hemifusion to pore opening is rate limiting for vacuole membrane fusion. *J Cell Biol*, 171(6):981–90, 2005.

[27] G. Schiavo, F. Benfenati, B. Poulain, O. Rossetta, P. Polverino de Laureto, B.R. DasGupta, and C. Montecucco. Tetanus and botulinum.b neurotoxins block neurotransmitter release by proteolytic cleavage of synaptobrevin. *Nature*, 359:832–834, 1992.

[28] G. Schiavo, A. Santucci, B.R. Dasgupta, P.P. Mehta, J. Jontes, F. Benfenati, M.C Wilson, and C Montecucco. Botulinum neurotoxins serotypes a and e cleave snap-25 at distinct cooh-terminal peptide bonds. *FEBS Letters*, 335:99–103, 1993.

[29] Susanne Schoch, F Deak, A Konigstorfer, M Mozhayeva, Y Sara, T C Südhof, and E T Kavalali. SNARE function analyzed in synaptobrevin/VAMP knockout mice. *Science*, 294(5544):1117–22, 2001.

[30] Tabrez J Siddiqui, Olga Vites, Alexander Stein, Rainer Heintzmann, Reinhard Jahn, and Dirk Fasshauer. Determinants of synaptobrevin regulation in membranes. *Mol Biol Cell*, 18(6):2037–46, 2007.

[31] T. Söllner, S. Whiteheart, M. Brunner, H. Erdjument-Bromage, M. Geromanos, P. Tempst, and J.E. Rothman. Snap receptors implicated in vesicle targeting and fusion. *Nature (London)*, 362:318–323, 1993.

[32] J. B. Sørensen, R. Fernandez-Chacon, T. C. Südhof, and E. Neher. Examin-

ing synaptotagmin 1 function in dense core vesicle exocytosis under direct control of ca2+. *J Gen Physiol*, 122(3):265–76, 2003.

[33] J. B. Sørensen, K. Wiederhold, E. M. Muller, I. Milosevic, G. Nagy, B. L. de Groot, H. Grubmuller, and D. Fasshauer. Sequential n- to c-terminal snare complex assembly drives priming and fusion of secretory vesicles. *Embo J*, 25(5):955–66, 2006.

[34] Jakob B. Sørensen. Formation, stabilisation and fusion of the readily releasable pool of secretory vesicles. *Pflugers Arch*, 448(4):347–62, 2004.

[35] Alexander Stein, Anand Radhakrishnan, Dietmar Riedel, Dirk Fasshauer, and Reinhard Jahn. Synaptotagmin activates membrane fusion through a Ca2+-dependent trans interaction with phospholipids. *Nat Struct Mol Biol*, 14(10):904–11, 2007.

[36] Alexander Stein, Gert Weber, Markus C Wahl, and Reinhard Jahn. Helical extension of the neuronal SNARE complex into the membrane. *Nature*, 460(7254):525–8, 2009.

[37] Thomas C Südhof and James E Rothman. Membrane fusion: grappling with SNARE and SM proteins. *Science*, 323(5913):474–7, 2009.

[38] R.B. Sutton, D. Fasshauer, R. Jahn, and A.T. Brunger. Crystal structure of a snare complex involved in synaptic exocytosis at 2.4 resolution. *Nature*, 395:347–353, 1998.

[39] Ward C Tucker, Thomas Weber, and Edwin R Chapman. Reconstitution of Ca2+-regulated membrane fusion by synaptotagmin and SNAREs. *Science*, 304(5669):435–8, 2004.

[40] G. van den Bogaart, M. G. Holt, G. Bunt, D. Riedel, F. S. Wouters, and R. Jahn. One SNARE complex is sufficient for membrane fusion. *Nat. Struct. Mol. Biol.*, 17(3):358–64, 2010.

[41] Alexander M Walter, Katrin Wiederhold, Dieter Bruns, Dirk Fasshauer, and Jakob B Sørensen. Synaptobrevin N-terminally bound to syntaxin-SNAP-25 defines the primed vesicle state in regulated exocytosis. *J Cell Biol*, 188(3):401–13, 2010.

[42] Philip Washbourne, Peter M Thompson, Mario Carta, Edmar T Costa, James R Mathews, Guillermina Lopez-Bendito, Zoltan Molnar, Mark W Becher, C Fernando Valenzuela, L Donald Partridge, and Michael C Wilson. Genetic ablation of the t-SNARE SNAP-25 distinguishes mechanisms of neuroexocytosis. *Nat Neurosci*, 5(1):19–26, 2002.

[43] T. Weber, B.V. Zemelman, J.A. McNew, B. Westermann, M. Gmachl, F. Parlati, T.H. Söllner, and J.E. Rothman. Snarepins: minimal machinery for membrane fusion. *Cell*, 92:759–772, 1998.

[44] R.M. Wightman, J.A. Jankowski, R.T. Kennedy, D.T. Kawagoe, T.J. Schroeder, D.J. Leszczyszyn, J.A. Near, E.J. Diliberto jr., and O.H. Viveros. Temporally resolved catecholamine spikes correspond to single vesicle release from individual chromaffin cells. *Proceedings of the National Academy of Sciences of the United States of America*, 88:10754–10758, 1991.

[45] Tae-Young Yoon, Xiaobing Lu, Jiajie Diao, Soo-Min Lee, Taekjip Ha, and Yeon-Kyun Shin. Complexin and Ca2+ stimulate SNARE-mediated membrane fusion. *Nat Struct Mol Biol*, 15(7):707–13, 2008.

[46] J. Zimmerberg, M. Curran, and F.S. Cohen. A lipid/protein complex hy-

pothesis for exocytotic fusion pore formation. *Annals of the New York Academy of Sciences*, 635:307–317, 1991.

CHAPTER 2

EXPERIMENTAL PROCEDURES

2.1 Abstract

The influx of calcium ions is needed to trigger the immediate fusion of vesicles with the plasma membrane, thus the instantaneous release of neurotransmitters. In recent years, the caged-calcium flash photolysis technique has been developed. It provides the advantage that calcium molecules can rapidly and homogeneously be released into the cell, while the fusion of vesicles with the plasma membrane is monitored via the change of the cell membrane capacitance.

2.2 Introduction

Calcium ions play an important role during exocytosis in neurons and in neuroendocrine cells. Physiologically, exocytosis in neurons and in chromaffin cells is activated by action potentials. The action potential opens voltage-gated Ca^{2+} channels, Ca^{2+} ions flow into the cells elevating the free intracellular Ca^{2+} concentration and stimulating the fusion of secretory vesicles with the plasma membrane. In whole-cell patch-clamp experiment, in voltage clamp mode, depolarizing pulses can be given to activate Ca^{2+} current and to stimulate exocytosis [10, 9]. The disadvantage of this method is that the free intracellular Ca^{2+} concentration is not homogeneous throughout the cell. When the Ca^{2+} channels open, the Ca^{2+} concentration near the channels and near the plasma membrane tend to be higher than the Ca^{2+} concentration deeper in the cell. Thus, in response to depolarization, a Ca^{2+} concentration gradient occurs inside the cell. To overcome this limitation, the caged-calcium flash photolysis was developed

[14, 8, 11, 15, 16, 13]. The main advantage of this technique is that, exocytosis can be stimulated with a known calcium concentration that is homogeneous throughout the cell, while the fusion of vesicles with the plasma membrane is being monitored.

2.3 Whole-cell capacitance measurement

The whole-cell patch-clamp configuration provides a means to dialyze the interior of the cell with a pipette solution, while also monitoring the entire cell's electrical properties. The whole-cell configuration is typically obtained by using a glass micro pipette with a diameter of 1-3 μm. The pipette tip is coated with wax, and fire polished for smoothness as well as noise and stray capacitance reduction. The pipette is used to make contact with the cell surface. Upon touching the cell membrane, a small suction is applied such that part of the membrane is sucked inside the micropipette tip forming an omega shape. For a good seal, the resistance between the pipette and the cell membrane should be on the order of GΩ. To have access to the interior of the cell, the patch is broken with a brief suction pulse (whole-cell configuration).

The cell membrane is made-up of a lipid bilayer which separates two conductive media of different potentials. Therefore, it can be modeled as a parallel plate capacitor. Fig. 2.1 shows the minimal equivalent circuit of the whole-cell patch clamp configuration. The elements of the equivalent circuits are C_m the cell membrane capacitance, $G_m = 1/R_m$ the conductance of the cell membrane and R_a the access resistance. The smaller R_a the easier the pipette solution can diffuse into the cell. To measure the electrical current that passes through a cell membrane, an Ag|AgCl electrode connects the saline solution of the micropipette to a low noise amplifier, and another electrode is placed in the bath

solution and is connected to ground.

For capacitance measurement, a continuous sine wave of 70 mV peak to peak amplitude and 800 Hz frequency, is added to a -70 mV DC holding membrane potential, and is applied through the Ag|AgCl electrode, to charge or to discharge the cell membrane. The resulting membrane current is fed into a LockIn amplifier [7, 6] which distinguishes the real and the imaginary part of the current based on 90° phase shift.

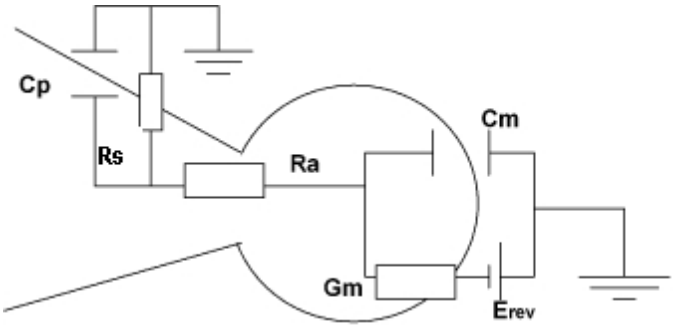

Figure 2.1: Equivalent circuit of a whole-cell patch-clamp configuration. C_m and G_m represent the cell membrane capacitance and conductance. E_{rev} is the reversal potential, and R_a is the access resistance. R_s is the seal resistance which is in the GΩ range and can be neglected. C_p is the pipette capacitance which can be compensated by the Cfast compensation circuit setting of the amplifier.

When the sinusoidal voltage $V(t)$ is applied across the cell membrane, the resulting current I is given by:

$$V(t) = V_0 \cos(\omega t). \tag{2.1}$$

$$I = VY(\omega). \tag{2.2}$$

Here, ω is the frequency and $Y(\omega)$ is the admittance of the equivalent circuit in Fig. 2.1 [3].

$$Y(\omega) = \frac{1 + \omega^2 R_m R_s C_m^2}{R_t(1 + \omega^2 R_s^2 C_m^2)} + \frac{j\omega R_m^2 C_m}{R_t(1 + \omega^2 R_s^2 C_m^2)} \tag{2.3}$$

R_t and R_s are given by:

$$R_t = R_m + R_a \tag{2.4}$$

$$R_s = \frac{R_m R_a}{R_m + R_a} \tag{2.5}$$

The DC holding potential V_{dc} is added to the sinusoidal voltage stimulus, and it is given by:

$$V_{dc} = I_{dc} R_t + E_{rev} \tag{2.6}$$

Where I_{dc} is the DC holding current and E_{rev} is the reversal potential.

From the equations 2.3 and 2.6, the equivalent circuit parameters are calculated [3]:

$$R_a = \frac{A + G_t}{A^2 + B^2 - AG_t} \tag{2.7}$$

$$R_m = \frac{1}{G_t} \frac{(A - G_t)^2 + B^2}{A^2 + B^2 - AG_t} \tag{2.8}$$

$$C_m = \frac{1}{\omega_c B} \frac{(A^2 + B^2 - AG_t)^2}{(A - G_t) + B^2} \tag{2.9}$$

Where A and B are:

$$A = \frac{1 + \omega^2 R_m R_s C_m^2}{R_t(1 + \omega^2 R_s^2 C_m^2)} \tag{2.10}$$

$$B = \frac{j\omega R_m^2 C_m}{R_t(1 + \omega^2 R_s^2 C_m^2)} \tag{2.11}$$

2.4 Calcium Flash Photolysis

Once the access to the interior of the cell is gained at whole-cell patch-clamp configuration, calcium ions bound to the photolabile o-nitrophenyl-EGTA (NP-EGTA) mixed in solution with two calcium dyes Fura-4F and Mag-fura-2 is loaded into the cell through a patch pipette. While Fura-4F has a high affinity for calcium ($K_d \sim 0.145\,\mu$M), Mag-fura-2 has a low affinity ($K_d \sim 25\,\mu$M) for calcium. These two dyes are used in combination to assess calcium concentrations ranging from ~50 nM to ~100 μM.

Calcium ions bound to the chelator NP-EGTA are inactive and unavailable for the cell to use [2, 5] [Fig. 2.2]. The chelator NP-EGTA is chosen because its K_d for calcium is ~80 nM, and upon the exposure of the complex NP-EGTA-calcium to UV light (350 nm), the NP-EGTA breaks down into products with reduced affinity for calcium ($K_d \sim 1$ mM). When a cell loaded with NP-EGTA-calcium complex is irradiated with UV light pulses, the calcium is liberated and its concentration increases throughout the cell, including at its site of action. This provides the advantage that the time of activation of exocytosis is fast and the time course of vesicle fusion with the plasma membrane can be resolved on a millisecond time scale. However, NP-EGTA should be used at concentration where it is saturated with calcium to avoid that the newly released calcium concentration bind back to the chelator.

2.5 Equipments

Whole-cell capacitance measurements were performed with an EPC 9 or EPC 10 amplifier (HEKA) using the internal LockIn detection software. The applied stimulus is a sine wave of 70 mV peak to peak amplitude added to a -70 mV holding membrane potential. The xenon flash lamp is one of the main com-

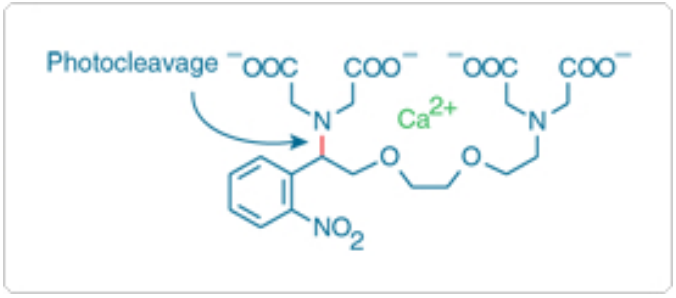

Figure 2.2: Calcium molecule bounds to NP-EGTA (Invitrogen).

ponents of the caged-calcium flash set-up [Fig.2.3], it produces a brief pulse of about 1 ms in the range of 250 to 1500 nm. The UV range is used to uncage the calcium ion from the NP-EGTA-calcium complex. A two-port condenser is mounted to an inverted light microscope in order to couple the lights from the flash lamp and the monochromator. The emitted photons are captured using a photomultiplier, and a computer is used to store and process data.

Microscope: The *Zeiss Axiovert 135* (Zeiss) inverted light microscope with a 40X NA 0.75 (Zeiss) objective is equipped with a photomultiplier and a camera. The photomultiplier is used to collect fluorescence emission from the cell and the camera is used to visually place the cells in the field of illumination.

A *two-port condenser*, type photometry (TILL Photonics GmbH, Germany) is attached to the microscope to merge lights from the flash lamp and the fluorescent excitation into the light path of the microscope. This condenser is equipped with a quartz beam splitter that transmits 92% of the flash lamp light and 8% of the fluorescence excitation light. The two-port condenser is also used to adjust the field stop and to restrict the illuminated area around the cell diameter.

Fluorescence excitation: *The monochromator* (Polychrome II, TILL Photonics GmbH, Germany) is connected to the microscope using a light guide which is inserted into the monochromator port of the two-port condenser. The UV light from

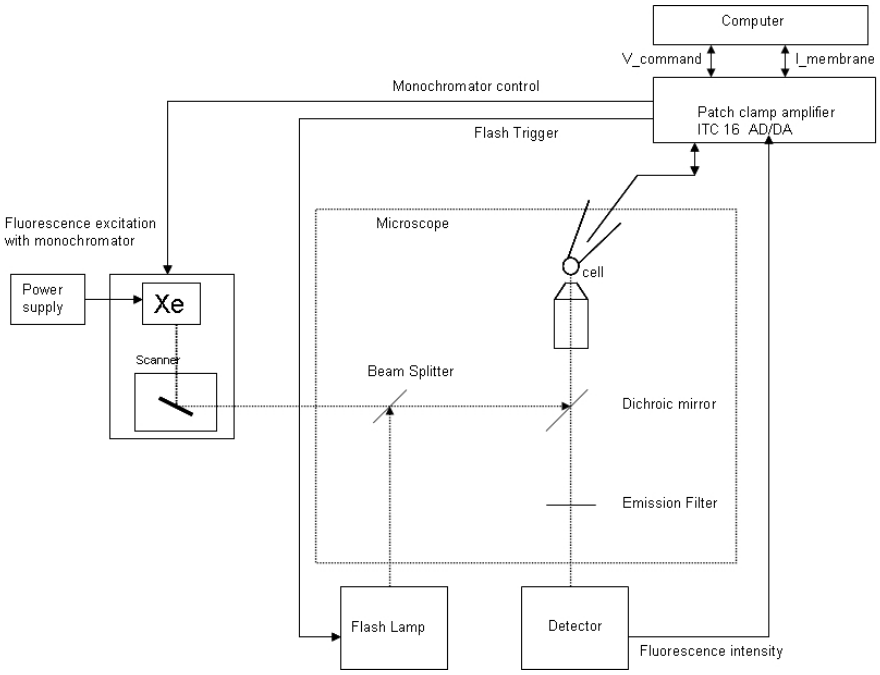

Figure 2.3: The EPC 9 amplifier is connected to the computer and is controlled by the patchmaster soltware. The voltage stimulus is applied to the cell through a pipette electrode. The monochromator and the flash lamp is controlled by the computer. 8% light from the monochromator and 92% light from the flash are coupled into the light path of the microscope via a beam splitter. The microscope is equiped with a dicroid mirror (415 - 570 nm) and an emission filter (510 nm/84 nm). The emission light from the fluorescent dyes is collected using a dectector (photomultiplier) which is connected to the amplifier.

the monochromator is used to excite the calcium indicator dyes by alternating wavelengths between 350 nm and 380 nm at 20 s interval (see calcium measurement). For accurate measurements, the monochromator is re-calibrated every time the lamp is exchanged. This is done following the manufacture instruction, and while wearing a protective UV eye glasses.

A xenon flash lamp (Gert Rapp Optoelektronik, Hamburg, Germany) is connected to the second input on the two-port condenser. The lamp produced a brief pulse of about 1 ms in the UV range 300-400 nm, in order to uncage the calcium from

the NP-EGTA. The intensity of the flash lamp is optimized for the uncaging of calcium concentrations ranging from ~25-30 μM.The light intensity of the flash lamp can be controlled by placing a neutral density filter in the illumination light path of the flash lamp. Nevertheless, the light intensity should be sufficiently high to uncage Ca^{2+} since the flash intensity determine the size of $[Ca^{2+}]_i$. While using the UV flash, caution must be taken to limit the production of free radicals resulting from the photodamage of the NP-EGTA, because they could interfere with physiological function of the cell.

Fluorescence detection: *A photomultiplier tube* is used for the detection of photons emitted from the cell as a result of the excitation of the calcium dyes.

Patch-clamp amplifier: The EPC 9 (Heka Elektronik, Lambrecht, Germany) amplifier is used to acquire whole-cell patch membrane current. The monochromator and the flash lamp are connected with a BNC cable to the D/A outputs of the EPC 9. The EPC 9 *head stage*, is connected to the glass pipette via a silver wire electrode. EPC 9 has the advantage that it has an integrated ITC-16 AD/DA which can be controlled by the *PatchMaster* (or *pulse*) software. The ITC-16 in the EPC 9 also acquires pipette current, performs C_m determination and records fluorescence intensity.

Amperometry amplifier (optional): An EPC 7 (HEKA) is used as the second amplifier to acquire the amperometric current. The amplifier's built in 3 kHz filter is used during the acquisition of the data. The *head stage* of the amplifier is connected to a carbon fiber electrode and shares the same ground with the EPC 9 *head stage*. A 7 volt constant voltage providing a holding potential of +700 mV is connected to the stimulus input of the ECP 7. A carbon fiber held at 700 mV can oxidize the catecholamine molecules released by chromaffin cells.

Softwares: *PatchMaster* (Heka Elektronik, Lambrecht, Germany) is a LockIn software used to control the EPC 9 or EPC 10 amplifier. The PatchMaster software is configured to continuously acquire two physical traces, the current trace of the cell and the emission intensity of the fluorescent dyes. The LockIn mode is set to "Sine+DC" and is used to extract the capacitance and the conductance values.

IgorPro software (WaveMetrics, Inc., Oregon) is used for offline data analysis.

2.6 Calibration

To calibrate the $[Ca^{2+}]$ measurement , multiple solutions with various concentrations of calcium from basal to saturation is used (Table 2.6). The calibration is achieved by infusing into a cell, solutions containing a known free calcium concentration buffered with 1,2-bis(2-aminophenoxy)ethane-N,N,N',N'-tetraacetate (BAPTA, $K_d \sim 150$ nM) at low calcium concentration and 1,3-diaminopropane-2-ol-N, N'-tetraacetate (DPTA ~81 μM) at high calcium concentration. In addition to calcium and buffers, the solutions also contained two fluorescent dyes Fura-4F and Mag-fura-2. Upon binding the calcium, the dyes

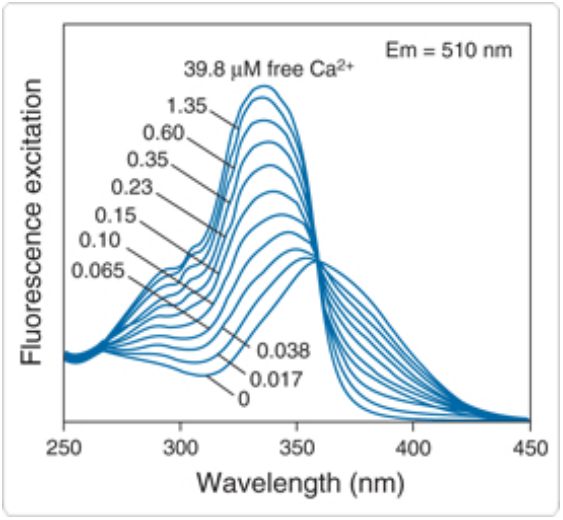

Figure 2.4: Fura-2 calcium binding spectrum (Invitrogen).

exhibit an absorption peak shift from 330 nm to 360 nm [Fig. 2.4] (Invitrogen), with little shift on the emission at 510 nm. This characteristic enables the application of a ratiometric analysis, which is done by alternating excitation of the dyes at 350 nm and 380 nm respectively while collecting the fluorescence emission at 510 nm. The ratiometric analysis is preferred to the absolute fluorescence analysis, because it eliminates artifacts from photobleaching, the slow diffusion of the solution in cells and problems due to the optical path length and the variation of illumination intensity.

A stock of the buffer solution containing 100 mM Cs-glutamate and 32 mM Hepes, titrated with CsOH to pH 7.2 was prepared separately. The buffer was added to individual solutions in Table 2.6 until the total osmolarity of the solution reached ~ 290 mOsM. To determine the free calcium concentration in solutions a custom-written IgorPro procedure was used, taking into account the calcium binding affinity for DPTA or BAPTA, for fluorescent dyes, ATP and nitrophenyl-EGTA. The computer programs MaxChelator which is freely available can also be used for the same purpose.

Table 2.1: The calibration solutions are supplemented with ascorbic acid because it protects the fura dyes against photodamage caused by UV light. Therefore, unlike previously described calibration procedure [15], the postflash calibration is omitted [4].

Solution	1	2	3	4	5	6	7	8	9
Mg-ATP(mM)	2	2	2	2	2	2	2	2	2
Na-GTP(mM)	0.3	0.3	0.3	0.3	0.3	0.3	0.3	0.3	0.3
Fura-4F (mM)	0.4	0.4	0.4	0.4	0.4	0.4	0.4	0.4	0.4
Mag-fura-2(mM)	0.4	0.4	0.4	0.4	0.4	0.4	0.4	0.4	0.4
Bapta (mM)	20	8	4.5	0.9			0.4	0	0
Ca-Bapta(mM)		12	15.5	19.1			0.4	0	0
Dpta (mM)		0	0	0	38.1	34.5	30.5	22.5	0
Ca-DPTA (mM)		0	0	0	1.9	5.5	9.5	17.5	0
ascorbic acid (mM)	1	1	1	1	1	1	1	1	1
$CaCl_2$ (mM)									12.5
$CaCl_{free}$ (μM)	0	0.331	0.741	3.356	3.913	11.57	23.736	72.769	12.5

2.7 Ratiometric measurements

2.7.1 Cell preparation

The chromaffin cells are isolated by enzymatic reaction from the adrenal gland as previously described [1, 11]. They are then plated onto coverslips and cultured for 2 to 4 days. During the experiment, the cells bathed in solution composed of (in mM): 145 NaCl, 1 $MgCl_2$, 2.8 KCl, 2 $CaCl_2$ and 10 HEPES. The pH and osmolarity are adjusted to 7.2 with NaOH and to 310 mOSM with D-glucose whenever necessary.

2.7.2 Calibration procedure

The fluorescence ratio signal is calibrated by infusing the calibration solutions into chromaffin cells at whole-cell patch clamp configuration through the patch pipette [15]. A cell loaded with the calibration solution is illuminated by alternating the monochromator light between 350 nm and 380 nm every 20 ms. The photomultiplier is used to collect photons emitted at 510 nm/84 nm by the fura dyes, and the ratiometric values (380/350) are calculated and plotted versus the calcium concentrations [Fig. 2.5].

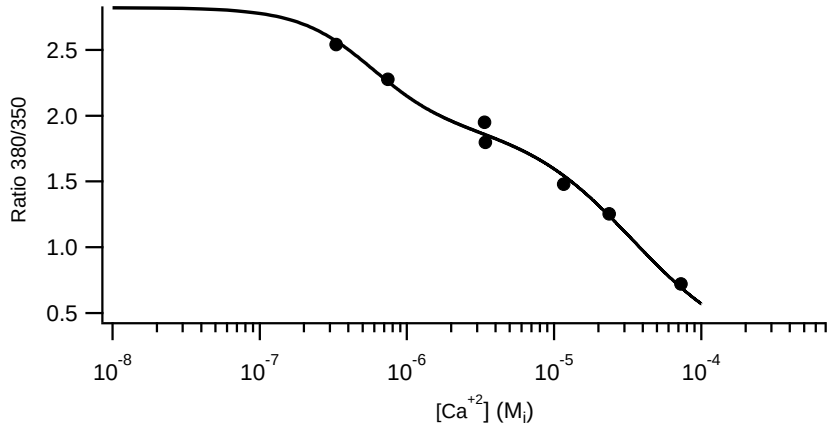

Figure 2.5: Each data point consisted of at least three measurements. The points are best fitted (solid line) with $R = R_0 - R_1 \frac{[Ca^{2+}]}{K_1+[Ca^{2+}]} + R_2 \frac{[Ca^{2+}]}{K_2+[Ca^{2+}]}$, which takes into account the binding of calcium ions to the two calcium dyes. The fit is used to convert the ratio R at 380/350 nm of the fluorescent signal into the $[Ca^{2+}]_i$ [15].

For given fluorescence ratio values, the free calcium concentration is calculated. For one fluorescence dye, the free calcium concentration is given by:

$$[Ca^{2+}] = K_{eff} \frac{(R - R_{min})}{R_{max} - R} \tag{2.12}$$

Where R_{min} is the fluorescence ratio obtained for the lowest free calcium, and R_{max} is the ratio obtained for the highest free calcium in solution. R_{min}, R_{max} and

K_{eff} parameters are obtained experimentally. Rearranging equation 2.12 as follows:

$$R_{max} - R = \frac{K_{eff}}{[Ca^{2+}]}(R - R_{min}) \tag{2.13}$$

$$R_{max} - R_{min}\frac{K_{eff}}{[Ca^{2+}]} = R\frac{K_{eff} + [Ca^{2+}]}{[Ca^{2+}]} \tag{2.14}$$

$$R = R_{min}\frac{K_{eff}}{K_{eff} + [Ca^{2+}]} + R_{max}\frac{[Ca^{2+}]}{K_{eff} + [Ca^{2+}]} \tag{2.15}$$

$$R = R_{min} - (R_{min} - R_{max})\frac{[Ca^{2+}]}{K_{eff} + [Ca^{2+}]} \tag{2.16}$$

$$R = R_{min} - (R_{min} - R_{max})\frac{[Ca^{2+}]}{K_{eff} + [Ca^{2+}]} \tag{2.17}$$

$$R = R_0 - R_1\frac{[Ca^{2+}]}{K_1 + [Ca^{2+}]} \tag{2.18}$$

Where $R_0 = R_{min}$ and $R_1 = R_{min} - R_{max}$ and $K_1 = K_{eff}$. This provides a convenient parametrization of the fluorescence ratio R as a function of the free $[Ca^{2+}]_i$.
When two fluorescence dyes are combined, this equation 2.18 becomes:

$$R = R_0 - R_1\frac{[Ca^{2+}]}{K_1 + [Ca^{2+}]} - R_2\frac{[Ca^{2+}]}{K_2 + [Ca^{2+}]} \tag{2.19}$$

where R_0 reflects the ratio R at $[Ca^{2+}]_i = 0$ and $R_0 - R_1 - R_2$ is the ratio at the highest value of $[Ca^{2+}]_i$. Fitting the parameters R0, R1, R2, K1, and K2 of equation 2.19 to the calibration data points as shown in Fig. 2.5 provides the calibration to determine $[Ca^{2+}]_i$ from the measured fluorescence ratio R.

2.8 Experimental procedures

To study exocytosis in chromaffin cells, cells are infused at whole-cell configuration with solution containing (in mM): 0.4 fura-4F, 0.4 Mag-fura-2 (Invitrogen),

5 Nitrophenyl-EGTA (NP-EGTA, Synaptic Systems), 100 Cs-glutamate, 0.3 Na-GTP, 2 Mg-ATP, 4 $CaCl_2$, 1 ascorbic acid and 32 HEPES, pH 7.2. Intracellular calcium measurements are performed by alternating the fura-4F/Mag-fura-2 excitation wavelength between 350 nm and 380 nm [Fig.2.6] [15]. Photolysis of NP-EGTA is achieved by a UV flash [Fig.2.6, arrow], calcium molecules are freed from the calcium chelator and this results in an increase of calcium inside the cell. The increase of $[Ca^{2+}]$ induced the increase of the cell membrane capacitance [Fig.2.6, brown line], indicating the fusion of vesicles with the plasma membrane.

The analysis of the capacitance trace [Fig.2.7] can yield information about the kinetics of the exocytotic process. The steep increase or the burst phase of the capacitance trace reflects the fusion of vesicles at the surface of the plasma membrane ready to fuse prior to the elevation of calcium. This phase can be fitted with the sum of two exponentials functions and has been associated with the fusion of vesicles of the readily releasable pool (RRP) and the slowly releasable pool (SRP) [15]. The sustained phase, which is the region of the capacitance trace which increases with a time constant of seconds, reflects the fusion of vesicles which slowly refill the ready releasable pool. These vesicles fuse immediately as long as the calcium concentration in the cell remained high. For a detailed review of the RRP and the SRP see [12].

2.9 Conclusion

Caged-calcium Flash Photolysis technique has become a very useful tool to study the kinetic of fusion in exocytosis. In all subsequent chapters this was

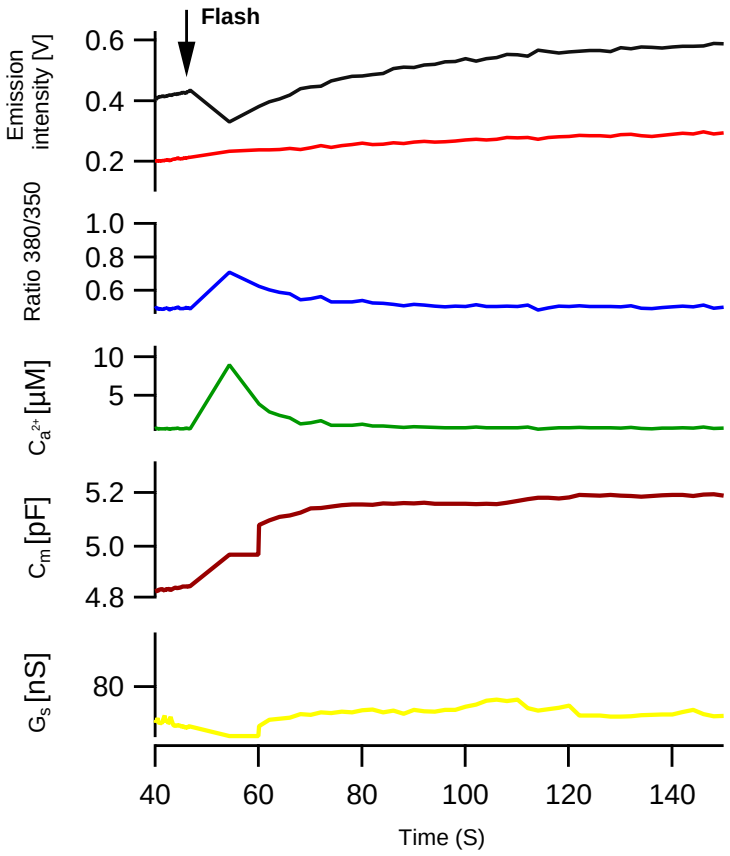

Figure 2.6: Sample calcium and capacitance measurements. Calcium dyes excited at 350 (black) and 380 (red). Calculated ratiometric (380/350) values (blue), and corresponding calcium changed (green). Change in cell membrane capacitance (brown) and the series conductance (yellow).

the main approach used to study the role of the transmembrane domain of the SNARE protein synaptobrevin-2 during vesicle fusion.

2.10 Acknowledgements

I have learned this technique from Prof. Jakob B. Sørensen with the assistance of Alexander Walter at Max Planck Institute for Biophysical Chemistry, Göttingen. With the help of Prof. Manfred Lindau, I have implemented this technique here

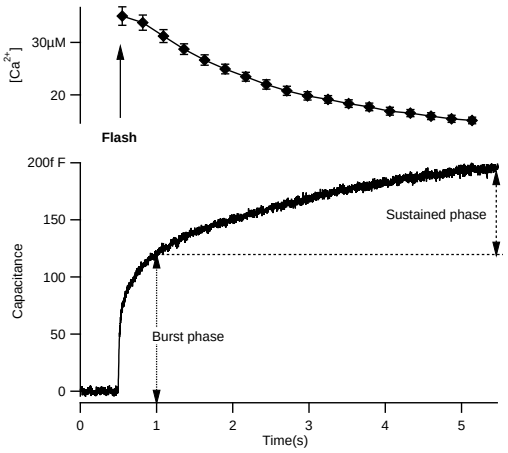

Figure 2.7: Example of simultaneous calcium and cell membrane capacitance measurement at whole-cell patch-clamp configuration from a chromaffin cell.

at Cornell in Prof. Lindau's lab. This work has been supported by the National Institutes of Health grants R01NS38200, R01GM085808, T32GM008267, the Nanobiotechnology Center (a National Science Foundation Science and Technology Center, agreement No. ECS-9876771).

BIBLIOGRAPHY

[1] M. Borisovska, Y. Zhao, Y. Tsytsyura, N. Glyvuk, S. Takamori, U. Matti, J. Rettig, T. Südhof, and D. Bruns. v-snares control exocytosis of vesicles from priming to fusion. *Embo. J.*, 24(12):2114–26, 2005.

[2] G C Ellis-Davies and J H Kaplan. Nitrophenyl-EGTA, a photolabile chelator that selectively binds Ca2+ with high affinity and releases it rapidly upon photolysis. *Proc Natl Acad Sci U S A*, 91(1):187–91, 1994.

[3] Kevin D. Gillis. Techniques of membrane capacitance measurements. In B. Sakmann and E. Neher, editors, *Single-Channel Recording*. Plenum Press, 1995.

[4] C Heinemann, R H Chow, E Neher, and R S Zucker. Kinetics of the secretory response in bovine chromaffin cells following flash photolysis of caged Ca2+. *Biophys J*, 67(6):2546–57, 1994.

[5] J H Kaplan and G C Ellis-Davies. Photolabile chelators for the rapid photorelease of divalent cations. *Proc Natl Acad Sci U S A*, 85(17):6571–5, 1988.

[6] M Lindau and E Neher. Patch-clamp techniques for time-resolved capacitance measurements in single cells. *Pflugers Arch*, 411(2):137–46, 1988.

[7] E Neher and A Marty. Discrete changes of cell membrane capacitance observed under conditions of enhanced secretion in bovine adrenal chromaffin cells. *Proc Natl Acad Sci U S A*, 79(21):6712–6, 1982.

[8] E Neher and R S Zucker. Multiple calcium-dependent processes related to secretion in bovine chromaffin cells. *Neuron*, 10(1):21–30, 1993.

[9] O Nusse and M Lindau. The dynamics of exocytosis in human neutrophils. *J Cell Biol*, 107(6 Pt 1):2117–23, 1988.

[10] O Nüsse and M Lindau. The calcium signal in human neutrophils and its relation to exocytosis investigated by patch-clamp capacitance and Fura-2 measurements. *Cell Calcium*, 14(4):255–69, 1993.

[11] J. B. Sørensen, R. Fernandez-Chacon, T. C. Südhof, and E. Neher. Examining synaptotagmin 1 function in dense core vesicle exocytosis under direct control of ca2+. *J Gen Physiol*, 122(3):265–76, 2003.

[12] Jakob B. Sørensen. Formation, stabilisation and fusion of the readily releasable pool of secretory vesicles. *Pflugers Arch*, 448(4):347–62, 2004.

[13] Jakob B Sørensen, Ulf Matti, Shun-Hui Wei, Ralf B Nehring, Thomas Voets, Uri Ashery, Thomas Binz, Erwin Neher, and Jens Rettig. The SNARE protein SNAP-25 is linked to fast calcium triggering of exocytosis. *Proc Natl Acad Sci U S A*, 99(3):1627–32, 2002.

[14] P Thomas, J G Wong, and W Almers. Millisecond studies of secretion in single rat pituitary cells stimulated by flash photolysis of caged Ca2+. *EMBO J*, 12(1):303–6, 1993.

[15] T Voets. Dissection of three Ca2+-dependent steps leading to secretion in chromaffin cells from mouse adrenal slices. *Neuron*, 28(2):537–45, 2000.

[16] S. Wei, T. Xu, U. Ashery, A. Kollewe, U. Matti, W. Antonin, J. Rettig, and E. Neher. Exocytotic mechanism studied by truncated and zero layer mutants of the c-terminus of snap-25. *Embo J*, 19(6):1279–89, 2000.

CHAPTER 3

ROLE OF THE SYNAPTOBREVIN C-TERMINUS IN FUSION PORE FORMATION

3.1 Abstract

Neurotransmitter release is mediated by the SNARE proteins synaptobrevin II (SybII, also known as VAMP2), syntaxin and SNAP-25 generating a force transfer to the membranes and inducing fusion pore formation. However, the molecular mechanism by which this force leads to opening of a fusion pore remains elusive. Here we show that the ability of SybII to support exocytosis is inhibited by addition of one or two residues to the SybII C-terminus depending on their energy of transfer from water to the membrane interface, following a Boltzmann distribution. These results suggest that following stimulation, the SNARE complex pulls the C-terminus of SybII deeper into the vesicle membrane, with this movement disrupting the vesicular membrane continuity and leading to fusion pore formation. In contrast to current models, the experiments suggest that fusion pore formation begins with molecular rearrangements at the intravesicular membrane leaflet and not between the apposed cytoplasmic leaflets.

Running Title:

Movement of synaptobrevin C-terminus induces fusion

3.2 Introduction

The SNARE proteins [21] mediate release of stored secretory products by exocytosis. In neurosecretion, the t-SNAREs syntaxin and SNAP-25 in the plasma membrane bind the v-SNARE synaptobrevin II (SybII, also known as VAMP2), which is anchored to the vesicle membrane by a single transmembrane domain (TMD) . Upon stimulation, the SNARE complex is thought to zip up more tightly proceeding in a vectorial manner from the N- to the C-terminus, towards the TMD of sybII and syntaxin [5, 18, 23, 29], thereby transferring a force to the membranes [16]. However, the molecular mechanism by which this force leads to opening of the fusion pore has not been determined [19].

Several models have been proposed to explain the mechanism of fusion pore formation. In the lipid-stalk-hemifusion hypothesis, the outer and the inner leaflets of the two membranes merge via formation of a hemifusion intermediate in response to forces exerted by proteins surrounding the fusion site [37]. In an alternative proteinaceous fusion pore model, the fusion pore is lined by the TMD of syntaxin [12] and possibly synaptobrevin [12]. However, it is not immediately evident how the hydrophobic transmembrane domains can line an aqueous fusion pore that allows for ion permeation by electrodiffusion [10]. When the C-terminal SNARE domain interactions are reduced by mutating or deleting the C-terminus of SNAP-25, or when flexible linkers are introduced between the sybII TMD and its SNARE domain, the rate of exocytosis is reduced [6, 7, 13, 30, 35] and the flux of transmitter through the early fusion pore is decreased [9, 13], consistent with a structural change in the fusion pore. In an attempt to interpret these findings, a proteolipidic fusion pore model has been proposed, in which the fusion pore formed by a molecular complex of both lipids and SNARE proteins [9]. However, even this model does not explain

the molecular mechanism by which the N-to C-terminal zipping of the SNARE complex leads to the formation of a fusion pore, a step that must somehow disrupt membrane continuity.

3.3 Results

3.3.1 Addition of polar amino acids to the SybII C-terminus inhibits fusion

To determine a possible role of the SybII TMD in fusion pore formation, SybII constructs were generated in which two charged residues (lysine or glutamate) were added to the C-terminus of SybII. To determine whether these C-terminal mutants localize to secretory vesicles, synaptobrevin constructs were generated that carried a GFP tag at their N-terminus. Wild-type GFP-SybII, GFP-SybII-KK, and GFP-sybII-EE were expressed in mouse chromaffin cells and imaged by Total Internal Reflection Fluorescence (TIRF) microscopy [Fig. 3.3.1A-C]. While a considerable fraction of the SybII constructs is localized in the plasma membrane as expected [32] and generates diffuse fluorescence, punctate fluorescence is clearly visible, indicating vesicular localization.

To determine if the vesicles carrying these constructs are fusion competent, simultaneous TIRF microscopy and recording of catecholamine release from the cell membrane in contact with the coverslip was performed using microfabricated electrochemical detector arrays [11]. This method allows determination of time and location of a fusion event by amperometric recordings with multiple electrodes. It can then be determined if a fusion event is accompanied by loss of a fluorescent granule. Amperometrically detected exocytotic events associated with disappearance of GFP-SybII fluorescence puncta were observed

when the construct carried the unmodified SybII TMD [Fig. 3.3.1 A], indicating that vesicles carrying GFP-sybII are fusion competent. In contrast, no such correlated events were observed for GFP-SybII-KK or GFP-SybII-EE fluorescence puncta, indicating that the modification of the SybII C-terminus by addition of these charged residues renders the vesicles fusion incompetent. However, those cells did show quantal release events [Fig.3.3.1 B,C], presumably from vesicles carrying mainly wild-type sybII with undetectable amounts of GFP-SybII-KK or GFP-SybII-EE. These wild-type SybII granules were presumably generated in the cell before the GFP construct was expressed.

To quantify the inhibition of exocytosis, chromaffin cells overexpressing a sybII construct and identified by GFP fluorescence were stimulated by flash photolysis of caged-calcium (NP-EGTA) [28], and exocytosis was monitored by whole-cell capacitance measurements [14] while the associated transmitter release was monitored by carbon fiber amperometry [33]. The exocytotic response in cells overexpressing wt sybII consists of an exocytotic burst on the millisecond time scale followed by a sustained phase on a time scale of seconds [Fig. 3.3.1 D, black trace], which is indistinguishable from the response of non-infected wild-type chromaffin cells (data not shown). When sybII-EE was expressed in wild-type chromaffin cells and exocytosis stimulated by photorelease of caged calcium [Fig. 3.3.1 D, red trace], the burst amplitude and the sustained phase were moderately reduced by 35% and 27%, respectively. This inhibition provides further evidence that the mutant protein is correctly sorted to secretory vesicles. The exocytotic burst kinetics was unchanged [Fig. 3.3.1E], consistent with the conclusion that the population of vesicles that carry the sybII-EE construct is unable to undergo exocytosis

To eliminate the contribution of wild-type SybII to the exocytotic respsonse, experiments were performed using double knock-out (DKO) embryonic

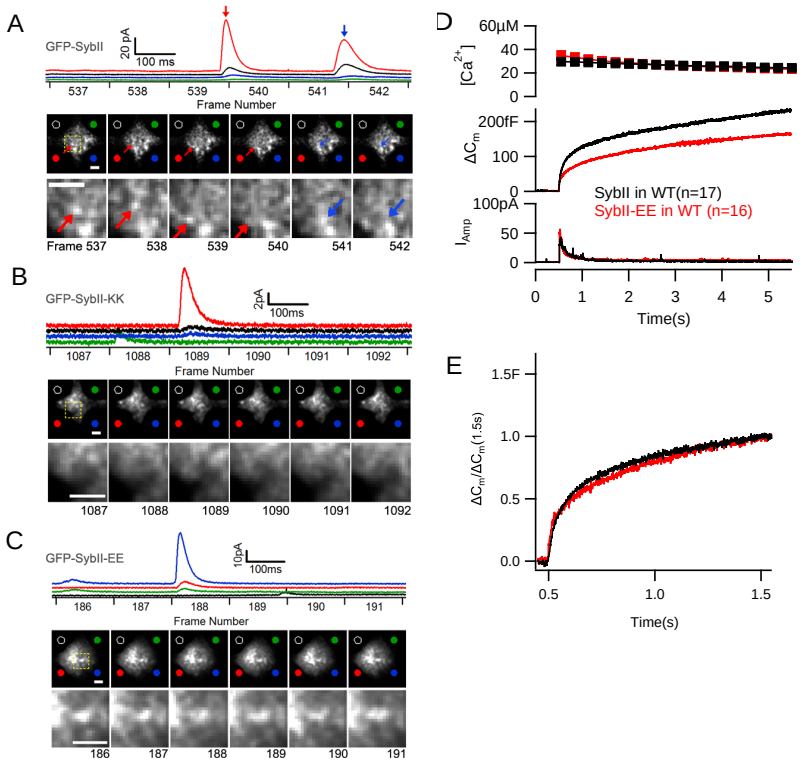

Figure 3.1: Vesicular localization of GFP-SybII, GFP-SybII-KK and GFP-SybII-EE in mouse chromaffin cells. (A-C) Simultaneous ECD array amperometry and TIRF microscopy imaging of wild-type cells expressing GFP-SybII (A), GFP-SybII-KK (B) and GFP-SybII-EE (C). Scale bars are 2 μm. Colors of amperometric traces (top panels) correspond to the respective electrodes as indicated by colored dots in images below. Frame acquisition timing of the image sequences is indicated below the amperometric traces. In a GFP-SybII cell (A), two amperometric events detected by multiple electrodes of the ECD array are associated with loss of fluorescence puncta between frames 539-540 (red arrow) and 541-542 (blue arrow). The area in the yellow rectangle is enlarged in the bottom panel. In a GFP-SybII-KK cell (B) and a GFP-SybII-EE cell (C) amperometric events (top) are not associated with loss of fluorescence puncta in TIRF images (bottom). (D) SybII-EE expression in wild-type cells (n=16) reduces the exocytotic burst amplitude by 35% (P<0.05) and the amplitude of the sustained phase by 27% (p=0.07) compared to cells overexpressing wild-type SybII. (e) Normalization of capacitance increase 0.6 s after the flash shows that SybII-EE overexpression in wild-type cells does not change the exocytotic burst kinetics.

mouse chromaffin cells deficient in SybII and cellubrevin [3, 20, 36]. As in wild-type chromaffin cells, vesicular localization of GFP-SybII, GFP-SybII-KK, and GFP-SybII-EE is clearly evident in DKO embryonic chromaffin cells by TIRF microscopy [Fig. 3.2]. In comparison with [Fig. 3.3.1 A-C], the vesicular localization is seen even more clearly. We attribute this difference to a lower background of SybII in the plasma membrane and/or a lower density of granules in embryonic cells that reduces overlap of fluorescence from adjacent granules and blurred by the microscope point spread function.

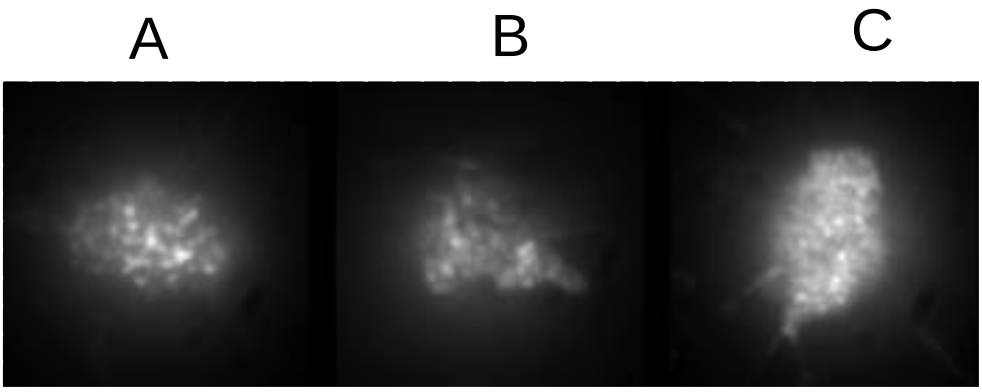

Figure 3.2: Expression of GFP-SybII (A), GFP-SybII-EE (B) and GFP-SybII-KK (C) in SybII/ceb DKO embryonic mouse chromaffin cells reveals vesicular localization of all three constructs in the absence of wild-type SybII.

To assess what properties determine the ability of the C-terminally modified constructs to support vesicle fusion, several constructs were generated where one or two polar or non-polar residues were added at the C-terminus of the protein [Fig. 3.3A]. These constructs were expressed in DKO embryonic mouse chromaffin cells and exocytosis was stimulated by flash photolysis of NP-EGTA. The amplitude and kinetics of exocytosis were quantified by capaci-

tance measurements and compared to those recorded in cells in which wild-type SybII was expressed using the same viral expression method.

As previously reported [3, 13], DKO chromaffin cells did not support exocytosis [Fig. 3.3 B blue traces], while viral expression of wild-type SybII restored a biphasic increase in capacitance [Fig. 3.3 B, black traces], indistinguishable from that observed in embryonic chromaffin cells from normal wild-type mice (data not shown). In contrast, when SybII-KK was expressed [Fig. 3.3 B, red traces], the response was indistinguishable from DKO [Fig. 3.3 C,D], indicating that this mutant protein failed to support vesicle fusion. Even addition of only a single lysine [SybII-K] reduced the exocytotic burst as well as the sustained phase by ~80% and similar reductions were observed with addition of other charged residues (-E, -EE, -HH) [Fig. 3.3 C,D].

3.3.2 Inhibition of fusion is related to amino acid polarity

To assess whether the inhibition of exocytosis is specifically due to the presence of charged residues at the C-terminius of SybII we tested the uncharged amino acids glutamine (SybII-QQ), glycine [SybII-GG] and valine [SybII-VV] [Fig.3.4]. While SybII-QQ expressing cells showed again only a very small exocytotic response, the response of cells expressing SybII-GG was not significantly different from control cells expressing wild-type SybII. The response of cells expressing SybII-VV was intermediate, showing a moderate reduction of 26% for the burst and of 40% (p=0.07) for the sustained phase [Fig. 3.4B]. When the responses were normalized [Fig.3.4C] the exocytotic burst shows slower kinetics for SybII-VV and more so for SybII-QQ. The delay between the flash-induced calcium release and the onset of the exocytotic burst also increased from 4.3 ms for wild-type SybII to 6.7, 8.5 and 19.6 ms for sybII -GG, -VV and -QQ, respec-

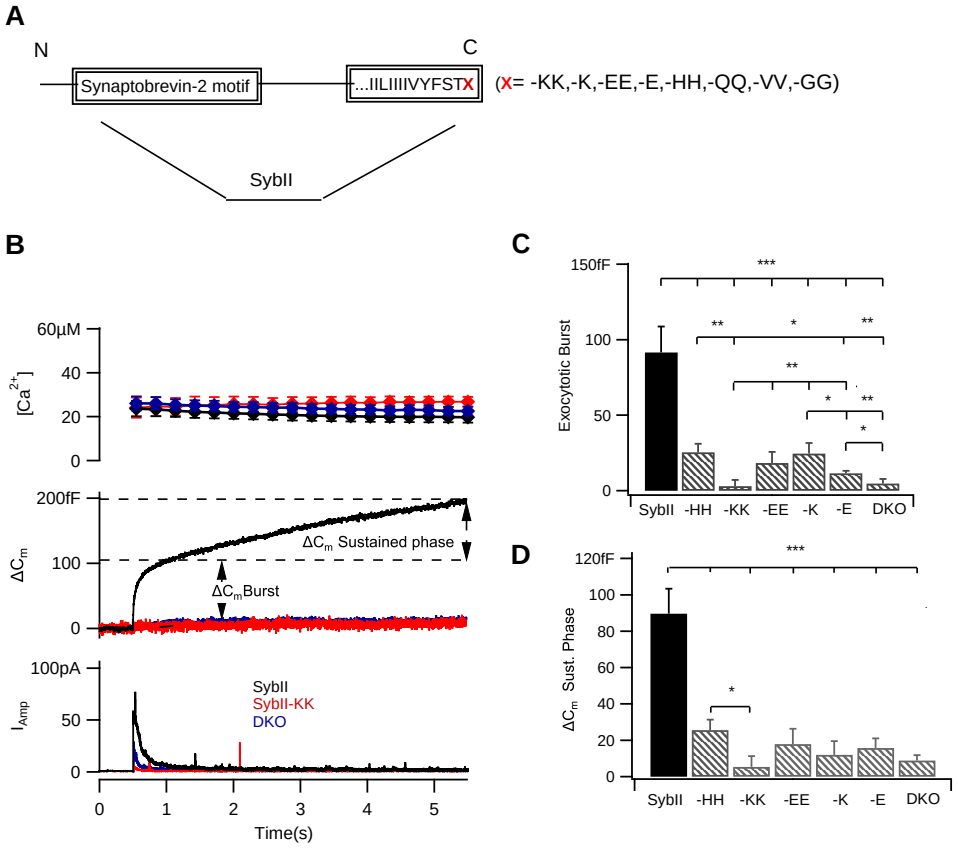

Figure 3.3: (A) SybII C-terminal mutations. X indicates added residues: single lysine (K) or glutamic acid (E), or double lysine (KK), glutamic acid (EE), glutamine (QQ), histidine (HH), valine (VV), or glycine (GG). (B) Exocytosis was stimulated with intracellular release of caged-calcium (top panel) using UV light at t = 0.5 s and monitored by patch clamp capacitance measurement (middle panel) and carbon fiber amperometry (lower panel). Exocytosis is virtually absent in DKO cells (blue traces) but is rescued by viral expression of wild-type sybII (black traces). Exocytosis is not rescued by expression of SybII-KK (red traces). Traces are averages from 8 to 17 cells. The exocytotic burst amplitude (C) was taken as the capacitance increase at 0.5 s after stimulation and the amplitude of the sustained phase (D) as the capacitance increase over the next 5 s. SybII-KK (n=8), SybII-K (n=17), SybII-EE (n=12), SybII-E(n=17), and SybII-HH(n=11). (*P<0.05, **P<0.01, ***P<0.001 student t-test).

tively [Fig. 3.4D]. The kinetics of exocytosis is thus slowed down in parallel with the reduction in exocytosis amplitude.

3.4 Discusion

Release of neurotransmitters from synaptic vesicles as well as exocytosis of chromaffin granules is mediated by the neuronal SNAREs SybII, syntaxin-1 and SNAP-25. The t-SNARE syntaxin and the v-SNARE synaptobrevin are anchored by a single TMD to the plasma membrane and the vesicle membrane, respectively. The SNARE domains of these proteins can form a four-stranded helical bundle as revealed by the crystal structure [25]. It has been suggested that SybII of vesicles in the readily releasable pool is bound tightly to the t-SNAREs only in the N-terminal part of the SNARE complex, zipping up fully only after stimulation [5, 18, 23]. Complexin interacts with the C-terminal part of the SNARE complex and thereby activates and clamps SNARE complexes such that Ca^{2+} can trigger Synaptotagmin to reverse the clamping function [16]. In the zipper model, this will allow N- to C-terminal zipping, which results in a force transfer to the membranes. But how does the force, which is exerted by this machinery, lead to fusion pore formation?

We have shown here that addition of polar residues to the intravesicular C-terminus of the SybII TMD inhibits fusion dramatically. This is an unexpected observation, because SybII has been modified by even adding a GFP variant to its C-terminus in the synapto-pHluorin construct [17] that is widely used to investigate exocytosis and recycling of secretory vesicles. However, in synapto-pHluorin a flexible linker with the sequence SGGSGGTGG was inserted between the SybII C-terminus and GFP. This linker is rich in glycine residues, which did not interfere with SybII function (see Fig. 3.4, SybII-GG construct). It

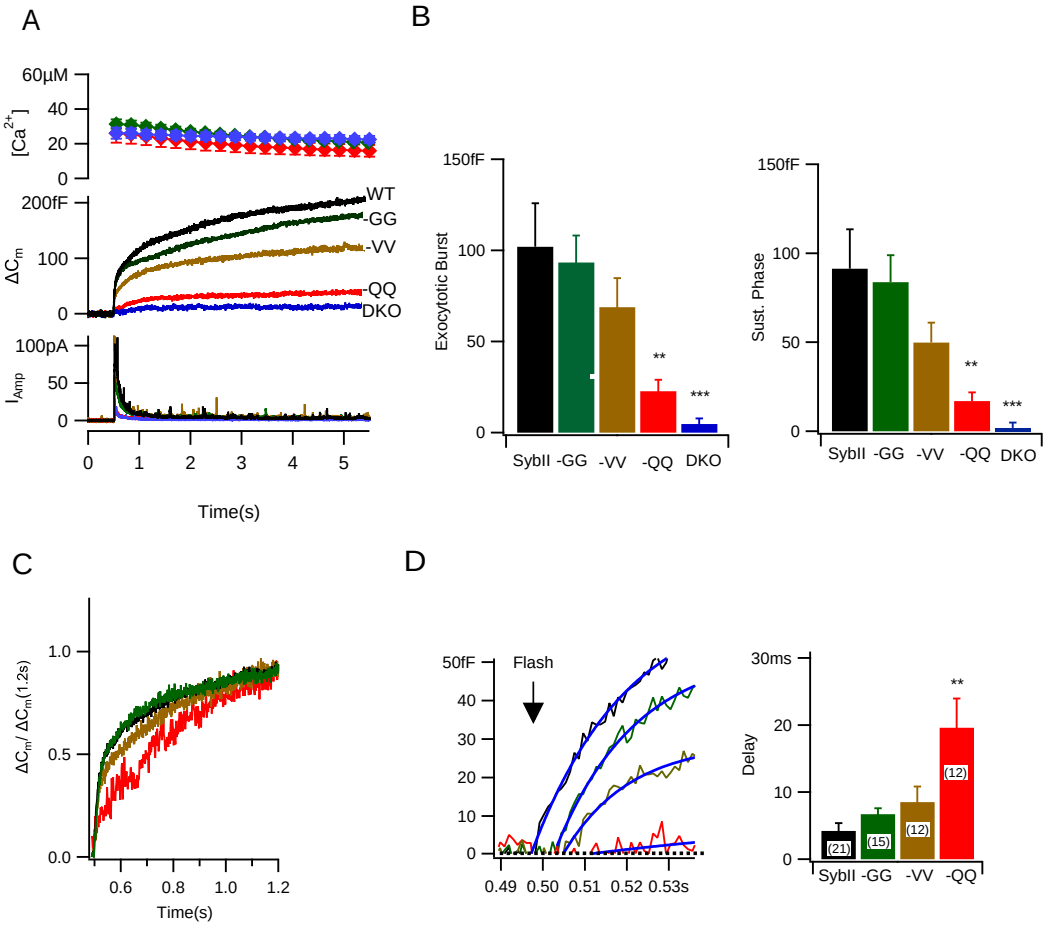

Figure 3.4: Polarity of C-terminal additions determines fusion competence. (a) Average biphasic capacitance responses (middle trace) and associated catecholamine secretion (Lower panel) after photorelease of caged Ca^{2+} (upper trace). Wild-type SybII (black, n=14), SybII-GG (green, n=20), SybII-VV (brown, n=17), SybII-QQ (red, n=12) and DKO (blue, n=20). (B) The amplitudes of the exocytotic burst and of the sustained phase are reduced in parallel. (C) Normalization of the capacitance amplitude at 0.7 s after the flash reveals slower kinetics of exocytosis associated with reduced amplitude. (D) SybII-GG and SybII-VV show increase in delay between flash and onset of exocytosis. Smooth curves (left panel) show the initial parts of multiexponential fits. Statistical analysis of delays (right panel) determined by backextrapolation of multiexponential fits to individual responses indicate that only the increase in SybII-QQ is significant. (*P<0.05, **P<0.01 ***P<0.001 student's t-test).

thus appears that the nature of the residues near the intravesicular membrane-water interface is of particular importance. The inhibition of fusion by addition of polar residues suggests that fusion may be the consequence of a movement of the C-terminus towards the hydrophobic core of the vesicle membrane. We therefore compared the ability of the different SybII mutants to support exocytosis to the free energies of transfer from water to the membrane-water interface (ΔG_{wif}) [31] for the residues added to the SybII C-terminus.

3.4.1 Inhibition of fusion depends on free energy of transfer from water to the membrane-water interface

The transfer energies for the residues used here are given in Table 3.5.5. It has been shown that the transfer energies for multiple residues are additive [34] and we therefore assigned the value given in [31] for addition of a single residue and twice that value for the addition of two residues. For glutamate and histidine ΔG_{wif} is uncertain because it strongly depends on the protonation state of these residues near the interfacial layer inside the acidic vesicle (see corresponding section in Experimental Methods). The relation between ΔG_{wif} for the added residues and the amplitude of the exocytotic burst is shown in Fig. 5a. The ability to support exocytosis decreases with increased ΔG_{wif}. The dashed line shows a fit of the function

$$\Delta C_{burst} = A \cdot \exp(\Delta G_{wif}/E) + B,$$

yielding $E = 0.66 \pm 0.16$ kcal/mol, consistent with a Boltzmann distribution [Fig. 3.5a, solid line] with $E \sim RT = 0.59$ kcal/mol for T=295 K. This result indicates that the ability of the different mutants to support the exocytotic burst correlates directly with the energy required to move the added residues from water into

the interfacial layer.

3.4.2 The mechanism of fusion pore formation

While it is possible that added residues with high ΔG_{wif} may change the position the SybII TMD in the membrane and could thereby compromise the ability of SybII to participate in SNARE complex formation, it appears more likely that fusion pore formation is initiated by pulling the SybII TMD into the vesicle membrane, a movement that would translocate the C-terminally added residues from the water phase to the membrane interface. Such a mechanism is also supported by the finding that a reduction in exocytosis amplitude is accompanied by slowing of the kinetics [Fig. 3.4C,D], as expected for an increased height of the energy barrier. Consistent with this model is also the finding that introduction of flexible linkers between the SybII SNARE domain and its TMD reduces exocytosis in parallel with the length of the linkers [13].

Properties of the early fusion pore are reflected in amperometric foot signals. The SybII-VV construct was chosen for comparison with wild-type SybII because it produces limited inhibition allowing better statistical analysis of amperometric foot signals [Table 3.4.2]. Embryonic DKO chromaffin cells expressing SybII-VV showed no change in foot current amplitude indicating that this mutation does not affect the fusion pore structure. However, a small but significant decrease in foot duration by about 20% (data not shown) was observed for SybII-VV compared to wild-type sybII, which points to small change in the energetics of fusion pore expansion. This mutant has a higher energy in the interfacial layer (~0.14 kcal/mol for 2 valines) and it is thus expected to contribute some additional distortion of the vesicle membrane, thereby lowering the activation energy for fusion pore expansion. A reduction in fusion pore life-

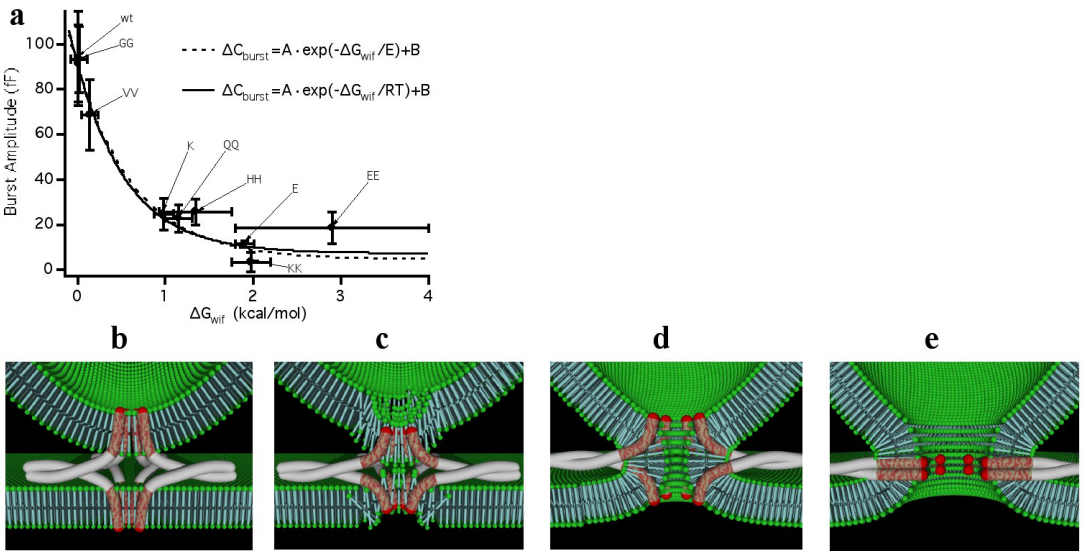

Figure 3.5: (a) Dependence of exocytotic burst amplitude on energy of transfer from water to the membrane-water interface (ΔG_{wif}) for the residues added to the SybII C-terminus. The single exponential fit of the function $\Delta C_{burst} = A \cdot \exp(-\Delta G_{wif}/E) + B$ yielded the fit parameters $A = 88 \pm 6$ fF, $B = 4 \pm 6$ fF, and $E = 0.66 \pm 0.16$ kcal/mol. The solid lines indicate a theoretical Boltzmann distribution fitting only amplitude A and baseline B of the exponential. The data points for SybII-HH and SybII-EE were excluded from the fit (see text). (b-e) Schematic model of fusion pore opening, for clarity only synaptobrevin and syntaxin are shown. Pre-fusion arrangement of N-terminally zipped SNARE complex (b). C-terminal zipping pulls C-termini of SybII and possibly syntaxin deeper into the membrane disrupting membrane continuity (c) leading to fusion pore formation (d) and pairing up of the SybII and syntaxin TMD (e).

time is thus also consistent with the model proposed here. Interestingly, using a simple activation energy model, the ~20% reduction in fusion pore lifetime corresponds to a change in activation energy by ~0.13 kcal/mol, which equals the transfer energy from water to the membrane interface of the two valine residues.

Table 3.1: SybII-VV single amperometry spikes. *P<0.05

							$T_{foot} > 2$ ms		
	I_{max}[pA]	$T_{1/2}$ [ms]	Q[pC]	I_{foot}[pA]	T_{foot} [ms]	Q_{foot} [pC]	I_{foot} [pA]	T_{foot} [ms]	Q_{foot} [pC]
SybII (n=19)	54.65±5.75	3.42± 0.36	0.34± 0.03	3.61± 0.34	3.73± 0.30	0.01± 0.002	5.11± 0.41	6.85± 0.56	0.038± 0.004
SybII-VV (n=24)	53.37±6.17	2.88±0.27	0.27±0.02	3.53±0.30	3.17±0.50	0.01±0.01	5.78±0.49	5.27±0.46*	0.034±0.004

The C-terminus of the wild-type SybII TMD is located in the interfacial layer of the vesicle membrane [4] [Fig. 3.5b]. The aromatic residues Y113 and F114 with their propensity for interfacial localization [31](are suitably positioned and are conserved in vertebrate SybII. Ceb, which also supports chromaffin granule exocytosis, has a tryptophan and a non-aromatic residue in the corresponding position, which yields a very similar energy minimum for interfacial localization. When the TMD is pulled deeper into the membrane, the polar residues S115 and T116 may be pulled into the interfacial or hydrophobic layers [Fig.3.5c]. In some species (human, horse, bovine) T116 is substituted by S116 but Thr and Ser have identical ΔG_{wif}. In ceb, there are also one or more polar residues at the C-terminus conserving the essential properties. As a consequence of this movement of the SybII C-terminus into the hydrophobic membrane domain, the stability of the vesicle membrane should be significantly reduced followed by structural rearrangements leading to disruption of membrane continuity and formation of a proteolipid fusion pore [Fig.3.5 d,e]. Consistent with this model is the recently reported X-ray structure of the neuronal SNARE complex, consisting of syntaxin 1A, SNAP-25 and SybII, includ-

ing the carboxy-terminal linkers and transmembrane regions [24]. In this post-fusion structure [8], the C-termini of syntaxin and SybII appear to be pulled towards the hydrophobic core of the membrane. In the zipper model of SNARE-mediated fusion, the movement of the SybII C-terminus as a prerequisite for fusion pore formation is expected to occur as a consequence of N- to C-terminal zipping of the SNARE domains. A movement of the SybII C-terminus is, however, also consistent with the recently proposed scissors mechanism involving a transition of the SybII TMD from a tilted conformation to one parallel to the membrane normal [26].

The possibility of a proteolipid fusion pore was originally proposed by [37] but the identity and function of the proteins participating in such a mechanism were unknown. In the model proposed here, the genesis of the pore formation starts at the inner leaflet of the vesicle membrane and is induced by movement of the C-terminal end of SybII. This movement is activated in response to calcium stimulation via synaptotagmin, which may in addition aid fusion pore formation by inducing membrane curvature [15]. It is possible that the TMD of syntaxin plays a complementary role in disrupting the continuity of the plasma membrane as depicted in Fig.3.5c of the model. However, we have not performed experiments with corresponding syntaxin mutants to support or discard such a role. The energy of C-terminal zipping of the SNARE complex appears to be remarkably balanced with respect to overcoming the energy barrier for fusion. It is just sufficient for the required SybII TMD movement as the additional energy of a few k_BT required for translocation of the added residues significantly inhibits fusion competence.

3.5 Experimental Procedures

SybII/ceb DKO mouse E17- E18 embryos were obtained and chromaffin cells isolated and plated as described [3, 22]. Recombinant Semliki Forest Virus was used to introduce SybII mutants into the cells after day 2 or 4 in culture [3, 1]. Full-length rat SybII plasmid was a kind gift from Dr. Thomas Südhof. The SybII TMD ...WWKNLKMMIILGVICAIILIIIIVYFST was extended at the C-terminal end by addition of K, E, KK, EE, QQ, HH, VV, or GG amino acids. All constructs were confirmed by DNA sequencing.

3.5.1 Whole-cell capacitance measurement

Whole-cell patch clamp experiments were performed 4-6 hrs after transfection at room temperature. The extracellular solution contained in mM: 145 NaCl, 1 $MgCl_2$, 2.8 KCl, 2 $CaCl_2$ and 10 HEPES pH 7.2, adjusted to 310 mOSM with D-glucose. The whole-cell pipette solution contained in mM: 0.4 fura-4F, 0.4 mag-fura-2 (Invitrogen), 5 Nitrophenyl-EGTA (NP-EGTA, Synaptic Systems), 100 Cs-glutamate, 0.3 Na-GTP, 2 Mg-ATP, 4 $CaCl_2$, 1 ascorbic acid and 32 HEPES, pH 7.2. Photolysis of NP-EGTA was achieved by a UV flash lamp (Rapp Optoelektronik). Intracellular calcium measurements were performed by alternating the fura-4F/mag-fura-2 excitation wavelength between 350 nm and 380 nm as described [27]. Capacitance changes were measured using an EPC9 using the "sine + dc" technique [14]. The amplitude of the exocytotic burst was taken as the capacitance increase 500 ms after the flash. The sustained phase of exocytosis was quantified as the capacitance increase over the next 5 s. Amperometric recordings were performed with homemade 10 mm carbon fiber electrodes using an EPC7 amplifier and filtered at 3 KHz.

3.5.2 Total Internal Reflection Fluorescence (TIRF) Microscopy

An inverted microscope (Axiovert 135 TV, Zeiss, Thornwood, NY) modified for TIRF microscopy as described [2] and fitted with a Zeiss plan-fluar 1.45 NA 100x oil emersion objective was used to observe the cells during experiments. Illumination was provided by a 100 W mercury arc lamp (HBO 103W/2, Osram, Danvers, MA), with 480/40 nm excitation filter, 515 nm dichroic, and 520 nm long pass emission filter (Chroma Technology, Rockingham, VT). Images were collected using an EMCCD camera (Andor iXon, South Windsor, CT) and its accompanying software. For each cell, a 2000 frame image sequence was collected. The exposure time for each frame was 100-150 ms, with an interframe time of 1.8 ms.

3.5.3 Electrochemical Detector Arrays

Microfabricated platinum electrode arrays were used to amperometrically detect the release of catecholamines from the transfected chromaffin cells. Each electrochemical detector (ECD) array consists of a set of four planar Pt electrodes fabricated on a glass coverslip. The four electrodes of an ECD reside at the corners of a square sized such that a cell can be placed atop the array and viewed through the glass coverslip while amperometric currents are recorded from all four electrodes simultaneously. The ECD arrays were fabricated as described (Dias et al., 2002; Hafez et al., 2005) except for an improved insulation layer, which was created by chemical vapor deposition of approx. 300 nm of SiO_2 onto the electrodes (IPE 1000 PECVD), and subsequent etching of the SiO_2 layer via reactive ion etching (PlasmaLab 80Plus, Oxford Instruments, Concord, MA) to expose the active areas of the electrodes and contact pads.

3.5.4 Combined TIRF microscopy and ECD amperometry

GFP was linked to the N-terminus of SybII, SybII-KK, or SybII-EE and the constructs expressed in wild-type mouse chromaffin cells or in embryonic DKO chromaffin cells as described above. Cells expressing the construct were located using a 20x Zeiss air objective under epifluorescence illumination. Cells chosen for experiments had a characteristic green GFP fuorescence, and exhibited a concentration of the label in the ER. The cells of interest were also inspected under bright field illumination to insure healthy cells were chosen. Cells were picked up and positioned on the ECD arrays using a micropipette as described [11]. TIRF microscopy (see above) was performed simultaneously with measurement of catecholamine by amperometry using the ECD array as described [11] . Amperometric currents were low pass filtered at 500 Hz, acquired with 5 kHz sampling rate and analyzed as described [11]. For analysis, a 5 pA minimum current peak height was used as threshold, with a minimum of four analyzable events per cell. The camera output signal was recorded in order to synchronize the timing of the fluorescence image frames with electrochemical signals.

3.5.5 Assignment of free energies of transfer from water to membrane interface

The whole residue transfer energies from water to the membrane interface of the residues added to the C-terminus were taken from [31] [Table 3.5.5]. For Lys the value in the table was used. The double additions LysLys, GlnGln, GlyGly, and ValVal were assigned twice the values in the table. Assuming a pK of 4.3 for glutamic acid and an intravesicular pH of 5.5, one would expect 94% in Glu^-

and 6% in Glu^0 state. We thus assigned a transfer energy for single Glu addition: $\Delta G_{wif} = 0.94 \times (2.02 \pm 0.11(+0.06 \times (-0.01 \pm 0.15) = 1.90 \pm 0.11$ kcal/mol.

For the GluGlu addition, ΔG_{wif} could be twice that value ($\Delta G_{wif} = 3.8 \pm 0.22$). However, it appears possible that a negative charge on one Glu will significantly change the pK of the second Glu, which may thus lead to ~50% protonation between the two added Glu residues corresponding to $\Delta G_{wif} = 2.01 \pm 0.26$. For GluGlu we thus estimate a range$\Delta G_{wif} = 1.75 - 4.0$ or 2.9 ± 1.1 kcal/mol. Assuming a pK of 6.0 for histidine one would expect 76% in His^+ and 24% in His^0 state. We thus assigned a transfer energy for a single His addition: $\Delta G_{wif} = 0.76 \times (0.96 \pm 12) + 0.24 \times (0.17 \pm 0.06) = 0.77 \pm 0.11$ kcal/mol.

For the HisHis additon, ΔG_{wif} could be twice that value ($\Delta G_{wif} = 1.54 \pm 0.22$). However, protonation of the first His may shift the pK of the second His such that there could again be an average ~50% protonation giving $\Delta G_{wif} = 1.13 \pm 0.18$. For HisHis we thus estimate a range $\Delta G_{wif} = 0.95 - 1.76 = 1.35 \pm 0.41$. Due to these uncertainties the data points for sybII-HH and sybII-EE were not included in the fits of Fig. 3.5 A.

3.6 Acknowledgements

This chapter was submitted to a journal and the authors listed on the paper are: Annita N. Ngatchou, Kassandra Kisler, Qinghua Fang, Alexander M. Walter, Ying Zhao3, Dieter Bruns, Jakob B. Sørensen and Manfred Lindau

We thank Dirk Reuter, Joan Lenz and Ina Herfort for expert technical assistance and Stephan Weiss for the fusion pore artwork. We are grateful to Dr. Erwin Neher for critical reading of the manuscript. This work has been supported by the National Institutes of Health grants R01NS38200, R01GM085808,

Table 3.2: Selected whole residue transfer energies from water to membrane interface from [31].

Amino Acids	ΔG_{wif} (kcal/mol)
Gln	0.58 ± 0.08
Glu^{-}	2.02 ±0.11
Glu^{0}	-0.01 ± 0.15
Gly	0.01 ± 0.05
His^{+}	0.96 ± 0.12
His^{0}	0.17 ± 0.06
Lys^{+}	0.99 ± 0.11
Val	0.07 ± 0.05

T32GM008267, the Nanobiotechnology Center (a National Science Foundation Science and Technology Center, agreement No. ECS-9876771) and the Deutsche Forschungsgemeinschaft (SFB523-B16 to JBS and SFB530-C10 to DB).

BIBLIOGRAPHY

[1] U. Ashery, A. Betz, T. Xu, N. Brose, and J. Rettig. An efficient method for infection of adrenal chromaffin cells using the Semliki Forest virus gene expression system. *Eur. J. Cell. Biol.*, 78(8):525–32, 1999.

[2] D. Axelrod. Selective imaging of surface fluorescence with very high aperture microscope objectives. *J. Biomed. Opt.*, 6(1):6–13, 2001.

[3] M. Borisovska, Y. Zhao, Y. Tsytsyura, N. Glyvuk, S. Takamori, U. Matti, J. Rettig, T. Südhof, and D. Bruns. v-snares control exocytosis of vesicles from priming to fusion. *Embo. J.*, 24(12):2114–26, 2005.

[4] M. E. Bowen, D. M. Engelman, and A. T. Brunger. Mutational analysis of synaptobrevin transmembrane domain oligomerization. *Biochemistry*, 41(52):15861–6, 2002.

[5] Y A Chen, S J Scales, J R Jagath, and R H Scheller. A discontinuous SNAP-25 C-terminal coil supports exocytosis. *J Biol Chem*, 276(30):28503–8, 2001.

[6] M Criado, A Gil, S Viniegra, and L M Gutierrez. A single amino acid near the C terminus of the synaptosomeassociated protein of 25 kDa (SNAP-25) is essential for exocytosis in chromaffin cells. *Proc Natl Acad Sci U S A*, 96(13):7256–61, 1999.

[7] Ferenc Deak, Ok-Ho Shin, Ege T Kavalali, and Thomas C Südhof. Structural determinants of synaptobrevin 2 function in synaptic vesicle fusion. *J Neurosci*, 26(25):6668–76, 2006.

[8] Jeffrey F Ellena, Binyong Liang, Maciej Wiktor, Alexander Stein, David S Cafiso, Reinhard Jahn, and Lukas K Tamm. Dynamic structure of lipid-bound synaptobrevin suggests a nucleation-propagation mechanism for

trans-SNARE complex formation. *Proc Natl Acad Sci U S A*, 106(48):20306–11, 2009.

[9] Q. Fang, K. Berberian, L. W. Gong, I. Hafez, J. B. Sø rensen, and M. Lindau. The role of the c terminus of the snare protein snap-25 in fusion pore opening and a model for fusion pore mechanics. *Proc Natl Acad Sci U S A*, 105(40):15388–92, 2008.

[10] Liang-Wei Gong, Guillermo Alvarez de Toledo, and Manfred Lindau. Exocytotic catecholamine release is not associated with cation flux through channels in the vesicle membrane but Na+ influx through the fusion pore. *Nat Cell Biol*, 9(8):915–22, 2007.

[11] Ismail Hafez, Kassandra Kisler, Khajak Berberian, Gregor Dernick, Vicente Valero, Ming G Yong, Harold G Craighead, and Manfred Lindau. Electrochemical imaging of fusion pore openings by electrochemical detector arrays. *Proc Natl Acad Sci U S A*, 102(39):13879–84, 2005.

[12] Meyer B Jackson and Edwin R Chapman. Fusion pores and fusion machines in Ca2+-triggered exocytosis. *Annu Rev Biophys Biomol Struct*, 35(NIL):135–60, 2006.

[13] J. Kesavan, M. Borisovska, and D. Bruns. v-snare actions during ca(2+)-triggered exocytosis. *Cell*, 131(2):351–63, 2007.

[14] M Lindau and E Neher. Patch-clamp techniques for time-resolved capacitance measurements in single cells. *Pflugers Arch*, 411(2):137–46, 1988.

[15] Kara L Lynch, Roy R L Gerona, Dana M Kielar, Sascha Martens, Harvey T McMahon, and Thomas F J Martin. Synaptotagmin-1 utilizes membrane

bending and SNARE binding to drive fusion pore expansion. *Mol Biol Cell*, 19(12):5093–103, 2008.

[16] Anton Maximov, Jiong Tang, Xiaofei Yang, Zhiping P Pang, and Thomas C Südhof. Complexin controls the force transfer from SNARE complexes to membranes in fusion. *Science*, 323(5913):516–21, 2009.

[17] G Miesenbock, D A De Angelis, and J E Rothman. Visualizing secretion and synaptic transmission with pH-sensitive green fluorescent proteins. *Nature*, 394(6689):192–5, 1998.

[18] A. V. Pobbati, A. , and D. Fasshauer. N- to c-terminal snare complex assembly promotes rapid membrane fusion. *Science*, 313(5787):673–6, 2006.

[19] Josep Rizo and Han Dai. How much can SNAREs flex their muscles? *Nat Struct Mol Biol*, 14(10):880–2, 2007.

[20] Susanne Schoch, F Deak, A Konigstorfer, M Mozhayeva, Y Sara, T C Südhof, and E T Kavalali. SNARE function analyzed in synaptobrevin/VAMP knockout mice. *Science*, 294(5544):1117–22, 2001.

[21] T. Söllner, S. Whiteheart, M. Brunner, H. Erdjument-Bromage, M. Geromanos, P. Tempst, and J.E. Rothman. Snap receptors implicated in vesicle targeting and fusion. *Nature (London)*, 362:318–323, 1993.

[22] J. B. Sørensen, R. Fernandez-Chacon, T. C. Südhof, and E. Neher. Examining synaptotagmin 1 function in dense core vesicle exocytosis under direct control of ca2+. *J Gen Physiol*, 122(3):265–76, 2003.

[23] J. B. Sørensen, K. Wiederhold, E. M. Muller, I. Milosevic, G. Nagy, B. L. de Groot, H. Grubmuller, and D. Fasshauer. Sequential n- to c-terminal

snare complex assembly drives priming and fusion of secretory vesicles. *Embo J*, 25(5):955–66, 2006.

[24] Alexander Stein, Gert Weber, Markus C Wahl, and Reinhard Jahn. Helical extension of the neuronal SNARE complex into the membrane. *Nature*, 460(7254):525–8, 2009.

[25] R.B. Sutton, D. Fasshauer, R. Jahn, and A.T. Brunger. Crystal structure of a snare complex involved in synaptic exocytosis at 2.4 resolution. *Nature*, 395:347–353, 1998.

[26] Jiansong Tong, Peter P Borbat, Jack H Freed, and Yeon-Kyun Shin. A scissors mechanism for stimulation of SNARE-mediated lipid mixing by cholesterol. *Proc Natl Acad Sci U S A*, 106(13):5141–6, 2009.

[27] T Voets. Dissection of three Ca2+-dependent steps leading to secretion in chromaffin cells from mouse adrenal slices. *Neuron*, 28(2):537–45, 2000.

[28] T. Voets, E. Neher, and T. Moser. Mechanisms underlying phasic and sustained secretion in chromaffin cells from mouse adrenal slices. *Neuron*, 23(3):607–15, 1999.

[29] Alexander M Walter, Katrin Wiederhold, Dieter Bruns, Dirk Fasshauer, and Jakob B Sørensen. Synaptobrevin N-terminally bound to syntaxin-SNAP-25 defines the primed vesicle state in regulated exocytosis. *J Cell Biol*, 188(3):401–13, 2010.

[30] S. Wei, T. Xu, U. Ashery, A. Kollewe, U. Matti, W. Antonin, J. Rettig, and E. Neher. Exocytotic mechanism studied by truncated and zero layer mutants of the c-terminus of snap-25. *Embo J*, 19(6):1279–89, 2000.

[31] S H White and W C Wimley. Membrane protein folding and stability: physical principles. *Annu Rev Biophys Biomol Struct*, 28(NIL):319–65, 1999.

[32] Martin Wienisch and Jurgen Klingauf. Vesicular proteins exocytosed and subsequently retrieved by compensatory endocytosis are nonidentical. *Nat Neurosci*, 9(8):1019–27, 2006.

[33] R.M. Wightman, J.A. Jankowski, R.T. Kennedy, D.T. Kawagoe, T.J. Schroeder, D.J. Leszczyszyn, J.A. Near, E.J. Diliberto jr., and O.H. Viveros. Temporally resolved catecholamine spikes correspond to single vesicle release from individual chromaffin cells. *Proceedings of the National Academy of Sciences of the United States of America*, 88:10754–10758, 1991.

[34] W C Wimley and S H White. Experimentally determined hydrophobicity scale for proteins at membrane interfaces. *Nat Struct Biol*, 3(10):842–8, 1996.

[35] T Xu, T Binz, H Niemann, and E Neher. Multiple kinetic components of exocytosis distinguished by neurotoxin sensitivity. *Nat Neurosci*, 1(3):192–200, 1998.

[36] C Yang, S Mora, J W Ryder, K J Coker, P Hansen, L A Allen, and J E Pessin. VAMP3 null mice display normal constitutive, insulin- and exercise-regulated vesicle trafficking. *Mol Cell Biol*, 21(5):1573–80, 2001.

[37] J Zimmerberg, S S Vogel, and L V Chernomordik. Mechanisms of membrane fusion. *Annu Rev Biophys Biomol Struct*, 22(NIL):433–66, 1993.

CHAPTER 4

MODULATION OF SYNAPTOBREVIN-2 FUNCTION BY GFP TAGS IN CHROMAFFIN CELLS EXOCYTOSIS

4.1 Abstract

The green fluorescent protein (GFP) and its variants are commonly used to tag proteins in order to trace their localization or to follow their activities. GFP was previously linked to the vesicular protein synaptobrevin-2 to allow the visualization of vesicles fusion and recycling. However, it is unclear whether the hybridization of synaptobrevin-2 hinders its functionality in chromaffin cells. Here we study whether the linked proteins, GFP-synaptobrevin-2 and synapto-pHluorin can support calcium dependent exocytosis in chromaffin cells.

4.2 Introduction

Exocytosis is a process by which cells secrete their contents into the extracellular space. Many proteins regulate this process, among which is the vesicular protein synaptobrevin-2 (or VAMP), a member of the SNARE (Soluble N-ethylmaleimide-sensitive-factor Attachement protein REceptor) family.
Synaptobrevin-2 has three distinct regions, (i) a SNARE domain which forms a complex with syntaxin and SNAP-25 to drive fusion [11], (ii) a transmembrane domain (TMD) which is integrated into the bilayer membrane of vesicles [10], and (iii) an unstructured linker region that forms a bridge between the SNARE domain and the TMD [Fig. 4.2 A] [2].

pHluorin [7] is a histidine based mutation of the green fluorescent protein (GFP), whose fluorescence spectrum change as a response to the change in pH of its environment. When pHluorin is linked to the C-terminal end of

synaptobrevin-2 (synapto-pHluorin) and is targeted to the vesicle lumen (pH~5.6), its fluorescence is quenched due to the acidic pH [7]. However, upon the fusion of the vesicle with the plasma membrane, the pHluorin is exposed to the extracellular milieu (pH~7.4), resulting to its fluorescence un-quenching. Hence, by using synapto-pHlourin it has been possible to visualize exocytosis [7, 15, 4, 8]. However, it is unclear whether synapto-pHlourin can participate in the SNARE complex formation and mediates the fusion of vesicles, since synapto-phluorin is typically expressed in the presence of wild-type synaptobrevin. Here we expressed synapto-pHluorin in sybII/cellubrevin double knock out (DKO) chromaffin cells and assessed it functionality by caged-calcium flash photolysis and whole cell capacitance measurement.

4.3 Result

The fusion of vesicles in chromaffin cells was stimulated by the homogeneous release of photoreleasable calcium in the whole-cell patch clamp configuration [12]. The intracellular calcium concentration in cells was estimated by ratiometric measurements of the calcium dyes Fura-2 and Furaptra (Chapter II). The fusion of vesicles in response to the calcium stimulation was detected by the increase of the capacitance of the cell membrane, and the secretion of catecholamines that accompanied fusion was measured by amperometry.

Synapto-pHluorin partially rescued exocytosis in DKO Chromaffin cells

Synapto-pHluorin was constructed by fusing pHlourin at the carboxyl-terminus of synaptobrevin-2 (SybII) via a flexible linker (SGGSGGTGG) [7]. Synapto-pHluorin with this linker has been utilized in many experiments to monitor exocytosis in neuronal synapses [8, 7], suggesting that this construct should

not inhibit exocytosis in chromaffin cells. We overexpressed synapto-pHluorin in wild-type chromaffin cells using the Simliki Forest Virus expression system. Although synapto-pHluorin was expected to be targeted to vesicles, a considerable amount was also expressed at the surface of the cell membrane [8]. Since cells were bathed during the experiment in the bath solution with pH ~7.3, the fluorescence of synapto-pHluorins at the cells surface were dequenched, hence cells expressing the synapto-pHluorin were identified by their green fluorescence. Synapto-pHluorin expression in wild-type cells displayed robust capacitance and amperometric responses [Fig.4.1 B], indicating that the fusion of vesicles was not inhibited as expected [7, 15, 4, 8].

It is possible that in this experiment, exocytosis was mediated by both the endogenous synaptobrevin and synapto-pHluorin, or exclusively or predominantly by synaptobrevin. To distinguish between these possibilities, synapto-pHlourin was expressed in DKO embryonic chromaffin cells. DKO cells lacked both synaptobrevin and cellubrevin (DKO) because these proteins are functionally interchangeable in chromaffin cells [2]. When these null cells were stimulated by photorelease of calcium, the capacitance trace showed no exocytotic response [Fig.4.1 C, green]. However, when the cells expressed SybII and GFP as separate proteins, the capacitance amplitude rose to nearly ~200 fF at 5 s after the stimulus was given, indicating that the exocytotic response was rescued. Surprisingly, when synapto-Phluorin was expressed in these DKO cells, the capacitance amplitude was recuded by ~70 % of SybII capacitance at 5 s. However, synapto-pHluorin expressing cells gave a capacitance amplitude that was significantly higher than that observed in null cells [Fig.4.1 C], indicating that synapto-pHluorin was able to rescue exocytosis in DKO cells at sub-optiomal level.

The capacitance response to flash induced exocytosis displays a burst phase,

which reflects the fusion of vesicles that have established a stable link with the plasma membrane through SNARE complex formation prior to the elevation of $[Ca^{2+}]_i$ [9]. The burst was extracted by quantifying the change of the capacitance amplitude at 0.5 s after flash stimulation [Fig.4.1 C]. When we compared the burst amplitude, we observed that it was reduced for the synapto-pHluorin construct [Fig.4.1 D]. Scaling the burst phase revealed that its kinetic was slower than in SybII expressing cells [Fig.4.1 E]. Thus synapto-pHluorin decreased the amount of vesicles fusing during the exocytotic burst phase and also slowed down the kinetics of fusion.

The capacitance trace also displays a slower or sustained phase which has a time constant of seconds. This phase has been attributed to vesicles undergoing functional maturation as long as the intracellular calcium concentration remained high [13]. The sustained phase was quantified by taking the difference of the capacitance amplitude from 0.5 to 5 s. When cells expressed synapto-pHluorin, the sustained phase was reduced in comparison to control [Fig.4.1 D], indicating that synapto-pHluorin considerably slows down vesicle priming.

GFP-synaptobrevin-2 partially supports exocytosis

To determine whether the N-terminal fusion of GFP to synaptobrevin-2 also inhibits exocytosis, we engineered GFP-synaptobrevin-2 by fusing the fluorescent protein GFP, to the amino-terminus of SybII (GFP-SybII) [Fig.4.2, A] . The control experiment consisted of the co-expression of GFP with SybII protein. Cells co-expressing GFP and SybII proteins, showed diffuse fluorescence whereas those infected with GFP-SybII virus showed localized fluorescence [Fig.4.2, B], suggesting the accumulation of GFP-SybII proteins in the endoplasmic reticulum.

As we have seen in Chapter III, the expression of wild-type SybII in null

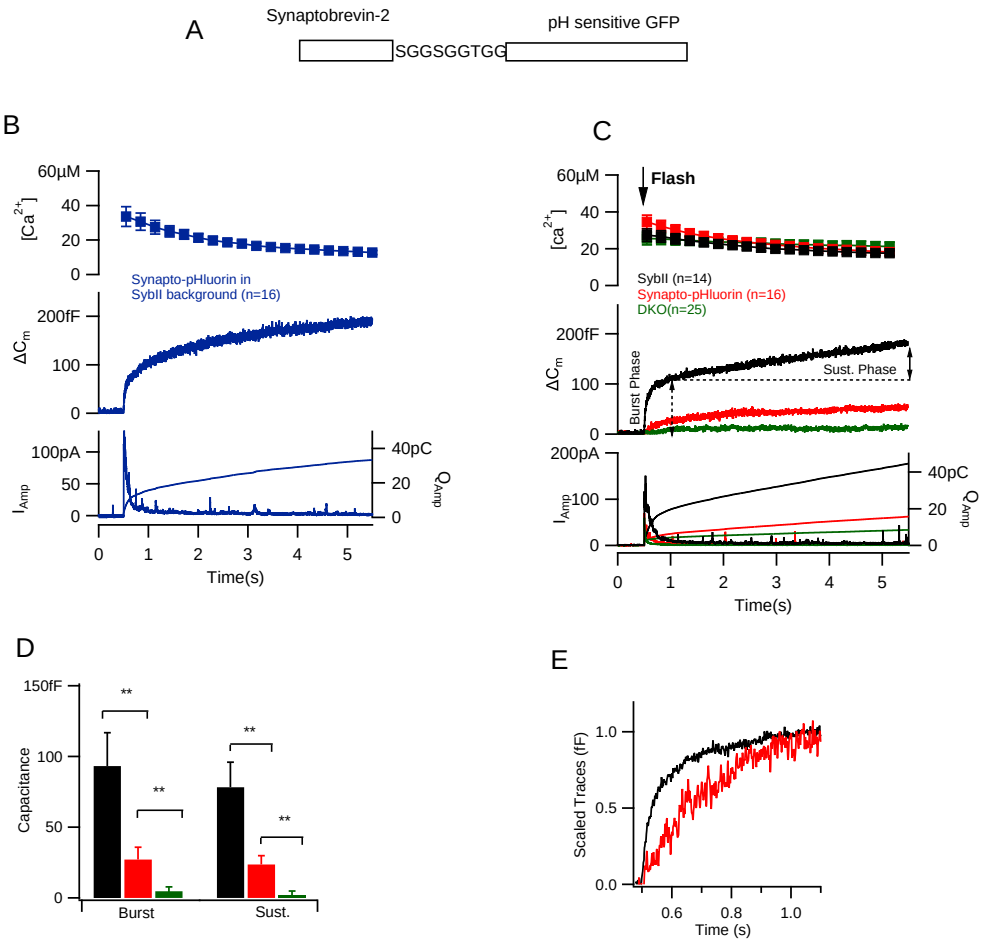

Figure 4.1: Synapto-pHluorin partially rescued secretion in DKO chromaffin cells. (A) Synapto-pHluorin was constructed by fusing pHluorin to the C-terminal end of synaptobrevin-2 protein via a linker region. (B) The expression of synapto-pHluorin in the presence of endogeneous SybII protein shows a robust secretion. (C) Rescued experiments showing a reduction the capacitance trace (middle panel) of DKO cells expressing synapto-pHluorin (red, n=16) in comparison to cells expressing SybII (black, n=14) and DKO cells (green, n=25). (C) Burst and sustained phase of the capacitance trace is reduced in mutant cells.

cells resulted in a two-phase increase of the capacitance trace [Fig.4.2, black trace], indicating that the exocytotic phenotype was rescued. However, when the GFP-SybII construct was expressed in null cells, the mean capacitance amplitude was reduced in comparison to the capacitance amplitude recorded in control cells [Fig.4.2], red trace]. This was consistent with the reduction of the amperometric current [Fig.4.2, bottom], indicating that fewer vesicles underwent exocytosis in cells expressing GFP-SybII.

When we compared the burst amplitudes, we observed that this phase was apparently reduced for the GFP-SybII construct, albeit not significantly [Fig.4.2 C], and scaling this region, did not show a difference in the kinetics in comparison to control. Thus, the GFP linked to SybII at the amino-terminus has little, if any effect on the exocytotic burst. The sustained phase on the other hand, was significantly reduced in comparison to the control [Fig.4.2 D], indicating that amino acid terminal GFP tag considerably slows downs the priming of vesicles.

4.4 Discussions

There is considerable evidences that the TMD of synaptobrevin-2 plays an important role in neurotransmitter secretion during exocytosis. For example, mutating key amino acids in the TMD of synaptobrevin-2 hinders its dimerization in vitro [6] and impaired exocytosis (Chapter VI). Furthermore, it has been found that lengthening the linker domain [5, 3] or adding extra residues at the C-terminal end of synaptobrevin-2 (Chapter III) inhibits exocytosis.

Synapto-pHlourin which is constructed by joining pHluorin to the carboxyl end of synaptobrevin-2, has been used to visualize vesicles secretion [7, 15, 4, 8], suggesting that synapto-pHluorin is functionally competent to mediate exocytosis.

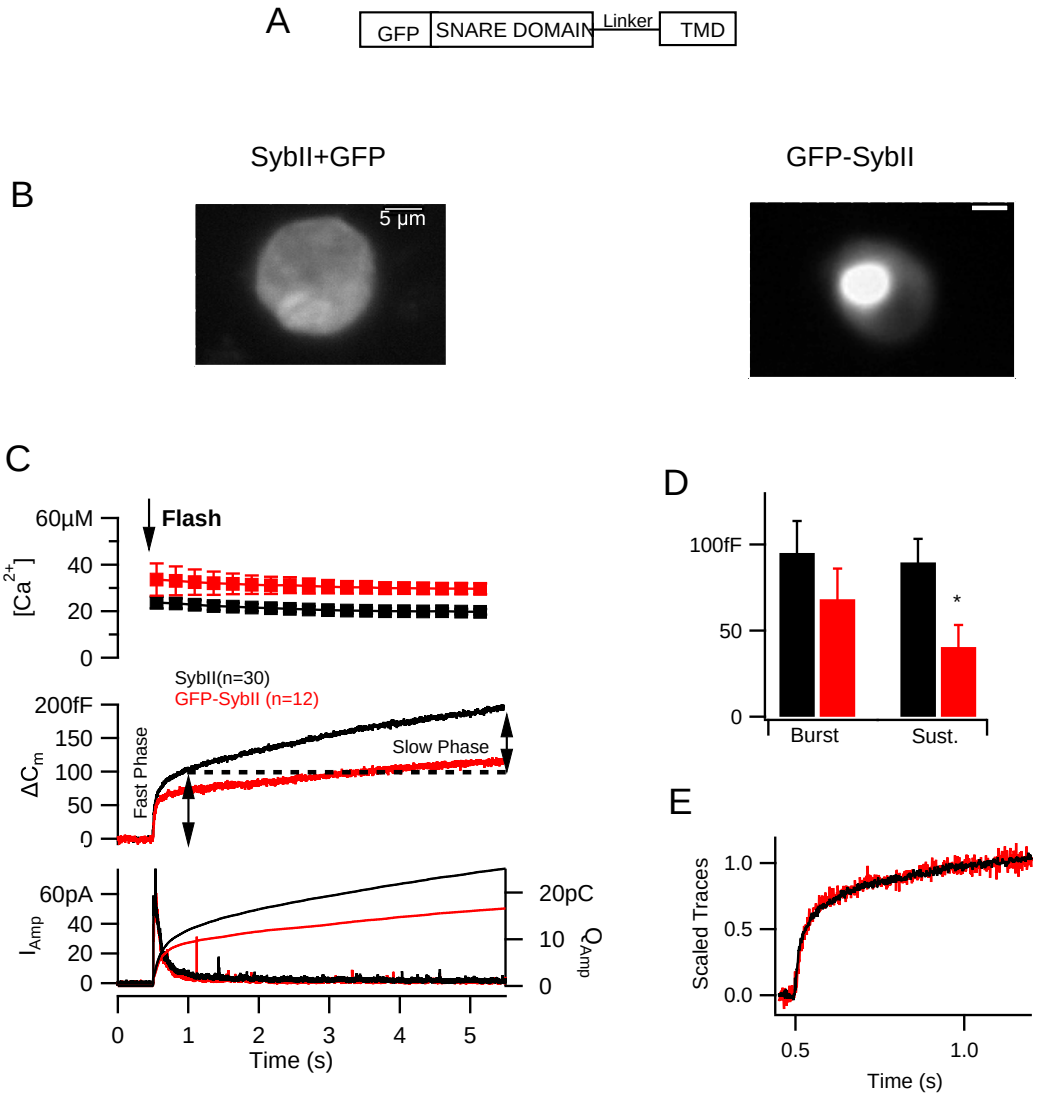

Figure 4.2: GFP-synaptobrevin-2 expression in DKO chromaffin cells. (A) Sketch of the GFP protein linked to the amino-terminus of SybII. (B) GFP-SybII cells show accumulation of fluorescence, whereas when SybII was co-expressed with GFP the fluorescence was diffused. (C) The mean capacitance response (middle panel) and amperomtry (bottom panel) in response to the $[Ca^{2+}]_i$ stimulus (upper panel) were reduced in cells expressing GFP-SybII (red, n=12) in comparison to cells expressing wild-type SybII (black, n=30). (D) Burst and sustained phase of the capacitance traces. (E) Scaled capacitance amplitudes taken at 0.5 s after the calcium stimulus.

However, these experiments were conducted in the presence of the endogenous synaptobrevin-2. We have looked at vesicle secretion in chromaffin cells by expressing synapto-pHluorin in the presence of the endogenous synaptobrevin-2, and our result demonstrates that exocytosis is also not inhibited in this system. However, when cells are devoid of the endogenous proteins, synapto-pHluorin fails to entirely rescue exocytosis, thus suggesting that synapto-pHluorin is unable to compete with synaptobrevin in cells expressing both proteins. In the absence of the endogenous SybII and cellubrevin, synapto-pHluorin supports exocytosis but the amplitude of exocytosis is inhibited by $\sim$ 70%. The C-terminal one or two amino acid additions inhibit exocytosis depending on the energy of transfer from water to the membrane interface (ΔG_{wif}) of the added residues following a Boltzmann distribution (Chapter III). In synapto-pHluorin, an SGGSGGTGG linker is used, thus the transfer of this linker into the water-lipid membrane interface may have induce the exocytotic inhibition.

The priming of vesicles entails in part the formation of the N-terminal domain of the complex formed by syntaxin, SNAP-25 and synaptobrevin [9, 14]. We have observed that GFP-SybII hinders vesicle priming, consistent with the notion that the GFP protein at the amino-terminal end of SybII may hinder the association of synaptobrevin with syntaxin and SNAP-25, thus obstructing with the formation of the SNARE complex. However, since we also have observed that GFP-SybII proteins were mainly located into the endoplasmatic reticulum, it is also possible that after the synthesis of GFP-SybII proteins by the ribosome, the proteins are missorted and as result, fewer GFP-SybII proteins could end up on their target vesicles.

Contrary to the results that we have reported here, fusing the GFP variants, Venus and eCFP at animo or carboxyl-terminus of synaptobrevin-2 does

not inhibit synaptic function in synaptobrevin-2 knock-out neurons [3]. This discrepancy could be due to the difference in experimental procedures. However to be able to draw any definitive conclusion, more results are clearly needed.

4.5 Methods

GFP-synaptobrevin-2 was engineered by amplifying synaptobrevin-2 by PCR to generate a 5′ XhoI and 3′ KpnI site. Then it was inserted into the XhoI/KpnI site of the pEGFP-N1 (Clontech), yielding GFP-synaptobrevin. Synapto-pHluorin a generous gift from Dr. Jurgen Klingauf, was amplified by PCR and DNA sequenced. The Cells were infected for 6 h using the Semliki Forest Virus expression [1] to allowed the expression of GFP-synaptobrevin-2 and synapto-pHluorin. To minimize the experiment variabilities, cells from the same animal were plated onto different coverslips and were incubated for 6 hours with SybII wild-type virus or with the hybridized SybII virus . Only the control (SybII wild-type) and the hybridized SybII data acquired from the same animal were considered for statistical analysis. Fluorescent cells were imaged by using bright field illumination microscopy with a 40X objective. The acquisition and the analysis of the electrophysiology data were carried out as previously described (Chapter III).

ACKNOWLEDGEMENTS

We thank Dr. Qinghua Fang who made the GFP-Synaptobrevin-2 construct. We are grateful to Dirk Reuter, Joan Lenz and Ina Herfort for expert technical assistance. This work has been supported by the National Institutes of Health grants R01NS38200, R01GM085808, T32GM007469, the Nanobiotechnology Center (a National Science Foundation Science and Technology Center, agreement No. ECS-9876771).

BIBLIOGRAPHY

[1] U. Ashery, A. Betz, T. Xu, N. Brose, and J. Rettig. An efficient method for infection of adrenal chromaffin cells using the Semliki Forest virus gene expression system. *Eur. J. Cell. Biol.*, 78(8):525–32, 1999.

[2] M. Borisovska, Y. Zhao, Y. Tsytsyura, N. Glyvuk, S. Takamori, U. Matti, J. Rettig, T. Südhof, and D. Bruns. v-snares control exocytosis of vesicles from priming to fusion. *Embo. J.*, 24(12):2114–26, 2005.

[3] Ferenc Deak, Ok-Ho Shin, Ege T Kavalali, and Thomas C Südhof. Structural determinants of synaptobrevin 2 function in synaptic vesicle fusion. *J Neurosci*, 26(25):6668–76, 2006.

[4] Sunil P Gandhi and Charles F Stevens. Three modes of synaptic vesicular recycling revealed by single-vesicle imaging. *Nature*, 423(6940):607–13, 2003.

[5] J. Kesavan, M. Borisovska, and D. Bruns. v-snare actions during ca(2+)-triggered exocytosis. *Cell*, 131(2):351–63, 2007.

[6] R Laage and D Langosch. Dimerization of the synaptic vesicle protein synaptobrevin (vesicle-associated membrane protein) II depends on specific residues within the transmembrane segment. *Eur J Biochem*, 249(2):540–6, 1997.

[7] G Miesenbock, D A De Angelis, and J E Rothman. Visualizing secretion and synaptic transmission with pH-sensitive green fluorescent proteins. *Nature*, 394(6689):192–5, 1998.

[8] S Sankaranarayanan, D De Angelis, J E Rothman, and T A Ryan. The use

of pHluorins for optical measurements of presynaptic activity. *Biophys J*, 79(4):2199–208, 2000.

[9] Jakob B. Sørensen. Formation, stabilisation and fusion of the readily releasable pool of secretory vesicles. *Pflugers Arch*, 448(4):347–62, 2004.

[10] Alexander Stein, Gert Weber, Markus C Wahl, and Reinhard Jahn. Helical extension of the neuronal SNARE complex into the membrane. *Nature*, 460(7254):525–8, 2009.

[11] R.B. Sutton, D. Fasshauer, R. Jahn, and A.T. Brunger. Crystal structure of a snare complex involved in synaptic exocytosis at 2.4 resolution. *Nature*, 395:347–353, 1998.

[12] T Voets. Dissection of three Ca2+-dependent steps leading to secretion in chromaffin cells from mouse adrenal slices. *Neuron*, 28(2):537–45, 2000.

[13] T. Voets, E. Neher, and T. Moser. Mechanisms underlying phasic and sustained secretion in chromaffin cells from mouse adrenal slices. *Neuron*, 23(3):607–15, 1999.

[14] Alexander M Walter, Katrin Wiederhold, Dieter Bruns, Dirk Fasshauer, and Jakob B Sørensen. Synaptobrevin N-terminally bound to syntaxin-SNAP-25 defines the primed vesicle state in regulated exocytosis. *J Cell Biol*, 188(3):401–13, 2010.

[15] Martin Wienisch and Jurgen Klingauf. Vesicular proteins exocytosed and subsequently retrieved by compensatory endocytosis are nonidentical. *Nat Neurosci*, 9(8):1019–27, 2006.

CHAPTER 5

ON THE IMPORTANCE OF SYNAPTOBREVIN-2 FOR THE FLUX OF NEUROTRANSMITTERS THROUGH THE FUSION PORE

5.1 Abstract

Neurotransmitters are stored in vesicles and are secreted into the extracellular space through a fusion pore. In SNARE mediated exocytosis, it has been speculated that the fusion pore is formed by the syntaxin transmembrane domain and potentially that of synaptobrevin-2. Here, we have introduced charged amino acids at position 113 of the synaptobrevin-2 transmembrane domain, close to its C-terminus. We have expressed the mutated proteins in synaptobrevin-2 and cellubrevin double knocked out (DKO) embryonic chromaffin cells and have studied whether these mutations can support exocytosis by using a combination of whole-cell calcium flash photolysis and amperometry measurements. We find that the mutated proteins partially rescued exocytosis, and significantly reduced the flux of neurotransmitters through the narrow fusion pore, thus suggesting that synaptobrevin-2 transmembrane domain is located in the fusion pore.

5.2 Introduction

The assembly of the SNARE proteins, namely that of the synaptosome associated protein of 25 KD (SNAP-25), syntaxin and synaptobrevin/Vamp (SybII) bridges the apposing membrane of the vesicle and the cell plasma membrane to drive calcium dependent exocytosis [19, 20, 16, 17]. Prior to full vesicle fusion, the SNARE proteins assemble into a complex thereby driving the formation of the fusion pore through which molecules can channel into the extracellular space [18, 11]. The fusion pore can expand to a diameter exceeding 3 nm [1], which allows neurotransmitters to diffuse out of the vesicle with a time course of few milliseconds [22, 11]. Even though the exact molecular composition of the pore is unclear, it is becoming evident that the SNARE proteins C-terminal domains modulate its structure.

The deletion of the last nine residues of SNAP-25 elongates the early fusion pore [5], and mutagenesis of the transmembrane domain (TMD) of syntaxin reduces the flux of neurotransmitters through the narrow fusion pore [6, 7]. From this latter result, it has been suggested that the syntaxin TMD lines the fusion pore. Since syntaxin and synaptobrevin-2 are both embedded into apposing lipid bilayers prior to exocytosis, and both mediate the formation of the pore, it is proposed that synaptobrevin-2 may also line the fusion pore [9].

However, direct evidence backing up this claim is still lacking, nonetheless, studies have shown that exocytosis is affected when the synaptobrevin-2 C-terminal region is altered [10, 13]. In particular, lengthening the flexible region that separates the cytosolic domain of synaptobrevin-2 to its TMD, reduces vesicles priming, and delays exocytosis [10]. Furthermore, adding charged residues at the C-terminal end of synaptobrevin-2 inhibits exocytosis (Chapter III). Based on these experimental observations, the synaptobrevin-2 TMD should receive

further attention. To investigate whether the introduction of charged residues into the synaptobrevin-2 transmembrane domain, near the C-terminus have any effect on exocytosis, we used a combination of capacitance and amperometry measurements.

5.3 Results

The TMD of synaptobrevin-2 (SybII) is composed of mostly hydrophobic residues (aa 97-116). We mutated the amino acids tyrosine at position 113 to either a lysine or a glutamate, because the alignment of SybII with its homologues vamp1 and the drosophila n_synaptobrevin [Fig. 5.1 A] suggested that a charged residue may be tolerated at position 113 of SybII. SybII mutations were reintroduced into cells using the Semiliki Forest Virus expression system, and exocytosis was triggered by infusing photoreleasable calcium at whole-cell patch. We cultured chromaffin cells from double knocked out (DKO) embryonic adrenal gland deprived of synaptobrevin-2 (SybII) and cellubrevin. The DKO chromaffin cells failed to express the exocytotic phenotype. However 4 h after SybII wild-type protein expression, the secretion defect was rescued [Fig.5.1 B] as previously observed (Chapter III).

5.3.1 The mutations SybII-Y113K and SybII-Y113E partially rescued vesicles fusion

Cells expressing SybII-Y113K and SybII-Y113E showed a reduction of the capacitance response in comparison to wild-type SybII [Fig.5.1 B]. The capacitance trace typically displays a burst and a sustained phase. We compared the burst amplitude of the mutated proteins to that of wild-type SybII by taking the ca-

pacitance increase at 0.5 s post stimulus. The burst amplitude with SybII-Y113E and with SybII-Y113K were ~57% and ~63% of that with wild-type SybII, respectively [Fig.5.1 C].

After scaling the burst phase to the same amplitude, it was evident that the glutamate mutation slowed down the burst kinetics, whereas the lysine did not change the fusion kinetics [Fig. 5.1 D]. The sustained phase which is the slowest component of the capacitance change was quantified by taking the difference in capacitance amplitude between 0.5 and 5 s after the step wise calcium increase. This phase was significantly reduced by ~55% [Fig.5.1 C] for both SybII-Y113E and SybII-Y113K [Fig. 5.1 B]. To rule out the possibility that the difference in exocytosis amplitudes are due to the dissimilarity in protein expression levels, SybII and its homologues were quantified by immunofluorescence. The result shows that the SybII, SybII-Y113K and SybII-Y113E are expressed at similar level after 4 hours of viral infection [Fig.5.2].

The differences in capacitance amplitudes of SybII-Y113K and SybII-Y113E versus SybII at whole-cell patch-clamp configuration, could have been caused by the change in individual vesicle sizes. Therefore, as a next step, we used cell-attached capacitance measurement to determine the size of single vesicles. Figure 5.1.E shows an example of a single vesicle capacitance step of 0.9 fF. The small transient increase in the real part (Re) of the admittance is produced by the low initial pore conductance. The capacitance increase (Cv) is calculated as $Cv = \frac{Re^2+Im^2}{Im}$ [12]. The mean±s.e.m capacitance step of embryonic chromaffin cells expressing SybII (0.36±0.02 fF) was similar to that recorded in wild-type non infected cells (0.38±0.03 fF). Also, cells expressing SybII-Y113K (0.34±0.04 fF) and SybII-Y113E (0.35±0.03 fF) had comparable mean capacitance step sizes. Assuming a specific vesicle membrane capacitance of 9 fF/μm [1], these mean capacitance step sizes correspond to vesicle diameters of 110-116 nm as expected

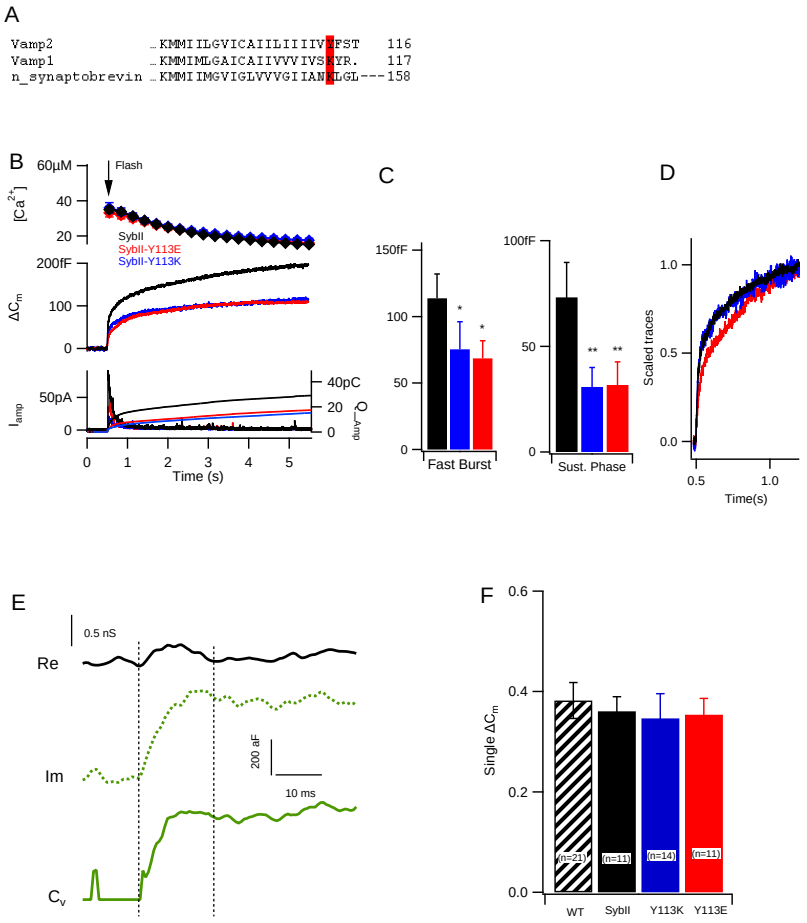

Figure 5.1: (A) Sequence alignment of synaptobrevin-2 homologues VAMP1 and n_synaptobrevin. The tyrosine residue at position 113 of synaptobrevin-2 was mutated to a single lysine (SybII-Y113K) or glutamate (SybII-Y113E). (B) Exocytosis was stimulated by photoreleasable calcium and was monitored by the change of the cell membrane capacitance and the release of catecholamine. At comparable $[Ca^{2+}]_i$ increase (top), cells expressing SybII-Y113K (n=17) and SybII-Y113E (n=14) show reduced capacitance amplitudes (middle) and amperometry currents (bottom) in comparison to wild-type SybII (n=11). (C) The mutations reduced the burst and the sustained phases of the capacitance change. (D) Scaled capacitance traces at 0.5 s after stimulus. (E) Example recording of a single vesicle step size acquired at cell-attached patch configuration. (F) Wild-type of non infected cells (n=21 cells,173 events), SybII expression (n=11 cells, 50 events), SybII-Y113K (n=14 cells, 52 events) and SybII-Y113E (n=11 cells, 79 events).

from the size of granules in mouse embryonic chromaffin cells ~130 nm [3].

5.3.2 Single vesicle amperometry characterization

Chromaffin granules contain catecholamine, which they release into the extracellular space through the fusion pore. To detect these molecules, a carbon fiber electrode was pressed down onto the cell membrane. The amperometry spike currents [Fig.5.3 B] resulting from the oxidation of catecholamine molecules at the surface of the electrode held at +700 mV, provide information on the amount, and kinetics of release of these molecules from individual vesicles. We used the amperometry measurement to assess whether the residues SybII-Y113K and SybII-Y113E altered the fusion pore properties.

Exocytosis was stimulated by infusing ~10 μM free calcium into cells. On average, ~23 events/min were recorded from cells expressing the wild-type SybII, with ~15 and ~17 events/min for cells expressing SybII-Y113K and SybII-Y113E respectively. This reduction of the rate of single release events is consistent with the reduction of capacitance amplitude at whole-cell patch-clamp [Fig.5.1]. In addition, the amount of catecholamine molecules released from the individual vesicles, assessed as the integrated charged of ameperometry spikes, were similar regardless of whether the cells expressed the wild-type or the mutated proteins, SybII (0.33±0.03 pC), SybII-Y113E (0.30±0.04 pC), SybII-Y113K (0.30±0.02 pC) [Fig.5.3 C]. The mean current amplitudes on the other hand differed, being lower (36.99±4.54 pA) and (22.12±2.40 pA) for SybII-Y113K and SybII-Y113E respectively, in comparison to (56.60±6.19 pA) for wild-type SybII [Fig.5.3 D]. The decrease in spike amplitude was accompanied by an increase in spike half width [Fig.5.3 E]

These results indicate that SybII-Y113K and SybII-Y113E slow down the

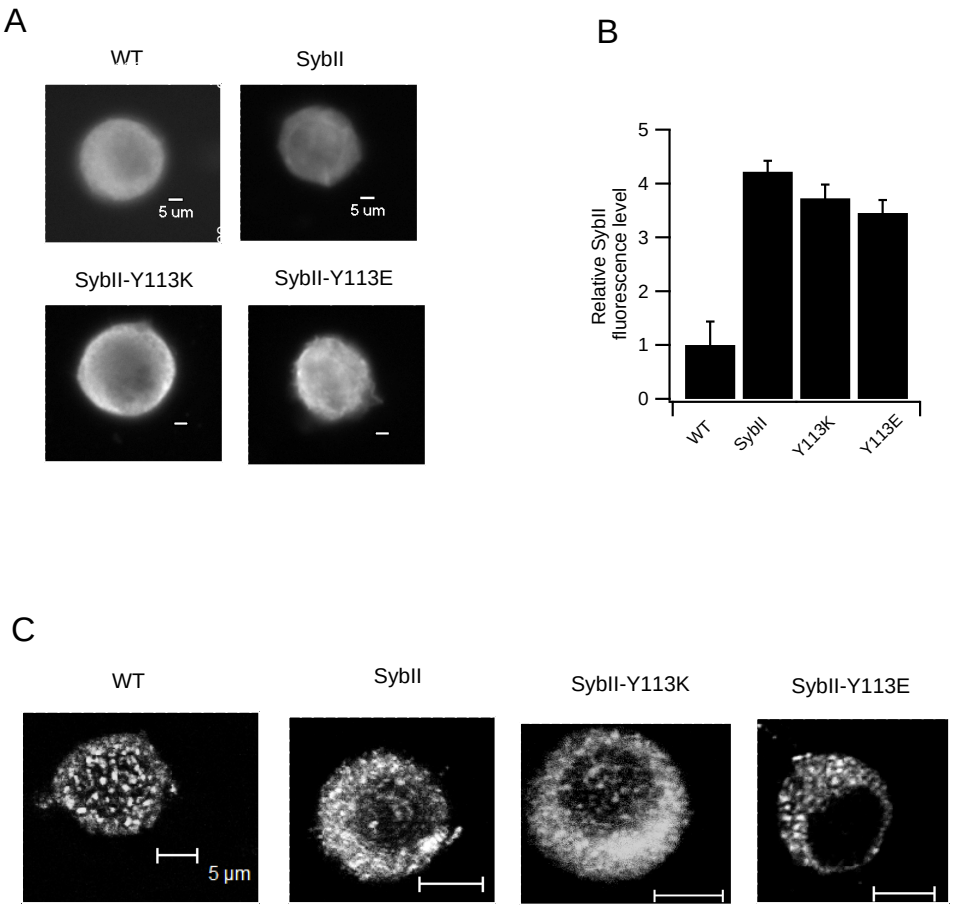

Figure 5.2: Synaptobrevin-2 isoforms quantification in embryonic mouse chromaffin cells. (A) Cells were immunostained with antibodies against SybII, those that were also successfully infected with viral particles and identified by their eGFP expression were selected for analysis. Exemplary fluorescent cells, wild-type non infected (WT+/+), cells overexpressing SybII, SybII-Y113K and SybII-Y113E. (B) Protein quantification using epifluorescence microscopy. SybII, SybII-Y113K and SybII-Y113E were overexpressed ~4 fold more than wild-type control (WT+/+) (>n=20 cells, 3 preparations, scale bar 5 μM). (C) The confocal images of WT+/+, SybII, SybII-Y113K, SybII-Y113E stained with sybII- antibody are granulated and in some cases the granules appear to circumvent the nucleus, indicating the synaptobrevin-2 were located in the vesicles.

release of catecholamine molecules from individual vesicles during the amperometry spike phase. The amperometry spike is often preceded by an amperometric foot current that reflects the formation of a metastable narrow fusion pore, which allows for a slow leakage of molecules from the vesicle. If the TMD of SybII is located at the mouth of the fusion pore or inside the fusion pore, the charged residues at position 113 may alter the flux of catecholamine. Therefore, we determined the foot current properties. The mean foot duration [Fig.5.3 F] was longer for SybII-Y113K (5.46±0.46 ms) and SybII-Y113E (7.27±0.42 ms), albeit only the value for SybII-Y113E was significantly different from wild-type SybII (5.03±0.34 ms). In addition, the foot current amplitudes were significantly smaller [Fig.5.3 G], indicating a slow flux of catecholamine molecules through the fusion pores of cells expressing the mutants proteins SybII-Y113E (0.021 ±0.002 pC) and SybII-Y113K (0.0171±0.002 pC), in comparison to SybII (0.032±0.003 pC).

Fusion pores exhibit dynamic fluctuations that lead to corresponding fluctuations in amperometric foot current. To determine if the foot currents are modified by the mutants SybII-Y113K and SybII-Y113E, we analyzed the fluctuations in the foot amperometry current. The example in Fig.5.4 A, the initial foot current amplitude is ~ 3.65 pA, and the foot current rises with a slope of ~ 138.39 pA/ms, where the slope of the foot current reflects the fusion pore expansion, and the initial foot current amplitude indicates the initial fusion pore conductance. Cells expressing SybII showed an initial foot current of 1.85 ±0.31 pA, whereas cells with the mutated proteins had a significant reduction of initial foot current of 0.65 ±0.18 pA, and 0.62 ±0.31 pA for SybII-Y113E and SybII-Y113K respectively [Fig.5.4 B]. The foot slope on the other hand, was similar for cells expressing SybII 873.14±60.12 pA/s (n=241 events) and those expressing SybII-Y113K 734.07±149.33 pA/s (n=128 events). Whereas the foot

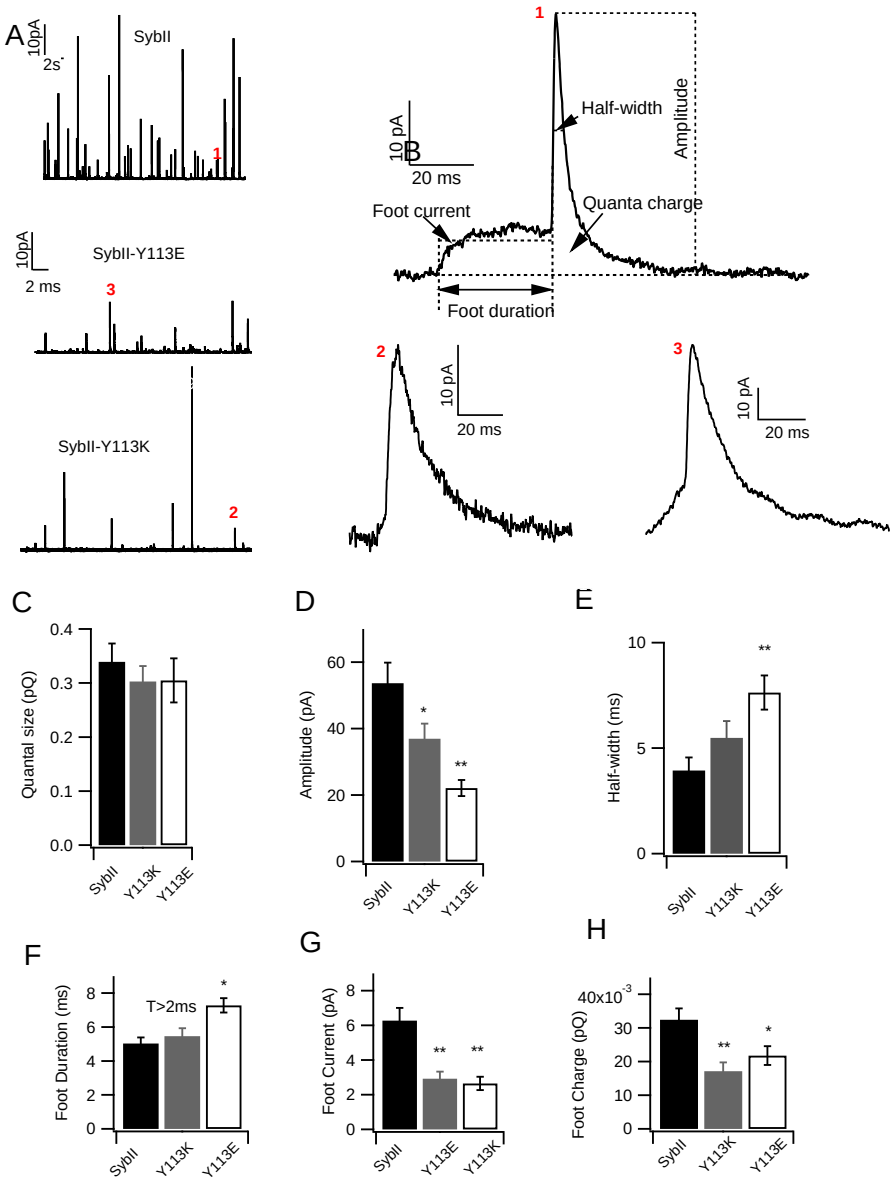

Figure 5.3: Charged residues at position 113 in the TMD of synaptobrevin-2 altered the fusion pore properties. (A) Sample amperometry trace recording from cells expressing wild-type SybII (top), SybII-Y113E (middle) and SybII-Y113K (bottom). (B) Representation of a single spike taken from SybII trace, with spike parameters as indicated (Foot current, half-width, quanta charge, foot duration, and spike amplitude). (D-H) The mean±s.e.m of >10 pA spikes properties, SybII-Y113E (n=17) and SybII-Y113K (n=17) and SybII (n=18) *P<0.05, **P<0.01.

slope for cells expressing SybII-Y113E (521.83±43.48 pA/s, n=216 events), was significantly slower than that for wild-type SybII [Fig.5.4 C].

The foot current deviates somewhat from its mean values during the foot current expansion [Fig.5.4 A], presumably reflecting the conductance property of the fusion pore at different times. The fluctuation of the foot current [Fig.5.4 D] were obtained by taking the difference between the actual foot current and its best linear fit [straight red line in Fig.5.4 A].

The variance, which was obtained by squaring the amplitudes of the residual current, increase with higher foot current amplitudes for cells expressing SybII. Whereas the variances of cells expressing the mutants proteins had smaller amplitudes and deviated less from their mean foot currents [Fig.5.4 E]. The power spectrum did not shows any preferred frequency, indicating that the currents fluctuated stochastically [Fig.5.4 F]. Furthermore, only the fluctuation amplitudes of cells expressing SybII-Y113E were apparently smaller than that of cells expressing SybII-Y113K and SybII.

5.4 Discussion

To achieve a rapid and effective neurotransmitter release, SNARE proteins preassembled into a complex [19, 20, 8] thus providing energy for the apposite membranes to merge, and thereby inducing the fusion pore formation. Synaptobrevin-2 modulates the fusion pore in synaptic vesicles and in chromaffin cells by means of its TMD [19, 14] (Chapter III, IV). We have previously established that the C-terminal end of synaptobrevin-2 disrupts the lipid bilayer continuity to initiate the fusion pore through which neurotransmitters are release into the extracellular space. However it was still unclear whether synaptobrevin-2 TMD is located in the fusion pore during the pore expansion.

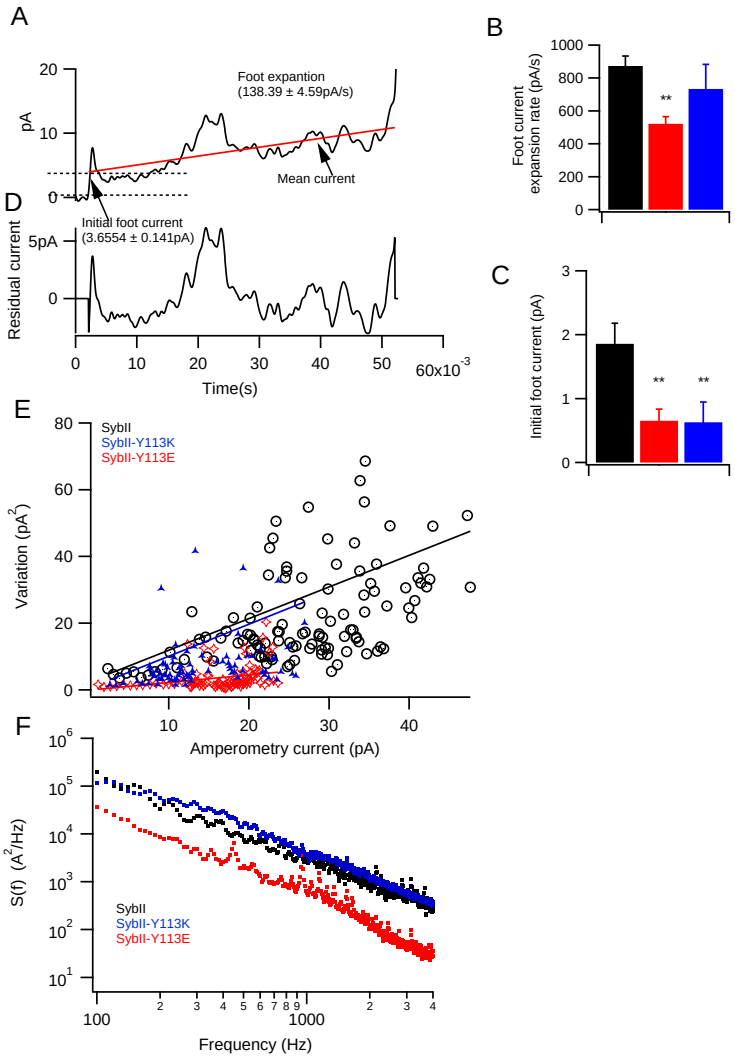

Figure 5.4: Foot current fluctuation analysis. (A) Example of a fluctuating foot current. The mean current was obtained by fitting the foot with a straight line (red line). From the fit, the initial foot current and the slope of the foot can be extracted. (B-C) Initial currents and foot current expansion rate of cells expressing SybII, SybII-Y113K and SybII-Y113E. (D) The residual current was obtained by taking the difference between the foot current and the linear fit. (E) Foot current variance plotted against mean current. (F) Power spectrum of wild-type SybII control, SybII-Y113K, SybII-Y113E (dot).

Here, we have introduced a single lysine or glutamate in the TMD of synaptobrevin-2, near the alleged location of the pore, this resulted in a significant reduction of the exocytotic amplitude at whole-cell patch.

By using single vesicle capacitance measurement, we excluded the possibility that this reduction of the total cell membrane area was due to the difference in the size of the vesicles. Thus it seems likely that these mutations partially inhibit exocytosis by rendering fewer vesicles fusion-competent. This phenotype was also confirmed by lower frequencies of observable single vesicles fusion found with the mutations.

5.4.1 Synaptobrevin-2 transmembrane domain modulates the fusion pore conductance

As vesicles fuse with the plasma membrane, a narrow fusion pore that allows for the flux of catecholamine into the extracellular space is formed. Charged residues in the TMD of synaptobrevin-2 if facing the fusion pore, may interfere with this migration because the released catecholamines carry a positive charge. In this frame work, we analyzed the catecholamine release during the first milliseconds of the fusion pore existence. Interestingly, the positively and the negatively charged mutants, SybII-Y113K and SybII-Y113E both led to a significant reduction of the amount of catecholamine molecules detected during the initial fusion pore expansion, indicating that the transmembrane domain of the mutated proteins interfere with the flux of catecholamine molecules.

It has also been reported that the TMD of synaptobrevin-2 lays at a tilt angle with respect to the vertical in the lipid bilayer [4]. Thus, the side chains of the lysine and glutamate residues at position 113 near the bilayer interphase may "snorkel" into the lipid head groups region to accommodate the charges on

the side chains while the hydrocarbons of the amino acids remained inside the lipid membrane. In this new configuration, the fusion pore structure may have been altered and synaptobrevin-2 transmembrane domain may have placed the charged side chains inside the fusion pore, leading to a reduction of the initial foot current as observed in [Fig.5.4, B].

Since the catecholamine molecules are positively charged at neutral and acidic pH, they may have interacted electrostatically with the charges on the side chains of the lysine or the glutamate residues during their passage through the narrow fusion pore, which may have led to fewer molecules being released during fusion pore expansion [Fig.5.3 H]. More importantly, the reduction of catecholamine molecules through the narrow fusion pore strongly suggests that synaptobrevin-2 C-terminal region is located in the fusion pore. A similar observation was previously reported when selected residues of the TMD of syntaxin were mutated to ionizable side chains [6, 7].

We observed that the foot current expansion rate is significantly slower for the negatively charged mutant and not for the positively charged mutant [Fig.5.4 D]. This is consistent with slower kinetic of vesicles fusion observed by scaling the burst phase of the capacitance increase [Fig.5.1 D], and the lower amplitude of frequencies observed in the power spectra. This suggest that the fusion pores formed by the negatively charged transmembrane domain slow down the fusion pore expansion rate. The specific reason for this phenotype is not yet well understood. Nevertheless, it is conceivable that, the glutamate being negatively charged would attract the positively charged catecholamines, and in the process may bind to them, thereby inducing a steric occlusion of the fusion pore and slowing down the movement of the transmembrane domain of synaptobrevin-2 (Chapter III). It is, however also possible that the structure of SybII TMD in the fusion pore is affected because the positive charge of the

lysine my accommodate better in the lipid head groups region than the negative charge of the glutamate. Also the potential snorkel for lysine is much longer than for glutamate.

5.5 Methods

5.5.1 Single Cell expression

Single chromaffin cells were isolated by enzymatic reaction from the medulla gland of E17-E19 embryonic littermate lacking both synaptobrevin-2 and cellubrevin. The cDNA encoding for SybII-Y113E and SybII-Y113K were produced by polymeric chain reaction (PCR) and verified by cDNA sequencing. Cells were infected after 3 to 4 days in cultures using the Semliki Forest Viral expression system [2].

5.5.2 Electrophysiology

Individual chromaffin cells were infected for 4 or 5 h to allow for the dual expression of eGFP and synaptobrevin-2. The flash photolysis and the capacitance measurement were carried at whole-cell patch configuration by infusing 0.4 M fura-4F, 0.4 M mag-fura-2 (Molecular Probes, Eugene, OR) and 0.4 M $CaCl_2$ bound to 0.5 M Nitrophenyl-EGTA . The ratiometric fluorescent measurement for calcium detection were performed as previously described [21]. Single vesicle capacitance was obtained at cell-attached patch configuration. The bath solution contained in mM: 145 NaCl, 1 $MgCl_2$, 2.8 KCl, 2 $CaCl_2$ and 10 HEPES. The pH and osmolarity was adjusted to 7.2 with NaOH and to 310 mOSM with D-glucose whenever necessary. The pipette solution contained in (mM) 50 NaCl, 100 TEA-Cl, 5 KCl, 5 $CaCl_2$, 1 $MgCl_2$, and 10 Hepes/NaOH (pH 7.2).

The experiments were performed using the EPC-7 amplifier (HEKA) and the lock-in amplifier (SR 830; Stanford Research Systems). A 20-KHz at 50 mV sine wave stimulus at 100 mV/pA was used to resolve the single capacitance steps. The phase was calibrated offline for each recording by using Igor Pro software (Wavemetrics, Lake Oswego, OR).

5.5.3 Amperometry

The high resolution amperometry measurement was used to detect the secretion of molecules from individual vesicles. The conventional carbon electrode with a 10 μM fiber diameter was used. To minimize the error due to diffusion, the carbon fiber was pressed onto the cell membrane and the tip of the electrode was cut before each experiment. The oxidation of molecules at surface of the electrode was detected as an amperometry spike and was acquired with EPC7 and filtered with 3 kHz with a sampling frequency of 20 kHz. To stimulate exocytosis, the cells were infused at whole-cell configuration with a solution containing in (mM) 100 Cs-glutamate, 0.3 Na-GTP, 2 Mg-ATP, 2.5 $CaCl_2$, 0.4 fura-4F, 0.4 furaptra, 20 DPTA and 32 HEPES, pH 7.2. The data are the mean of the median and One-way ANOVA was used for statistical analysis (*P<0.05, **P<0.01).

The foot current I_{foot} is proportional to the the flux J of neurotransmitters through the narrow fusion pore (5.1) [15].

$$I_{foot} \propto J = \frac{\pi \cdot R_{pore}^2 \cdot D \cdot \Delta C}{L_{pore}} \tag{5.1}$$

Where ΔC is the difference of neurotransmitters concentration between the interior and the exterior of the vesicle, D is the diffusion coefficient, R_{pore}^2, the radius and L_{pore}, the fusion pore length. Foot currents longer than 10 ms were obtained by fitting the foot trace I_{foot} with a line I_{mean} (5.2).

$$I_{mean}(t) = A \cdot (t) + I_{mean}(0) \tag{5.2}$$

Where A is the amplitude of the foot and $I_{mean}(0)$ the initial foot current. The residual current $I_{residual}$ was obtained by subtracting the I_{foot} from I_{mean}(5.3).

$$I_{residual}(t) = I_{foot}(t) - I_{mean}(t) \tag{5.3}$$

The variance was obtained by taking the squared amplitude of the residual current, and the power spectrum was obtained by taking the square of the Fourier transform of the residual current.

5.5.4 Immunofluorescence

Embryonic chromaffin cells were fixed after 4 h of viral infection with 3.7% formaldehyde for 20 min at room temperature. Cells were subsequently washed in phosphate-buffered saline (PBS), permeabilized for 10 min in 0.1% triton X-100 and quenched with 50mM NH_4Cl. The cells were then incubated for 2 h with the monoclonal primary antibodies (mouse anti-synaptobrevin-2) diluted 1:500 in 10% bovine serum albumin (Synaptic Systems, Göttingen, Germany) followed by 10 min wash in PBS. They were then exposed to the secondary antibody (cyanine (Cy)3-conjugated goat anti-mouse dilutions 1:200) for an 1 h at room temperature. Cells expressing the eGFP were chosen for synaptobrevin-2 proteins level quantification, using bright field illumination microscopy (Imaging Facility, Life Science Core Laboratiories Center, Cornell University) with excitation filter 560/55 and emission 645/75. The intensity of the region of interest was computed and subtracted from intensity of the local background. An average of 2-3 animals was used for this study. Confocal images were acquired using Leica confocal microscopy TCS SP2 with a 40x (NA 0.8/W.D. 3.3 mm) dipping objective.

5.6 Acknowledgements

This work was done in collaboration with Adam D. Herbst who did a fantastic job in building the program for fluctuation analysis. We are grateful to Dirk Reuter, Joan Lenz and Ina Herfort for expert technical assistance. We are also grateful to Ray Molloy for the antibody gift. This work has been supported by the National Institutes of Health grants R01NS38200, R01GM085808, T32GM007469, the Nanobiotechnology Center (a National Science Foundation Science and Technology Center, agreement No. ECS-9876771).

BIBLIOGRAPHY

[1] A. Albillos, G. Dernick, H. Horstmann, W. Almers, G. Alvarez de Toledo, and M. Lindau. The exocytotic event in chromaffin cells revealed by patch amperometry. *Nature*, 389:509–512, 1997.

[2] U. Ashery, A. Betz, T. Xu, N. Brose, and J. Rettig. An efficient method for infection of adrenal chromaffin cells using the Semliki Forest virus gene expression system. *Eur. J. Cell. Biol.*, 78(8):525–32, 1999.

[3] M. Borisovska, Y. Zhao, Y. Tsytsyura, N. Glyvuk, S. Takamori, U. Matti, J. Rettig, T. Südhof, and D. Bruns. v-snares control exocytosis of vesicles from priming to fusion. *Embo. J.*, 24(12):2114–26, 2005.

[4] M. E. Bowen and A. T. Brunger. Conformation of the synaptobrevin transmembrane domain. *Proc. Natl. Acad. Sci.*, 103(22):8378–83, 2006.

[5] Q. Fang, K. Berberian, L. W. Gong, I. Hafez, J. B. Sø rensen, and M. Lindau. The role of the c terminus of the snare protein snap-25 in fusion pore opening and a model for fusion pore mechanics. *Proc Natl Acad Sci U S A*, 105(40):15388–92, 2008.

[6] X. Han, C. T. Wang, J. Bai, E. R. Chapman, and M. B. Jackson. Transmembrane segments of syntaxin line the fusion pore of ca2+-triggered exocytosis. *Science*, 304(5668):289–92, 2004.

[7] Xue Han and Meyer B Jackson. Electrostatic interactions between the syntaxin membrane anchor and neurotransmitter passing through the fusion pore. *Biophys J*, 88(3):L20–2, 2005.

[8] P I Hanson, R Roth, H Morisaki, R Jahn, and J E Heuser. Structure and conformational changes in NSF and its membrane receptor complexes vi-

sualized by quick-freeze/deep-etch electron microscopy. *Cell*, 90(3):523–35, 1997.

[9] Meyer B Jackson and Edwin R Chapman. Fusion pores and fusion machines in Ca2+-triggered exocytosis. *Annu Rev Biophys Biomol Struct*, 35(NIL):135–60, 2006.

[10] J. Kesavan, M. Borisovska, and D. Bruns. v-snare actions during ca(2+)-triggered exocytosis. *Cell*, 131(2):351–63, 2007.

[11] Manfred Lindau and Guillermo Alvarez de Toledo. The fusion pore. *Biochim Biophys Acta*, 1641(2-3):167–73, 2003.

[12] K Lollike, N Borregaard, and M Lindau. The exocytotic fusion pore of small granules has a conductance similar to an ion channel. *J Cell Biol*, 129(1):99–104, 1995.

[13] J. A. McNew, T. Weber, D. M. Engelman, T. H. Söllner, and J. E. Rothman. The length of the flexible snarepin juxtamembrane region is a critical determinant of snare-dependent fusion. *Mol Cell*, 4(3):415–21., 1999.

[14] J. A. McNew, T. Weber, F. Parlati, R. J. Johnston, T. J. Melia, T. H. Söllner, and J. E. Rothman. Close is not enough: Snare-dependent membrane fusion requires an active mechanism that transduces force to membrane anchors. *J Cell Biol*, 150(1):105–17., 2000.

[15] Eugene V Mosharov and David Sulzer. Analysis of exocytotic events recorded by amperometry. *Nat Methods*, 2(9):651–8, 2005.

[16] G. Schiavo, F. Benfenati, B. Poulain, O. Rossetta, P. Polverino de Laureto, B.R. DasGupta, and C. Montecucco. Tetanus and botulinum.b neurotoxins

block neurotransmitter release by proteolytic cleavage of synaptobrevin. *Nature*, 359:832–834, 1992.

[17] T. Söllner, S. Whiteheart, M. Brunner, H. Erdjument-Bromage, M. Geromanos, P. Tempst, and J.E. Rothman. Snap receptors implicated in vesicle targeting and fusion. *Nature (London)*, 362:318–323, 1993.

[18] Jakob B Sørensen. Conflicting views on the membrane fusion machinery and the fusion pore. *Annu Rev Cell Dev Biol*, 25(NIL):513–37, 2009.

[19] Alexander Stein, Gert Weber, Markus C Wahl, and Reinhard Jahn. Helical extension of the neuronal SNARE complex into the membrane. *Nature*, 460(7254):525–8, 2009.

[20] R.B. Sutton, D. Fasshauer, R. Jahn, and A.T. Brunger. Crystal structure of a snare complex involved in synaptic exocytosis at 2.4 resolution. *Nature*, 395:347–353, 1998.

[21] T Voets. Dissection of three Ca2+-dependent steps leading to secretion in chromaffin cells from mouse adrenal slices. *Neuron*, 28(2):537–45, 2000.

[22] R M Wightman, T J Schroeder, J M Finnegan, E L Ciolkowski, and K Pihel. Time course of release of catecholamines from individual vesicles during exocytosis at adrenal medullary cells. *Biophys J*, 68(1):383–90, 1995.

CHAPTER 6

SYNAPTOBREVIN-2 DIMERIZATION IN CHROMAFFIN CELLS

6.1 Abstract

The exocytosis of neurons and neuroendocrine cells is driven by the formation of tight helical bundle. This complex is formed by the interaction of synaptobrevin-2, syntaxin and SNAP-25, and it mediates exocytosis by bringing the vesicle and the cell membranes in close apposition. Synaptobrevin-2 is anchored to the vesicle membrane by a transmembrane region. *Invitro*, this domain can self-interact, thus inducing the dimerization of synaptobrevin-2. However the physiological relevance of synaptobrevin-2 dimers has been questioned. Here we investigate whether the mutants L99A, C103A and I111A that inhibit synaptobevin-2 dimerization can support calcium dependent exocytosis in chromaffin cells. We find that, while the single point mutation L99A, and the double point mutation C103A/I111A partially rescue exocytosis in comparison to the wild-type synaptobrevin-2, the triple point mutant L99A/C103/I111A nearly abolishes secretion. We also find that the mutant C103N implicated in the increase of synaptobrevin-2 dimerization, also fails to rescue the exocytotic phenotype. Base on kinetic analysis, we infer that these defects are primarily due to the priming defect of vesicles.

6.2 Introduction

The neuronal SNARE (soluble N-ethylmaleimid-sensitive factor (NSF) attachment protein receptor) proteins play an important role in the release of neurotransmitters. Neurotransmitters are compartmentalized into vesicles, and in order to be released into the extracellular space, the vesicles dock and fuse with

the cell plasma membrane. This process is mediated by the so-called SNARE proteins, namely synaptobrevin, syntaxin and SNAP-25 [22, 15, 6, 9]. It has been established by crystallography that these proteins form a coiled-coil structure [22, 20] in which synaptobrevin SNARE motif binds to a pre-complex formed by syntaxin and SNAP-25 [7]. It has also been shown experimentally that, when the SNARE complex is cleaved by toxins, vesicle secretion is abolished in neurons and in chromaffin cells (view review [12]). Synaptobrevin has been of interest in recent years because it is the only protein of the complex which is anchored to the vesicle. In fact, synaptobrevin spans the vesicular bilayer through a single transmembrane domain (TMD). Although the function of this domain remains elusive, it has been proposed, based on *invitro* assays that synaptobrevin forms dimers [10, 11]. In SDS-PAGE assay, full length synaptobrevin molecules pairs up with other synaptobrevin via the interaction of their transmembrane domains. Three residues responsible for this interaction were identified [10], when leucine at position 99 (L99), cystine at position 103 (C103) and isoleucine at position 111 (I111) in the transmembrane domain were mutated to the amino acid alanine, the ratio of dimer-to-monomer synaptobrevin was significantly reduced [10] indicating that the protein lost its ability to form dimers. Furthermore, when L99, C103 and I111 were grafted onto an otherwise monomeric structure, this was sufficient to induce dimerization [11]. These observations suggested that, these three amino acids contained most of the dimers packing interaction and led to the conclusion that, the TMD of the synaptobrevin interacts via a set of selected residues, wherein amino acids facing each other form a link via their side chain interactions. Although synaptobrevin dimers have been detected in embryonic synaptosomes [1] the physiological relevance of synaptobrevin dimers has been questioned [4]. Here we explore

whether L99, C103 and I111 that have been previously identified to promote dimerization invitro are relevant in supporting $[Ca^{2+}]_i$ dependent exocytosis in chromaffin cell. We find that these mutations hinder the priming step of exocytosis.

6.3 Results

We studied whether replacing the residues L99, C103 and I111 [Fig.6.1] to alanine supports exocytosis in cells. To this end, we generated synaptobrevin-2 (SybII) constructs with either a single, double or triple mutations [Fig.6.1]. These mutants were expressed in E17-E19 embryonic chromaffin cells lacking synaptobrevin-2 and cellubrevin (DKO). DKO cells were necessary because cellubrevin can functionally substitute for SybII in this system [3]. Exocytosis was stimulated by raising homogeneously the intracellular free calcium to $\sim 30\,\mu$m by flash induced photorelease of caged Ca^{2+}. Vesicle fusion was monitored at whole-cell patch clamp by means of the cell membrane capacitance measurement, which capacitance increase reflected the fusion of vesicles with the plasma membrane. The capacitance measurement was combined with the detection of catecholamine molecules secreted by the vesicles during fusion [Fig.6.2 A (bottom panel)] [25]. We started by expressing SybII in DKO cells (data not shown), as previously described (Chapter III), DKO cells did not show a significant increase in membrane capacitance, whereas when they were infected by viral expression of wild-type SybII, the capacitance response was rescued.

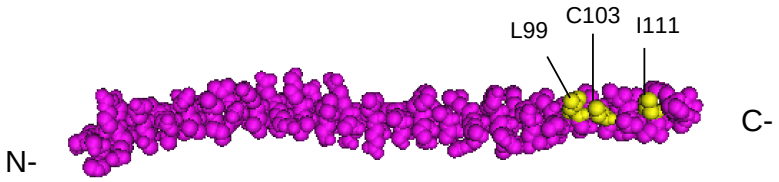

Figure 6.1: Mutations implicated in the dimerization of synaptobrevin-2 are located in the transmembrane region of the protein. Full length synaptobrevin-2 structure modified from 3IPD [20]. The residues L99, C103 and I111 are in yellow.

6.3.1 The dimerization mutants L99A, C103A and I111A partially inhibit exocytosis

The mutant SybII-I111A reduced SybII TMD dimerization *invitro* [10]. When we expressed SybII-I111A in chromaffin cells, the average capacitance increase at 5 s after stimulus [Fig.6.2 A (arrow)], was ~52 % of the capacitance amplitude recorded in cells expressing the wild-type SybII [Fig.6.2 A]. Introducing the double point mutation SybII-L99A/C103A, showed similar inhibition of ~43 % [Fig.6.2 A,B]. The triple point mutation SybII-L99A/C103A/I111A further reduced the capacitance amplitude to nearly ~23 % of control [Fig.6.2 C]. These results suggest that the dimerization mutants that are implicated in inhibiting SybII TMD dimerization, also inhibit the exocytotic response.

The capacitance response to a step-like calcium increase shows a rapid burst phase which typically last ~0.5 s after stimulus. This phase can be fitted with the sum of two exponential functions [Fig.6.2 D], where the fastest kinetic component reflects the fusion of the readily releasable pool (RRP) of vesicles, and the slower component, the fusion of the slowly releasable pool (SRP) of vesicles [23, 18, 26]. These pools reflect vesicles that have already undergone

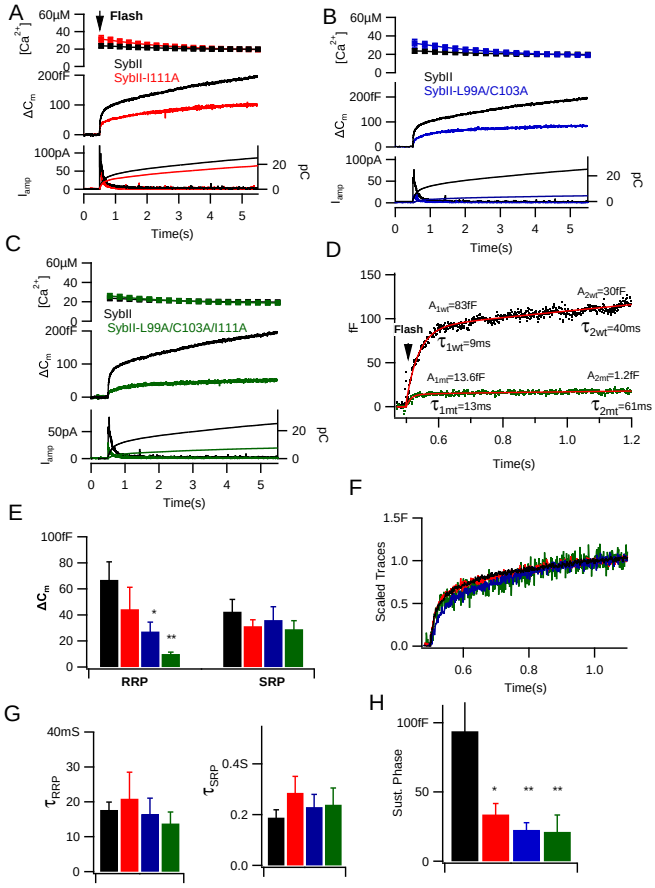

Figure 6.2: The expression of the dimerization mutants in chromaffin cells disrupts the exocytotic phenotype. (A) The single point mutation SybII-I111A (n=22), (B) the double point mutation SybII-L99A/C103A (n=20), and (C) the triple point mutation SybII-L99A/C103A/I111A (n=21) all display a reduction of the capacitance amplitude (middle), and amperometry current (bottom) in comparison to the control SybII (middle, black) (n=30), at similar calcium level (upper traces). (D) The kinetic parameters were evaluated by fitting the individual capacitance traces with a triple exponential function (Method). Sample fits of wild-type (black) and SybII-L99A/C103A/I111A (green) capacitance traces. (E-G) From the fit, we extracted the RRP and the SRP. The RRP amplitudes are reduced in the mutants whereas, the SRP amplitudes are similar to that of control SybII. Furthermore, the time constants of the different pools are similar for the mutants and the control. (F) Capacitance traces scaled at 0.5 s after the calcium stimulus. (H) All mutants impaired the sustained phase significantly (*P<0.05, **P<0.01, Student's t-test).

the priming step at the onset of the calcium stimulus. The sum of exponential fit yields multiple parameters, the amplitudes and the time constants. The amplitudes reflect the sizes of the pools whereas the time constants indicate the kinetics of fusion of their vesicles. Besides the burst phase, the capacitance response also displays a sustained phase which typically last several seconds. This phase reflects vesicles that replenish the SRP under the condition of sustained calcium increase [18]. In our experiments, the dimerization mutants reduced the RRP and the sustained phase amplitudes (capacitance increase during 0.5 s to 5 s after the calcium stimulus), while the SRP amplitudes remained constant [Fig.6.2 E,H]. However, the time constant of neither the RRP nor the SRP was affected by the mutations [Fig.6.2 G] [Table 6.3.2]. This indicates that, although the dimerization mutants affect the RRP sizes, they do not hinder the fast fusion of vesicles with the plasma membrane. In addition, the reduction of the sustained phase indicates that the amount of vesicles undergoing priming during the 5 s of our data acquisition was reduced, suggesting a defect in the priming step of vesicles.

6.3.2 Increasing synaptobrevin-2 dimerization inhibits calcium dependent exocytosis

Given that we observed the inhibition of exocytosis with mutations implicated in inhibiting SybII dimerization, we next investigated SybII-C103N, which was reported to increase SybII TMD dimerization *invitro* by ~ 14 fold [4]. The expression of SybII-C103N in cells also gave sub-optimal secretion as attested by the reduction of the capacitance and the amperometry amplitudes [Fig. 6.3 A] compared to cells expressing wild-type SybII. The RRP, SRP and sustained phase amplitudes were all significantly smaller in comparison to wild-type SybII

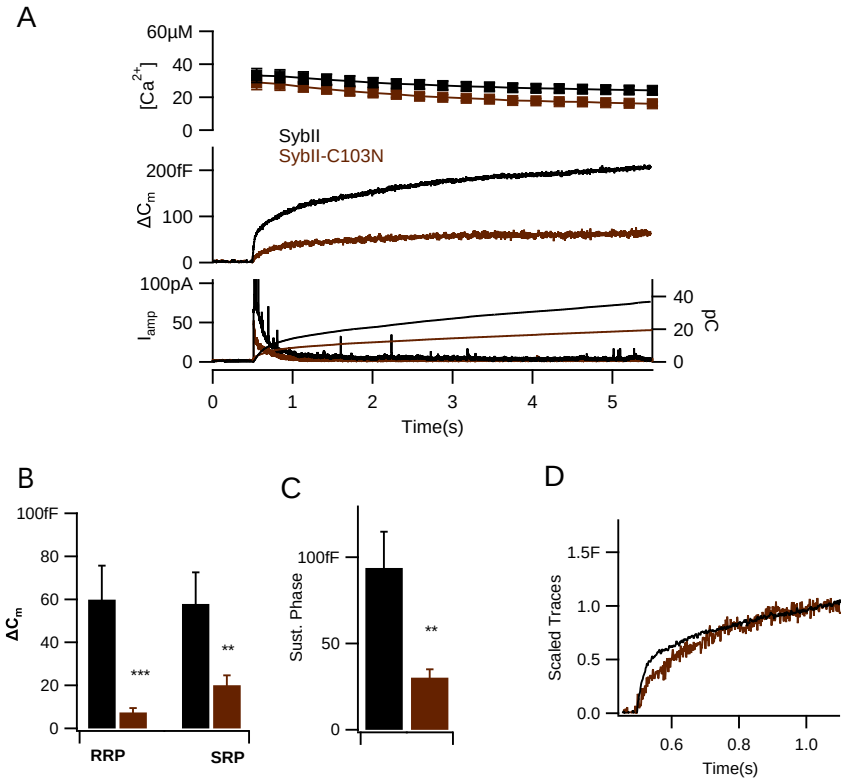

Figure 6.3: (A) The rescued experiment shows that the capacitance amplitude is reduced by ~69% (middle, n=15) of wild-type (black,n=12), this is consistent with the reduction in catecholamine released as visualized by amperometry (bottom) trace. (B,C) The RRP and the SRP sizes and the sustained phase are significantly reduced in cells expressing SybII-C103N in comparison to wild-type cells expression. (D) The burst phase of the capacitance trace is scaled to 0.5 s after stimulus.(*P<0.05, **P<0.01 ***P<0.001, Student's t-test).

[Fig. 6.3 B,C]. Unlike the kinetics of vesicles fusion mediated by the mutations that inhibit dimerization, SybII-C103N which increase dimerization in *invitro*, slowed down the fusion of the burst phase of exocytosis, as observed after scaling the capacitance amplitudes [Fig.6.3 D].

Table 6.1: Exponential fit parameters of the capacitance trace.

Dimerization Mutations	RRP (fF)	τ_{RRP}(ms)	SRP(fF)	τ_{SRP}(s)	Sust. Phase (fF)	Dimerization (%)
SybII	66.9±13.8	17.7±2.2	42.5±9.4	0.18±0.03	92.9± 20.01	
SybII-L99A	44.4±16.7	20.9±7.6	31.4±4.8	0.2±0.06	33.7± 7.8	~ 49 ± 12.5 [10]
SybII-L99A/I111A	27.3±7.2	16.5±4.5	36.1±10.1	0.2±0.04	22.6±5.2	
SybII-L99A/C103A/I111A	10±1.4	13.8±3.2	29.1±6.4	0.2±0.06	21.2± 1.2	~ 30 ± 10 [10]
SybII	59.9±15.7	16.2±4.5	57.9±14.6	0.20±0.07	93.9± 21.01	100
SybII-C103N	7.4±1.9	21.9±7.0	20.1±4.5	0.24±0.04	30.3±4.82	1400±600 [4]

6.4 Discussion

The dimerization of the TMD of synaptobrevin-2 has been controversial because *invitro* studies have yielded inconsistent conclusions [4, 10, 11]. Here we examined the physiological relevance of synaptobrevin-2 transmembrane mutants that have been linked to its TMD dimerization *invitro*. We have observed that the single point mutation SybII-I111A and the double point mutation SybII-L99A/C103A partially rescued exocytosis when they are expressed in DKO embryonic chromaffin cells. This result is in agreement with ~50% reduction of dimerization-to-monomer ratios obtained *invitro* [10]. Conversely, the

triple point mutation SybII-L99A/C103A/I111A nearly abolishes vesicle secretion, consistent with significant reduction of dimerization previously reported [10]. Our data strongly correlates the inhibition of exocytosis by these mutants with their impairment of dimerization, thus suggesting that synaptobrevin-2 dimerization is an intermediate step in exocytosis.

The SNARE complex "zipped" from the N- to the C-terminal [17]. This assembly follows a two steps process where the N-terminal assembles during priming, followed by a calcium dependent C-terminal association [24, 17, 19]. Our mutations slow down vesicles priming while keeping the fusion rate constant. This can be explained by the fact that the dimerization mutants interfere with the assembly of the N-terminal assembly of the SNARE complex. Furthermore, the kinetic of fusion was not affected by these mutants, suggesting that synaptobrevin-2 dimerization is not important for the triggering of exocytosis.

Computation studies have shown that synaptobrevin-2 transmembrane domains are at closest at position C103 [8]. We mutated C103 to asparagine because this alteration was reported to increase SybII TMD-TMD interaction. Here we have shown that the expression of this mutant in chromaffin cells, also inhibits the vesicles priming and slows down fast vesicles fusion. This can be explained by the fact that asparagine is polar amino acid, thus its position in the lipid bilayers is not favorable and is likely to change the protein/lipid dynamic. This is not unexpected since in Chapter III, and V, we have reported the inhibition of exocytosis by charged residues in the transmembrane domain of synaptobrevin-2.

The importance of synaptobrevin-2 dimerization is not yet fully understood, however, it is speculated that the multimerization of the SNAREs facilitates the release of neurotransmitters [5, 2, 21]. However, the exact number of SNARE complexes required for single vesicle fusion is still subject of debate

(review [13]). If multiple SNARE complexes were required to facilitate vesicle fusion, synaptobrevin-2 dimerization could stabilize this super SNARE complex structure. However, here we have found that increasing the interaction between synaptobrevin-2 also inhibit vesicles fusion.

Thus alternatively, we envision a scenario in which, similarly to syntaxin forming clusters [16], synaptobrevin-2 would also form clusters. A synaptobrevin-2 cluster would result from the interaction of multiple synaptobrevin-2 transmembrane domains. The role of this cluster could be to act as a reservoir to facilitate the availability of synaptobrevin-2 in participating in the SNARE complex formation. It is possible that our mutations render the cluster too tight (increase in dimerization) or too lose (decrease in dimerization), both states unfavorable for vesicles priming. To achieve vesicle priming, synaptobrevin-2 on the vesicle needs to find a way to bind to SNAP-25 and syntaxin on the plasma membrane. This step could be mediated by an accessory protein whose main function will be to direct synaptobrevin-2 from the cluster site to its target complex. We propose that this accessory protein could potentially be synaptophysin. Similar to synaptobrevin-2, synaptophysin is embedded into the vesicle via a transmembrane region, and it has been determined that synaptobrevin-2 forms an hetero structure with synaptophysin [14, 1], and this interaction is mediated by their transmembrane domains interaction. When a toxin is used to cleave synaptobrevin-2, synaptophysin can still bind to its C-terminal transmembrane region (residues 68-116) [27]. Interestingly, synaptophysin can only bind one synaptobrevin-2 [1] and when this composite structure is formed, synaptobrevin-2 can no longer interact with either syntaxin or SNAP-25. Therefore, it is possible that synaptophysin recruits synaptobrevin from the cluster via TMD-TMD interaction and retains it until the pre-complex formed by syntaxin-SNAP-25 is achieved [7]. In so doing protein recognition is be facilitated as well

as the achievement of vesicle priming and fast vesicle fusion.

6.5 Method.

The high resolution calcium flash photolysis data were collected as previously described (Chapter III) The chromaffin cells were isolated from E17-E19 mice and were cultured for 2 to 3 days. The infection of cells were typically carried for 4 to 5 hours using Semliki Forest Virus expression system. During the recording of the traces, the cells bathed in saline solution containing (mM): 145 NaCl, 2.8 KCl, 2 $CaCl_2$, 1 $MgCl_2$, and 10 Hepes plus 2 mg/ml D-glucose, pH 7.2. To stimulate exocytosis, the cells were infused with intra cellular solution containing (mM): 100 Cs-glutamate, 4 $CaCl_2$, 32 Hepes, 2 Mg-ATP, 0.3 GTP, 1 ascorbic acid, 5 nitrophenyl-EGTA, 0.4 fura-4F, and 0.4 furaptra, pH 7.2. For the capacitance analysis, each trace was fitted with the sum of three exponential functions:

$$f(x) = A_0 + A_1(1 - \exp[-t/\tau_1]) + A_2(1 - \exp[-t/\tau_2]) + A_3(1 - \exp[-t/\tau_3]),$$

where A_0 is the capacitance of the whole-cell membrane before the stimulus, A_1,A_2 τ_1 and τ_2 are the amplitude and time constant of the RRP and SRP, respectively. The parameters A_3 and τ_3 were not considered because this component consist of a mixture of exocytosis and endocytosis [23, 18]. The values reported are mean ± s.e.m. and the student's t-test was used to determine the statistical significance (*P<0.05, **P<0.01 ***P<0.001)

BIBLIOGRAPHY

[1] A. Becher, A. Drenckhahn, I. Pahner, M. Margittai, R. Jahn, and G. Ahnert-Hilger. The synaptophysin-synaptobrevin complex: a hallmark of synaptic vesicle maturation. *J. Neurosci.*, 19(6):1922–31, 1999.

[2] S. Bevan and L. M. Wendon. A study of the action of tetanus toxin at rat soleus neuromuscular junctions. *J Physiol*, 348(NIL):1–17, 1984.

[3] M. Borisovska, Y. Zhao, Y. Tsytsyura, N. Glyvuk, S. Takamori, U. Matti, J. Rettig, T. Südhof, and D. Bruns. v-snares control exocytosis of vesicles from priming to fusion. *Embo. J.*, 24(12):2114–26, 2005.

[4] M. E. Bowen, D. M. Engelman, and A. T. Brunger. Mutational analysis of synaptobrevin transmembrane domain oligomerization. *Biochemistry*, 41(52):15861–6, 2002.

[5] S G Cull-Candy, H Lundh, and S Thesleff. Effects of botulinum toxin on neuromuscular transmission in the rat. *J Physiol*, 260(1):177–203, 1976.

[6] Dirk Fasshauer. Structural insights into the SNARE mechanism. *Biochim Biophys Acta*, 1641(2-3):87–97, 2003.

[7] Dirk Fasshauer and Martin Margittai. A transient N-terminal interaction of SNAP-25 and syntaxin nucleates SNARE assembly. *J Biol Chem*, 279(9):7613–21, 2004.

[8] K G Fleming and D M Engelman. Computation and mutagenesis suggest a right-handed structure for the synaptobrevin transmembrane dimer. *Proteins*, 45(4):313–7, 2001.

[9] Reinhard Jahn and Richard H Scheller. SNAREs−−engines for membrane fusion. *Nat Rev Mol Cell Biol*, 7(9):631–43, 2006.

[10] R Laage and D Langosch. Dimerization of the synaptic vesicle protein synaptobrevin (vesicle-associated membrane protein) II depends on specific residues within the transmembrane segment. *Eur J Biochem*, 249(2):540–6, 1997.

[11] R Laage, J Rohde, B Brosig, and D Langosch. A conserved membrane-spanning amino acid motif drives homomeric and supports heteromeric assembly of presynaptic SNARE proteins. *J Biol Chem*, 275(23):17481–7, 2000.

[12] E Link, J Blasi, E R Chapman, L Edelmann, A Baumeister, T Binz, S Yamasaki, H Niemann, and R Jahn. Tetanus and botulinal neurotoxins. Tools to understand exocytosis in neurons. *Adv Second Messenger Phosphoprotein Res*, 29(NIL):47–58, 1994.

[13] Cesare Montecucco, Giampietro Schiavo, and Sergio Pantano. SNARE complexes and neuroexocytosis: how many, how close? *Trends Biochem Sci*, 30(7):367–72, 2005.

[14] Maria Pennuto, Dario Bonanomi, Fabio Benfenati, and Flavia Valtorta. Synaptophysin I controls the targeting of VAMP2/synaptobrevin II to synaptic vesicles. *Mol Biol Cell*, 14(12):4909–19, 2003.

[15] Josep Rizo, Xiaocheng Chen, and Demet Arac. Unraveling the mechanisms of synaptotagmin and SNARE function in neurotransmitter release. *Trends Cell Biol*, 16(7):339–50, 2006.

[16] Jochen J Sieber, Katrin I Willig, Rainer Heintzmann, Stefan W Hell, and Thorsten Lang. The SNARE motif is essential for the formation of syntaxin clusters in the plasma membrane. *Biophys J*, 90(8):2843–51, 2006.

[17] J. B. Sørensen, K. Wiederhold, E. M. Muller, I. Milosevic, G. Nagy, B. L. de Groot, H. Grubmuller, and D. Fasshauer. Sequential n- to c-terminal snare complex assembly drives priming and fusion of secretory vesicles. *Embo J*, 25(5):955–66, 2006.

[18] Jakob B. Sørensen. Formation, stabilisation and fusion of the readily releasable pool of secretory vesicles. *Pflugers Arch*, 448(4):347–62, 2004.

[19] Jakob B Sørensen. Conflicting views on the membrane fusion machinery and the fusion pore. *Annu Rev Cell Dev Biol*, 25(NIL):513–37, 2009.

[20] Alexander Stein, Gert Weber, Markus C Wahl, and Reinhard Jahn. Helical extension of the neuronal SNARE complex into the membrane. *Nature*, 460(7254):525–8, 2009.

[21] B A Stewart, M Mohtashami, W S Trimble, and G L Boulianne. SNARE proteins contribute to calcium cooperativity of synaptic transmission. *Proc Natl Acad Sci U S A*, 97(25):13955–60, 2000.

[22] R.B. Sutton, D. Fasshauer, R. Jahn, and A.T. Brunger. Crystal structure of a snare complex involved in synaptic exocytosis at 2.4 resolution. *Nature*, 395:347–353, 1998.

[23] T. Voets, E. Neher, and T. Moser. Mechanisms underlying phasic and sustained secretion in chromaffin cells from mouse adrenal slices. *Neuron*, 23(3):607–15, 1999.

[24] Alexander M Walter, Katrin Wiederhold, Dieter Bruns, Dirk Fasshauer, and Jakob B Sørensen. Synaptobrevin N-terminally bound to syntaxin-SNAP-25 defines the primed vesicle state in regulated exocytosis. *J Cell Biol*, 188(3):401–13, 2010.

[25] R.M. Wightman, J.A. Jankowski, R.T. Kennedy, D.T. Kawagoe, T.J. Schroeder, D.J. Leszczyszyn, J.A. Near, E.J. Diliberto jr., and O.H. Viveros. Temporally resolved catecholamine spikes correspond to single vesicle release from individual chromaffin cells. *Proceedings of the National Academy of Sciences of the United States of America*, 88:10754–10758, 1991.

[26] T Xu, T Binz, H Niemann, and E Neher. Multiple kinetic components of exocytosis distinguished by neurotoxin sensitivity. *Nat Neurosci*, 1(3):192–200, 1998.

[27] Sowmya V Yelamanchili, Clemens Reisinger, Anja Becher, Stefan Sikorra, Hans Bigalke, Thomas Binz, and Gudrun Ahnert-Hilger. The C-terminal transmembrane region of synaptobrevin binds synaptophysin from adult synaptic vesicles. *Eur J Cell Biol*, 84(4):467–75, 2005.

CHAPTER 7

CONCLUSIONS

Exocytosis is definitely a fascinating subject, by studying this process we can decipher not only how information is transmitted from neurons to neurons, but also how other secretory cells discard their contents into the extracellular space.

Katz and Del Castillo in 1956 postulated the existence of membrane packets containing neurotransmitters, from a simple drawing showing membrane packets approaching a cell membrane and releasing their molecules into the extracellular space, they gave birth to the idea of neuronal exocytosis. The existence of these membrane packets or vesicles were later confirmed by electron micrography. Today, not only we know that several cell types encompass vesicles, but we also know that the fusion of these vesicles with the cell membrane depends not only on calcium but also on the so-called SNARE proteins. When neurons or neuroendocrine cells are infused with toxins that cleave these SNARE proteins, exocytosis is abolished. Furthermore, we know that for a vesicle to fuse with the plasma membrane, it has to reach a maturation state also called priming, it has to dock with the cell plasma membrane, and a fusion pore has to be created to allow the diffusion of neurotransmitters into the extracellular space.

Although the Sørensen group have identified the role of SNARE proteins in vesicle priming and docking, it was still unclear whether the SNARE proteins are also involved in the fusion pore formation. Based on experimental evidences described in Chapter III, we have established that the transmembrane domain of SNARE protein synaptobrevin-2 disrupts the vesicular lipid bilayer continuity to initiate the fusion pore formation. We have also speculated that the cell lipid bilayer could also be disrupt with the movement of the transmembrane domain

of syntaxin, however this should be confirmed in future experiments.

Synapto-pHluorin is protein that has been extensively used in optical measurements of exocytosis because it is pH sensitive, which means that when Synapto-pHluorin is in an acidic environment, the fluorescence of the pHluorin on the protein is quenched. However, when the pH value exceeds 7.2 the fluorescence is dequenched. Hence synapto-pHluorin has been used to monitor the fusion of vesicles with the plasma membrane. The interior of the vesicle has a pH of 5.6 thus, when synapto-pHluorin is located on the vesicles, it appears dark under a fluorescence microscope. When the vesicles fuse with the plasma membrane, synapto-pHluorin is now exposed to the cytoplasm (pH 7.2), and there it brightened. However, synapto-pHluorin is composed of pH sensitive GFP protein or pHluorin attached to the C-terminal end of the synaptobrevin-2 protein. Our data in Chapter III indicate that when extra amino acids are added at the C-terminal end of synaptobrevin-2, the protein partially loses its functionality. Thus, it was important to assess whether synapto-pHluorin was functional in mediating exocytosis. We find that in general, synapto-pHluorin mediates vesicle exocytosis but not to full level, as it hinders the priming and the fast fusion of vesicles with the cell plasma membrane. However, exocytosis is not inhibited when synapto-pHluorin is in the presence of synaptobrevin-2. Overall this means that synapto-pHluorin is better used as an optical tool to visualize the process of exocytoisis however care should be taken when using it to assess the kinetic of exocytosis.

Even though the concept of multiple SNARE protein interaction is widely accepted, such as in the case of the SNARE protein syntaxin, whose self interaction leads to syntaxin clusters, the idea of synaptobrevin interactions has been disputed. In Chapter VI we have explored whether the amino acids at the center of synaptobrevin-2 TMD-TMD dimerization in vitro also hold in cells. We

find that the mutations that inhibited synaptobrevin dimerization *in-vitro* also inhibit calcium dependent exocytosis in cells. Hence, base on functional similarities between synaptobrevin and syntaxin, we postulate that synaptobrevin-2 may also form clusters. However, it remains to be established experimentally the existence of these clusters and to define their role.